



Brain & Cognitive
Sciences



University of Wisconsin
**SCHOOL OF MEDICINE
AND PUBLIC HEALTH**

NeuroImage Analysis

Moo K. Chung

Department of Brain and Cognitive Sciences
Seoul National University

Department of Biostatistics and Medical Informatics
Waisman Laboratory for Brain Imaging and Behavior
University of Wisconsin-Madison

www.stat.wisc.edu/~mchung

SNU PBCS lecture
October 4, 2011

Where I work?



Waisman Laboratory for Brain Imaging and Behavior, Madison

<http://brainimaging.waisman.wisc.edu>

Brain Image Analysis

Image Acquisition

I. Image collection
MRI, fMRI, PET, CT,
EEG, MEG
Inverse problem
DTI Q-ball imaging

2. Reading Image into computer
Image formats ascii, binary
DIACOM, MINC, ANALYZER, BRIK

Image Segmentation

3. Gaussian mixture
EM algorithm and a Bayesian prior

4. Deformable model
and surface model
Active contour, snake

5. PDF curve evolution
Level set, 0-levelset of spline

Image Registration

6. Similarity metric
Intensity correlation, mutual information
Kullback-Leibler divergence

7. Curve & surface registration
dynamic time warping,
iterative shifting

8. Image volume registration
Intensity-based, PDE-based

Flowchart illustrating the process of Brain Image Analysis:

Statistical Modeling

Geometric Modeling

Image Smoothing

9. Random fields

Mean-square convergence
Hilbert space
Karhunen-Loeve expansion
White noise, Brownian motion

10. Linear additive model

General linear model (GLM)
Fixed & Random effect models
Regression on manifolds

11. Curve modeling

Curvature estimation,
Riemannian metric tensor

12. Surface modeling

Curvature estimation,
Riemannian metric tensor

13. Kernel Smoothing

Fourier transform
Nadaraya-Watson kernel estimator

14. Diffusion Smoothing

Diffusion equations,
Spherical harmonics,
Finite element method

16. Tensor smoothing

Edge preserving
smoothing
Vector fields smoothing

15. Heat kernel smoothing

Iterative kernel smoothing,
Laplace-Beltrami operator

Multiple comparisons

17. False discovery rate (FDR)

18. Random fields theory
Corrected P-value
Euler characteristic

19. Permutation test
Checking image processing artifacts

Classification

21. Linear discriminant

22. Logistic discriminant
Classification accuracy

23. Support Vector Machines

Network modeling

24. Functional connectivity
Effective connectivity
Covariance modeling

25. Structural connectivity
DTI-based graph network model

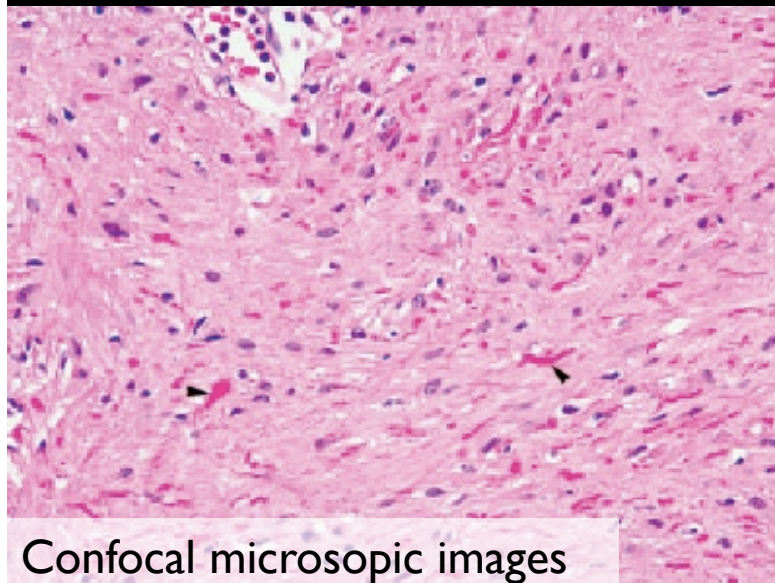
26. Topological network modeling
Rips complex, epsilon-neighbor

Image acquisition

Microscope

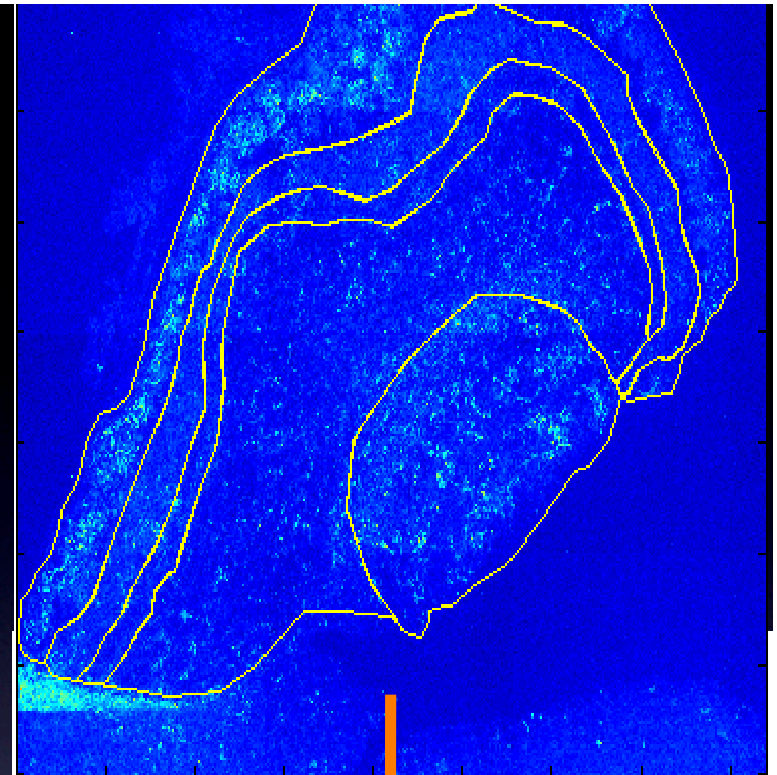


Rosenthal Fiber Segmentation (mouse brain)

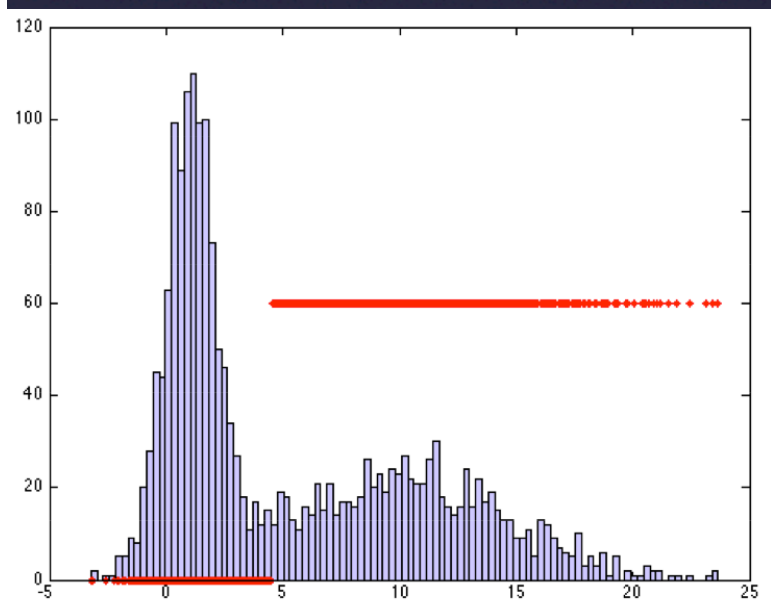
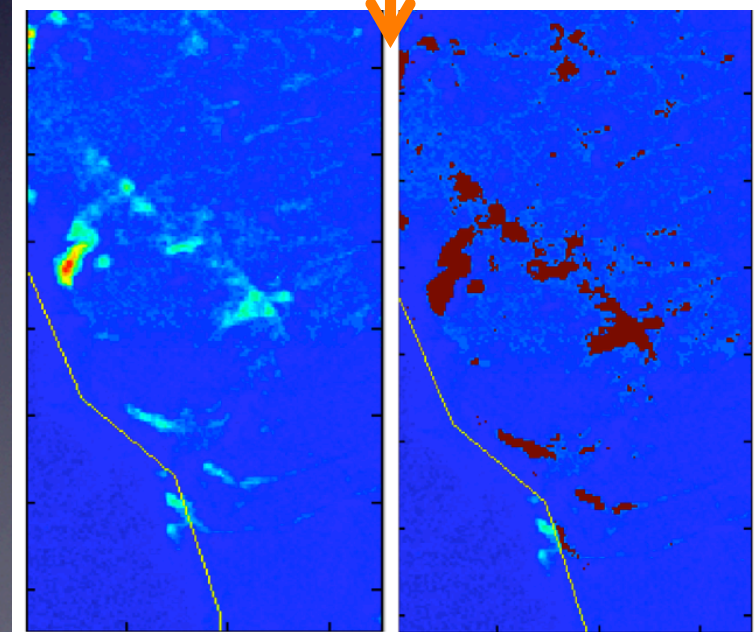


Confocal microscopic images

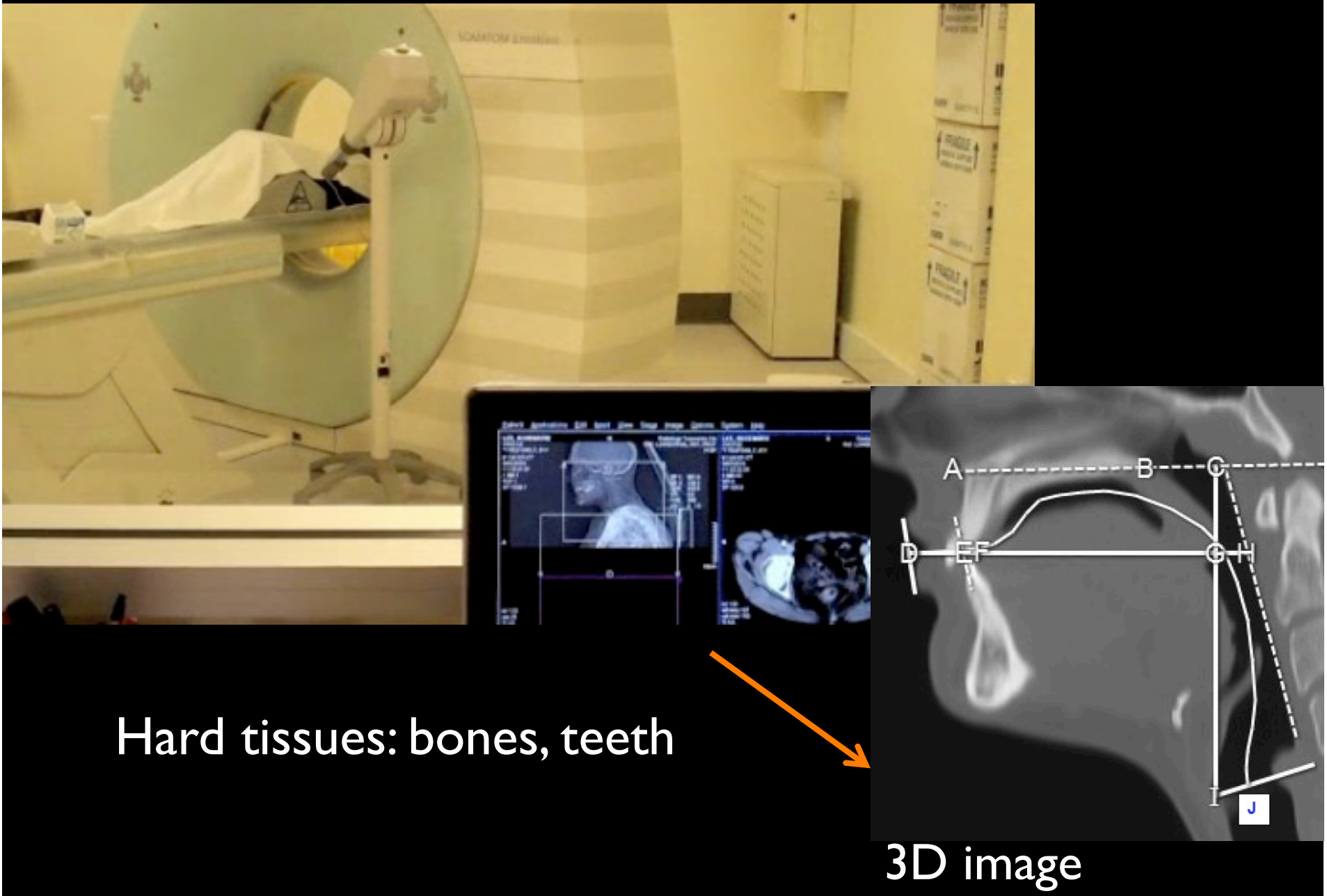
ROI-drawing

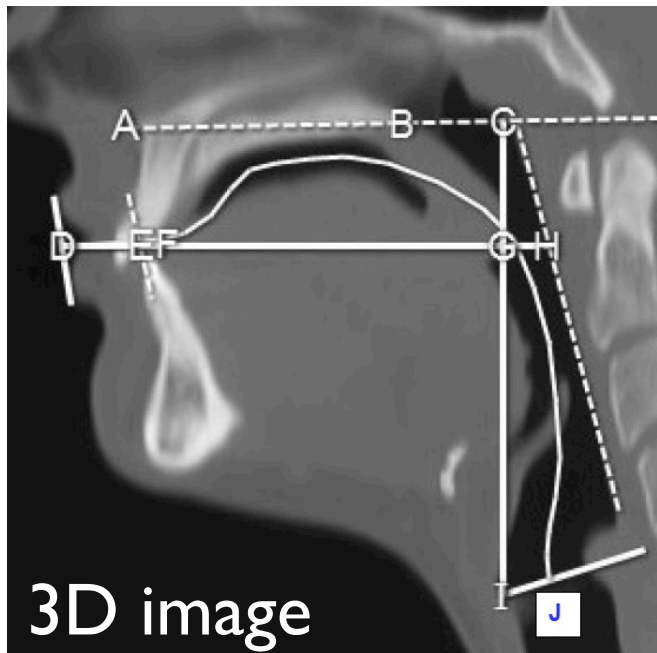


Gaussian
Mixture model

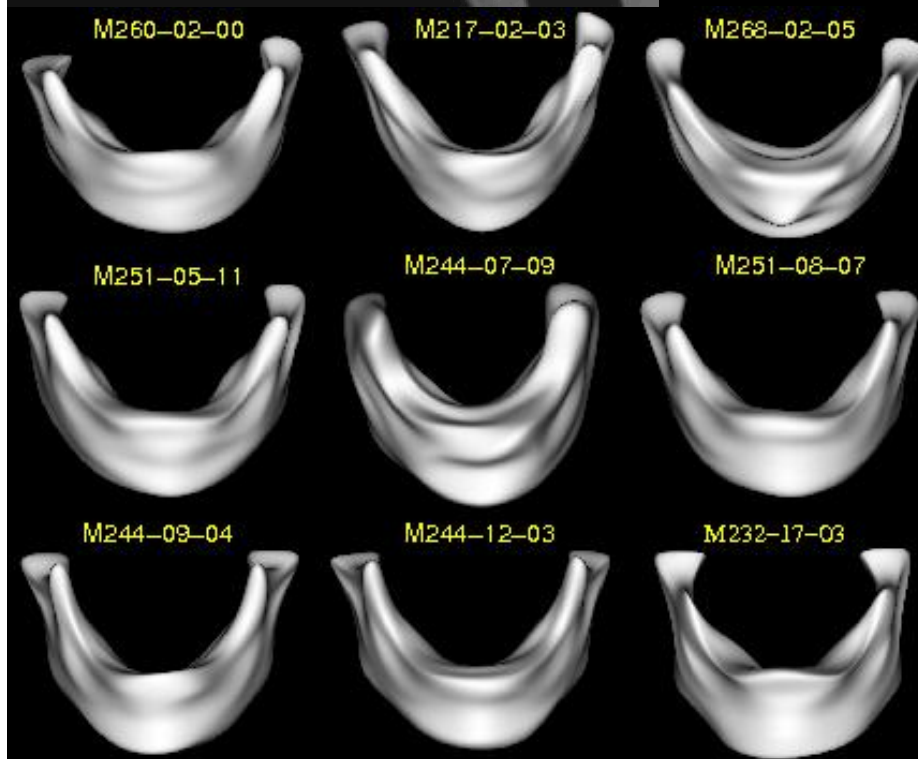


Computed Tomography (CT)





3D image



Binary
segmentation

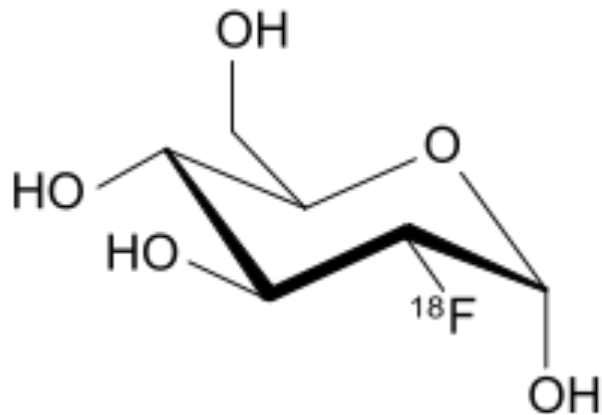


Surface models

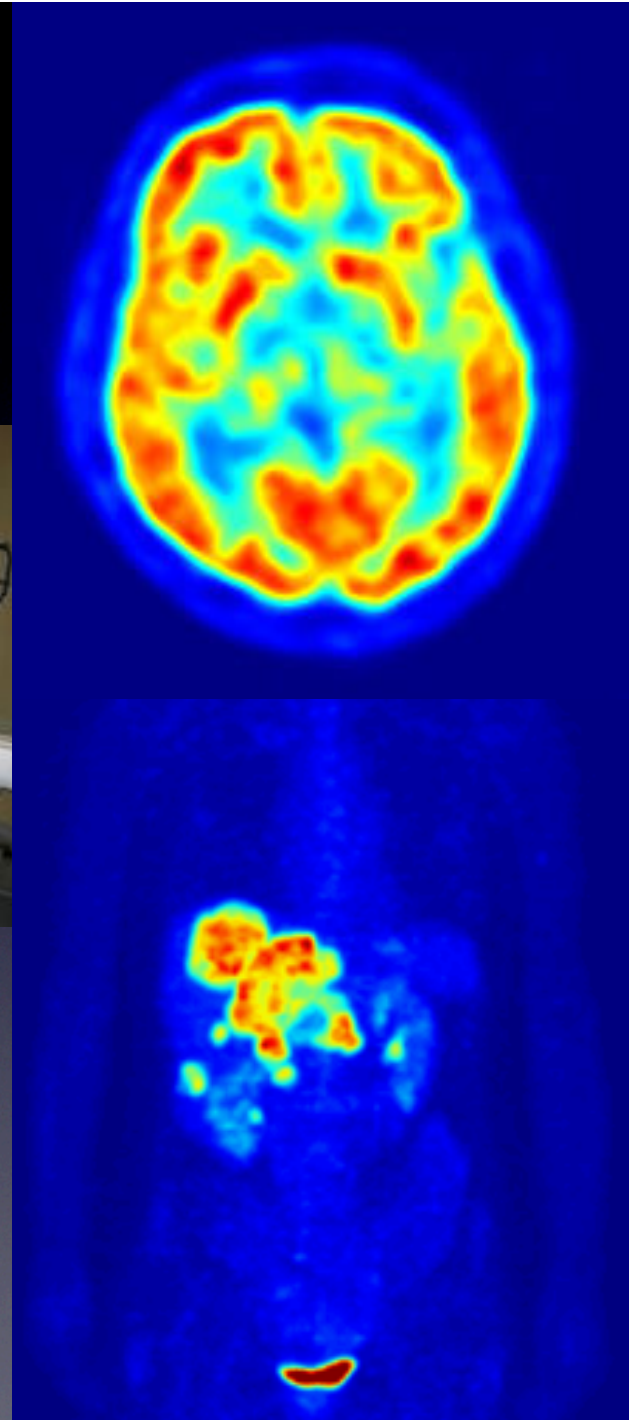
Waisman vocal tract laboratory

FDG-PET

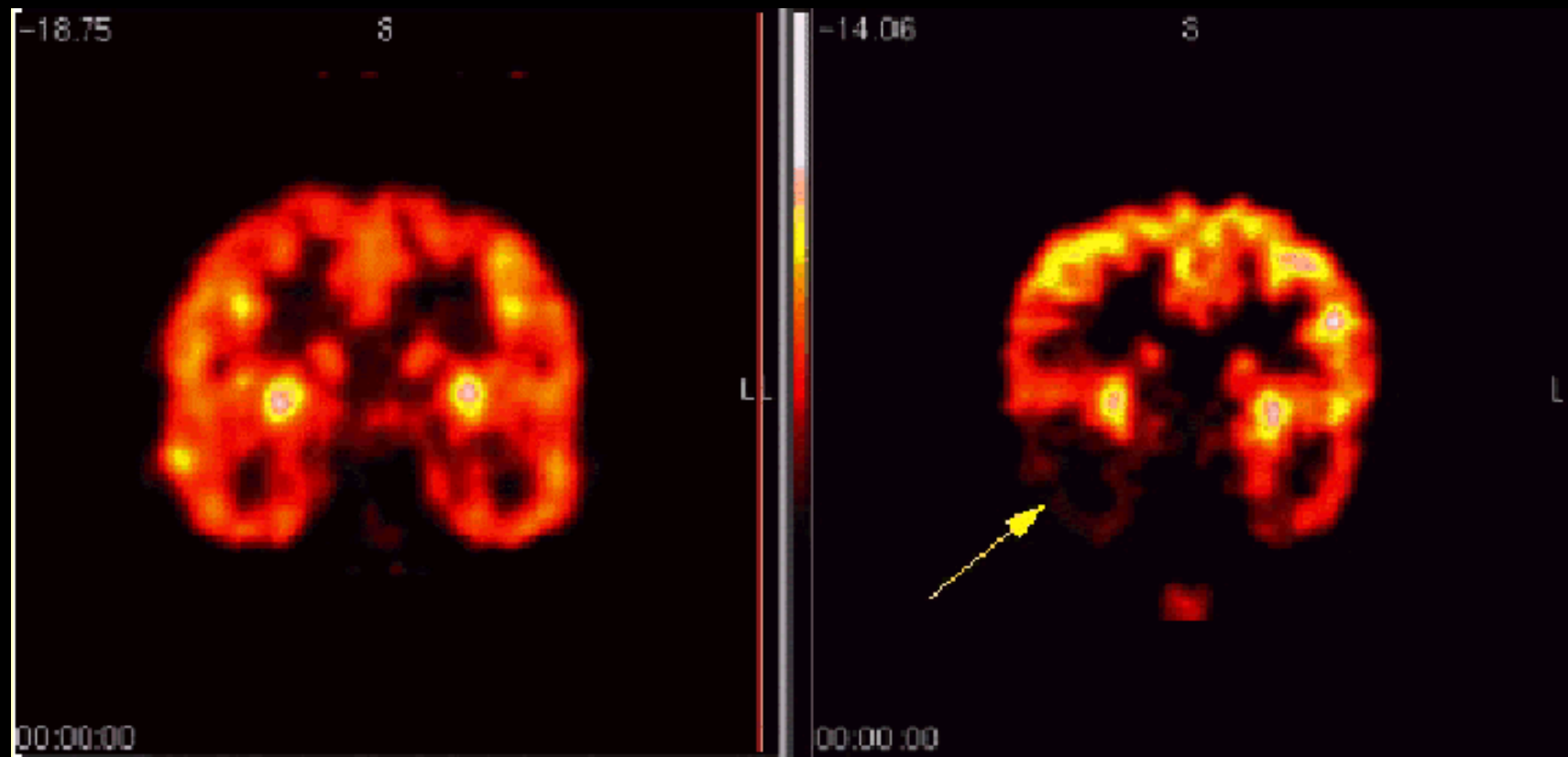
The PET scanner detects pairs of gamma rays emitted from a positron-emitting radioactive tracer.



¹⁸F-FDG is the most widely used tracer used for measuring tissue metabolic activity, in terms of regional glucose uptake.



Positron Emission Tomography (PET)



Normal Brain

Brain of 9 year old girl
suffering from epilepsy

Montreal Neurological Institute

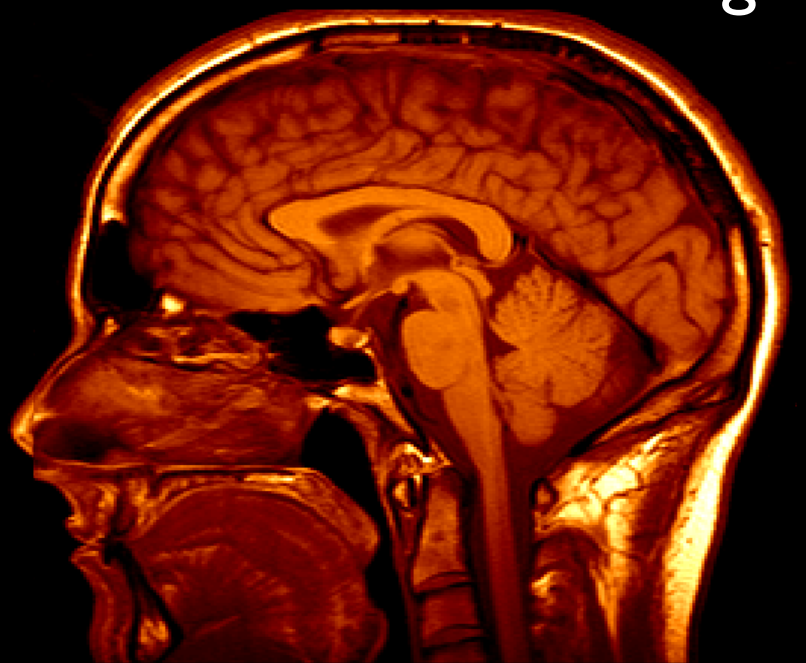
Magnetic Resonance Imaging (MRI)



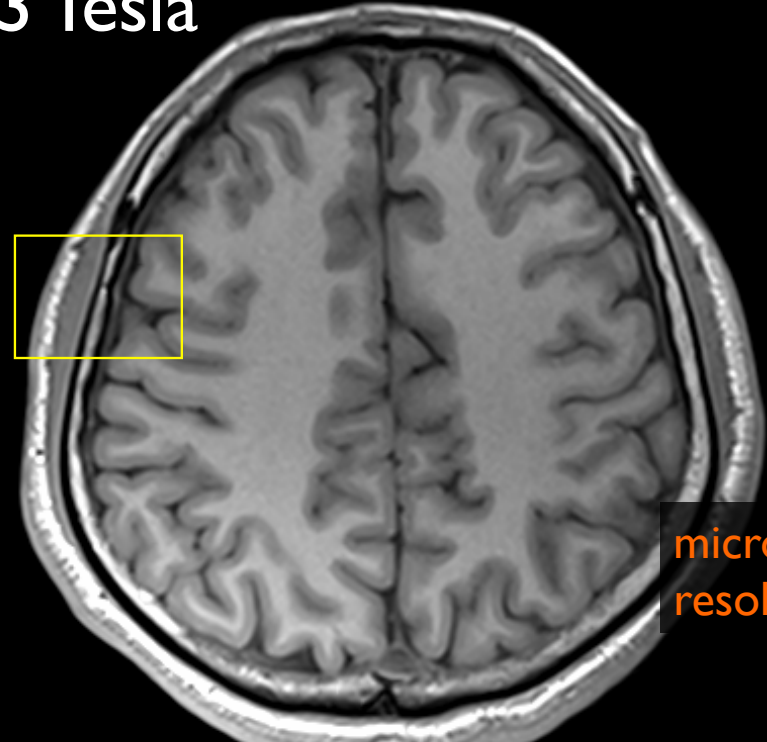
3.0 Tesla GE Scanner

Soft tissues

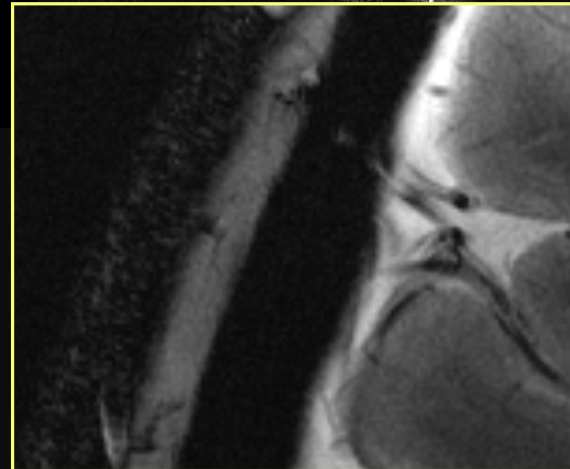
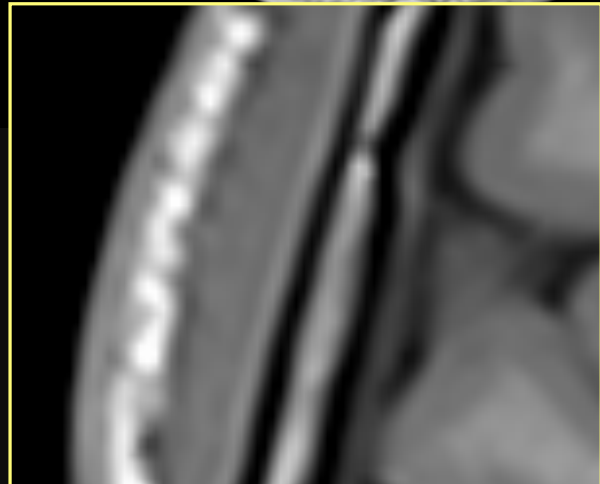
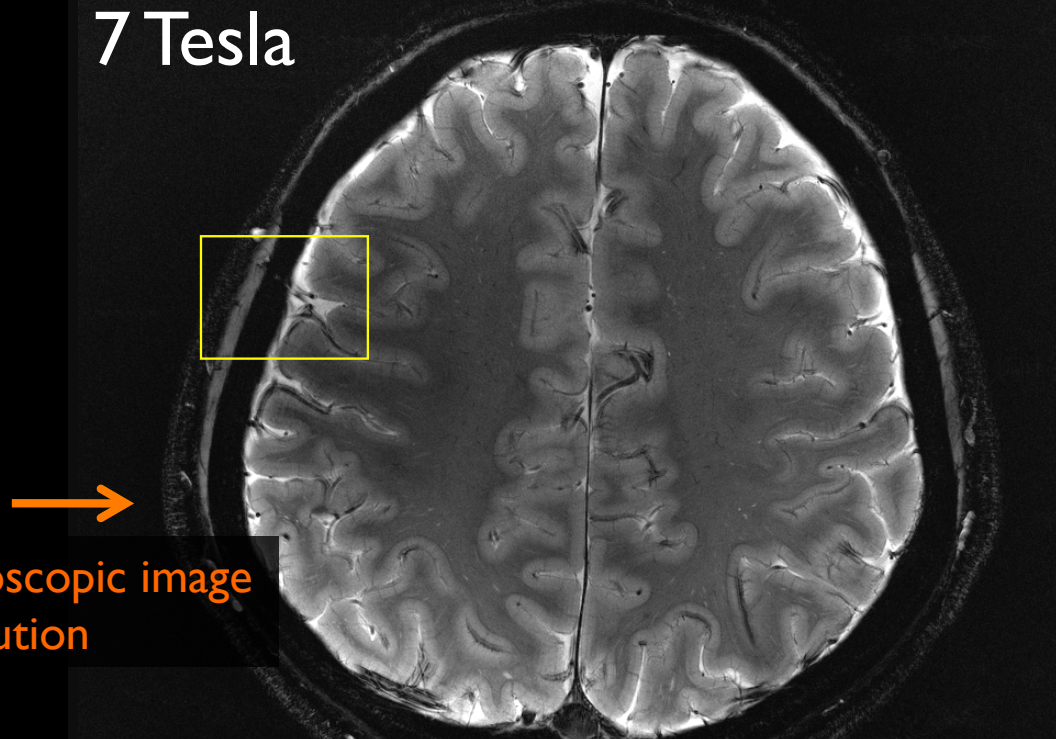
3D image



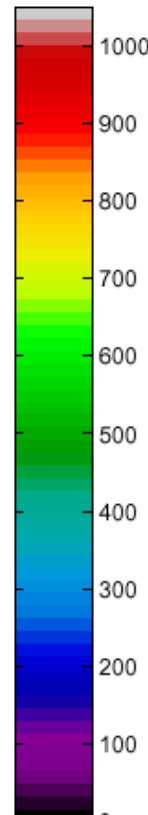
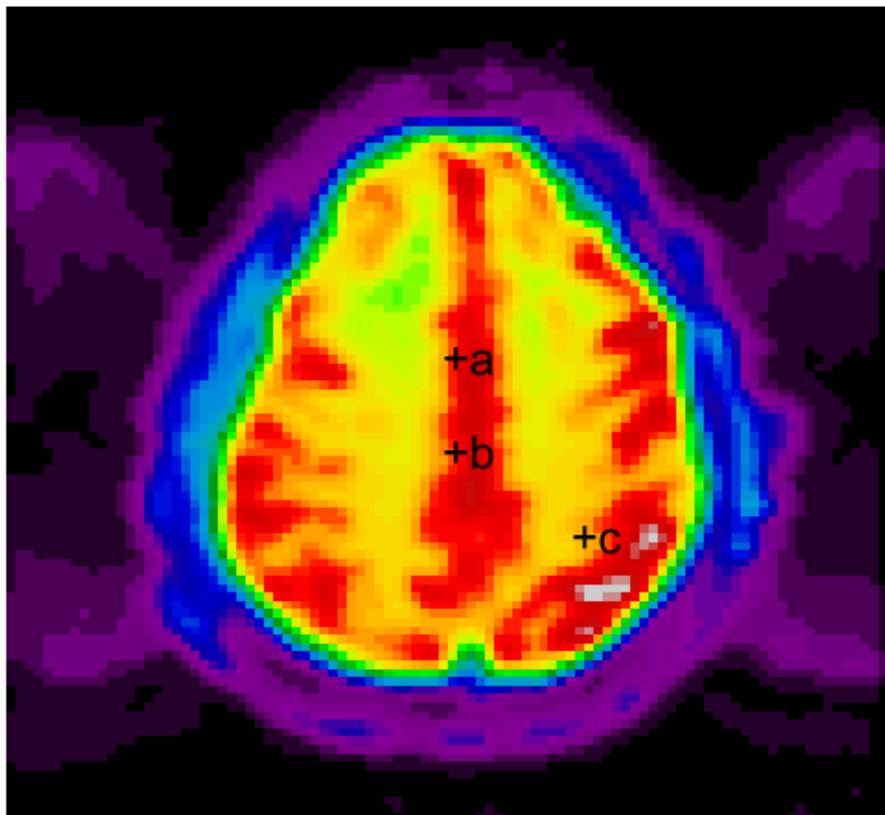
3 Tesla



7 Tesla

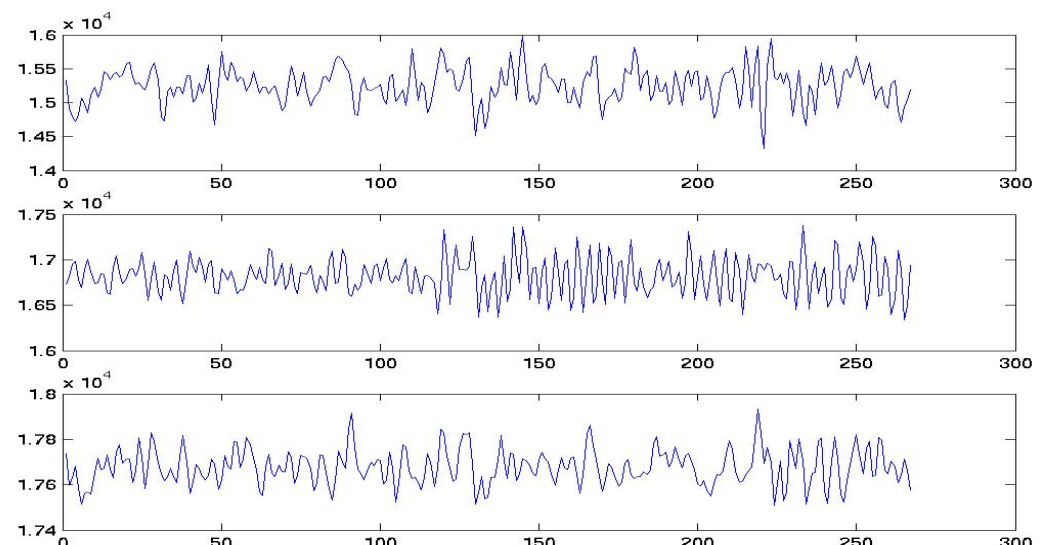


Seo H. Lee, Zang-Hee Cho, Gachon Univ.



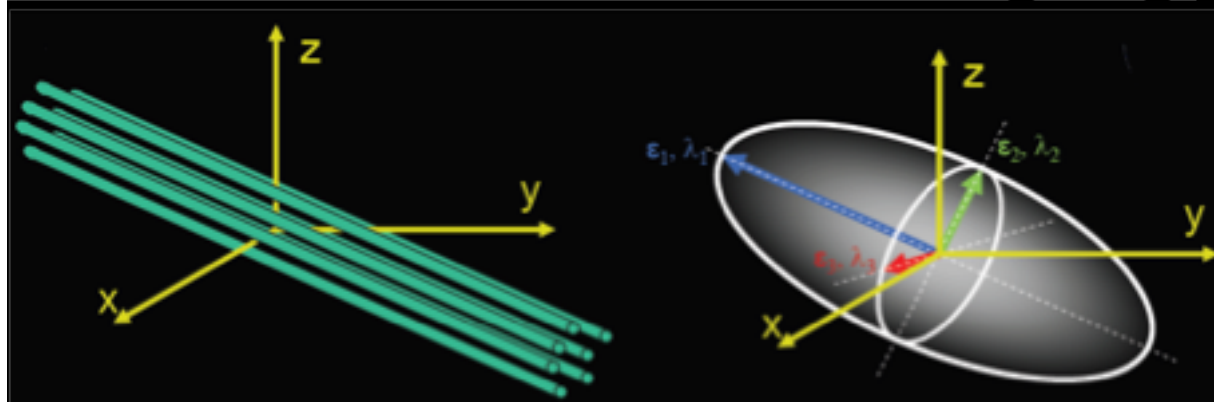
Functional MRI

Measures hemodynamic response (change in blood flow)

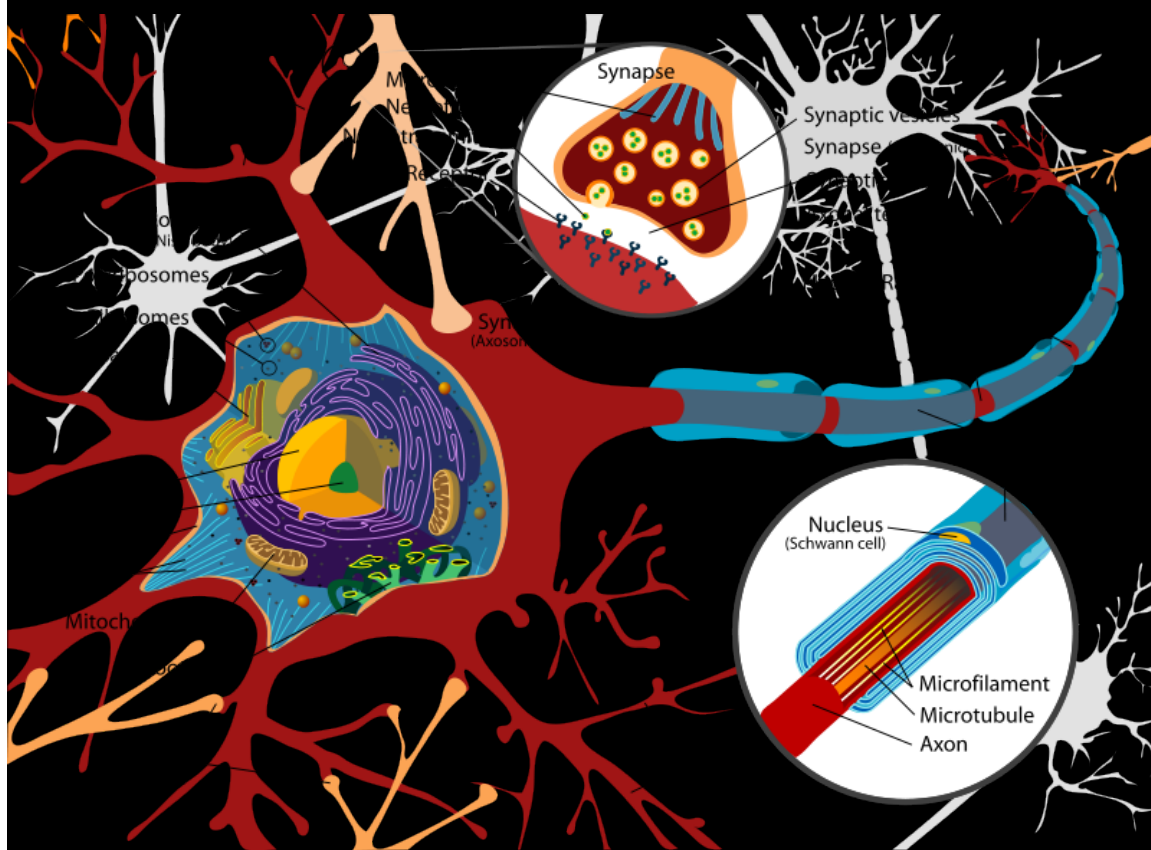


Diffusion Tensor Imaging

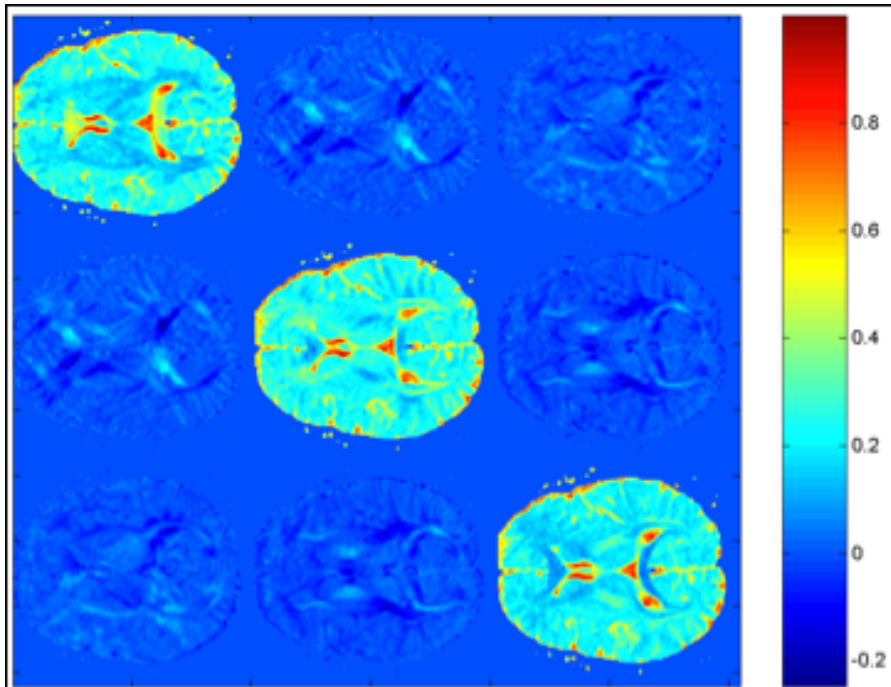
Mori and van Zijl NMR Biomed 2002



The movement of anisotropic water diffusion can be measured using DTI



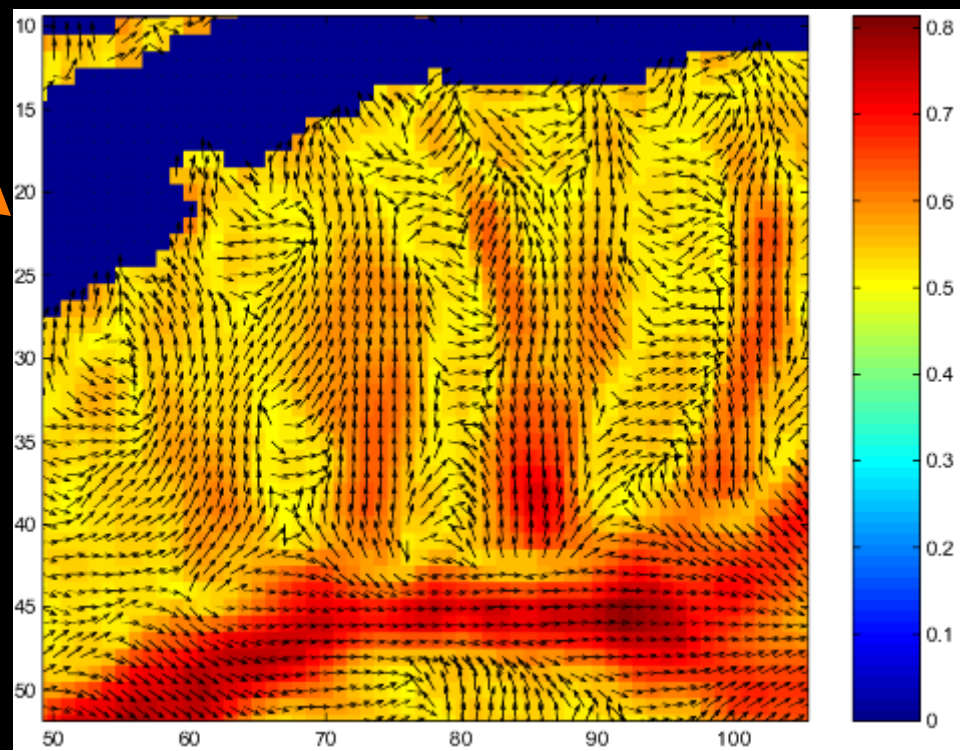
The direction of neuronal filaments in the axon dictates the movement of water diffusion.



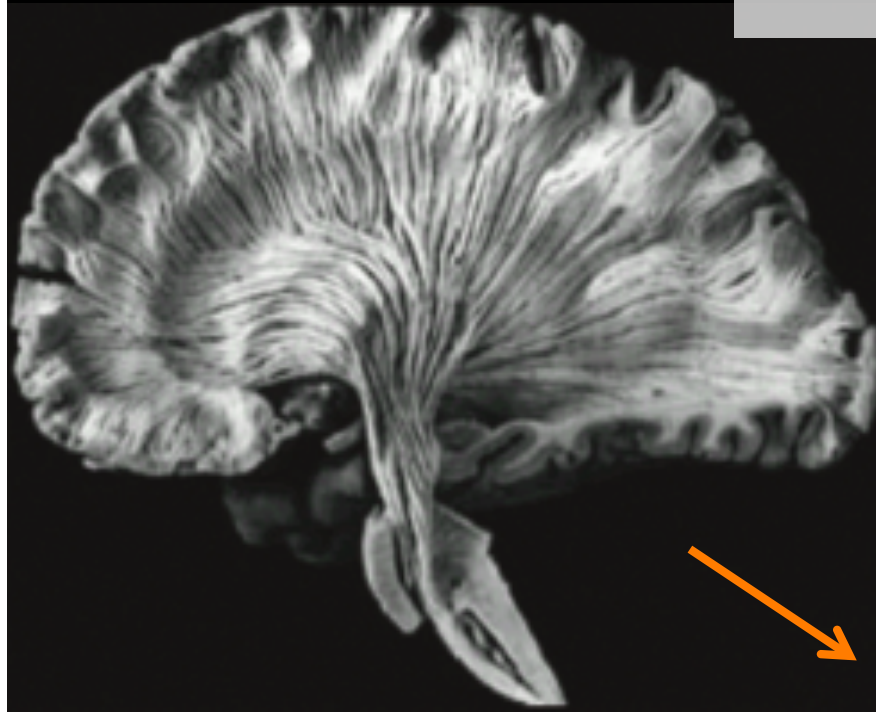
Direction of diffusion is
encoded in 3×3 matrix D
(diffusion tensor)

Principal
eigenvectors of D

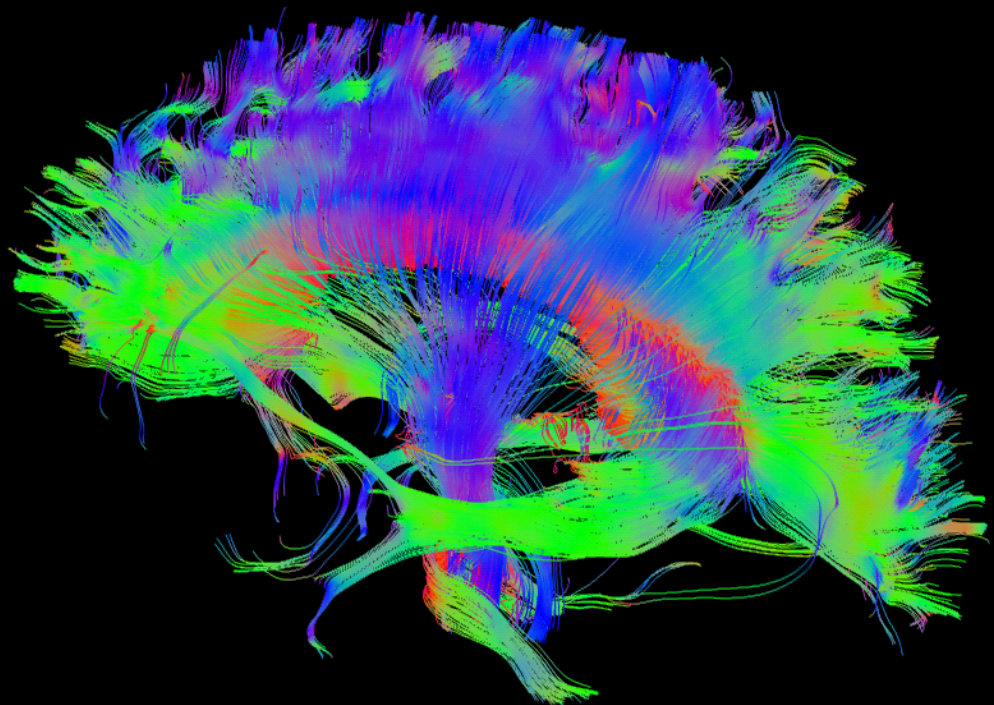
Tractography done using the second order
Runge-Kutta algorithm with TEND (Lazar
et al., HBM 2003)



White Matter Fiber Tractography



Postmortem

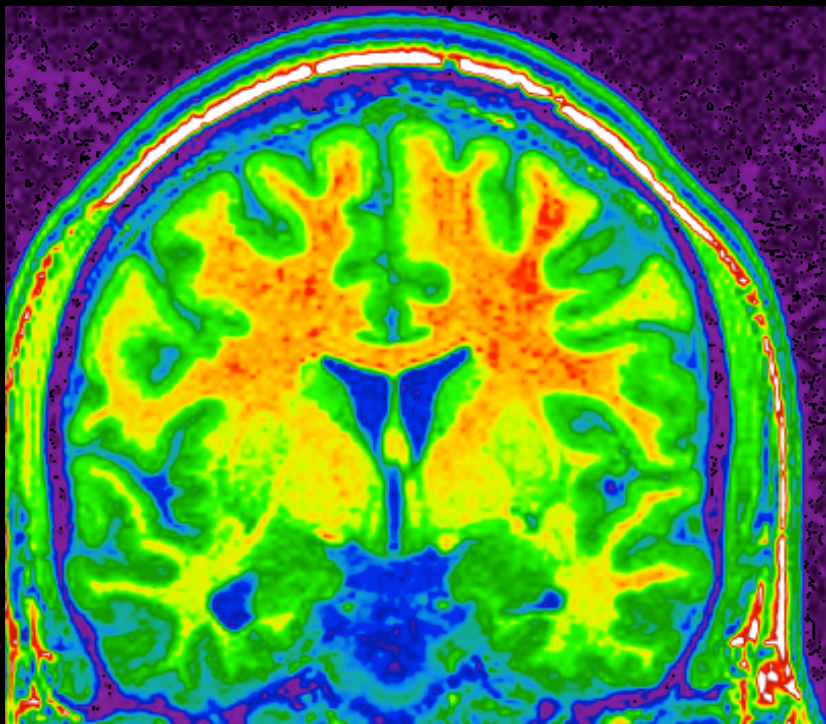


Reconstructed
0.5 million tracts

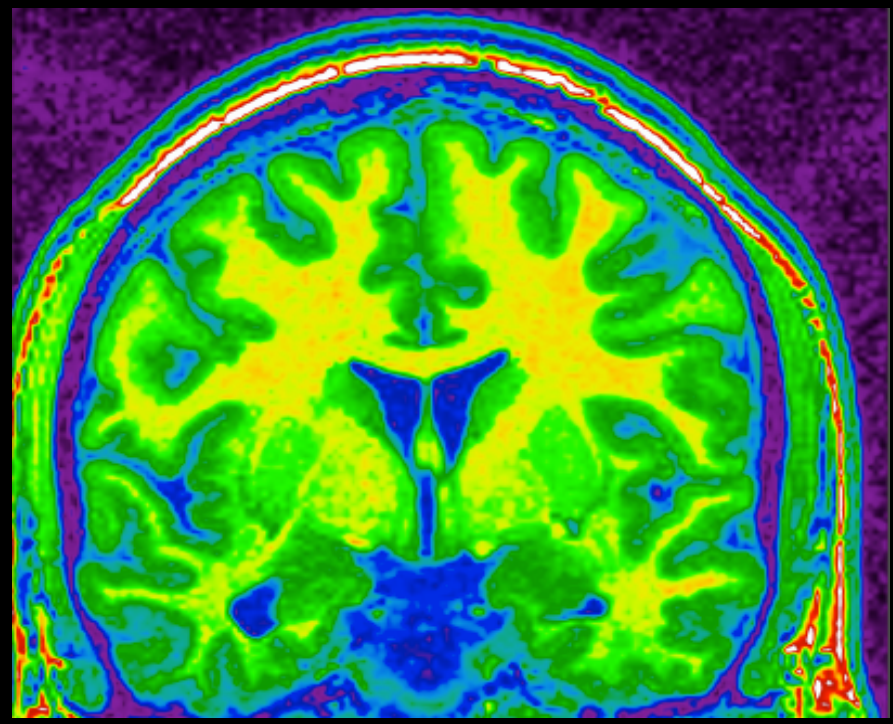
Image, tissue and structure segmentation

Image intensity non-uniformity correction

Original MRI

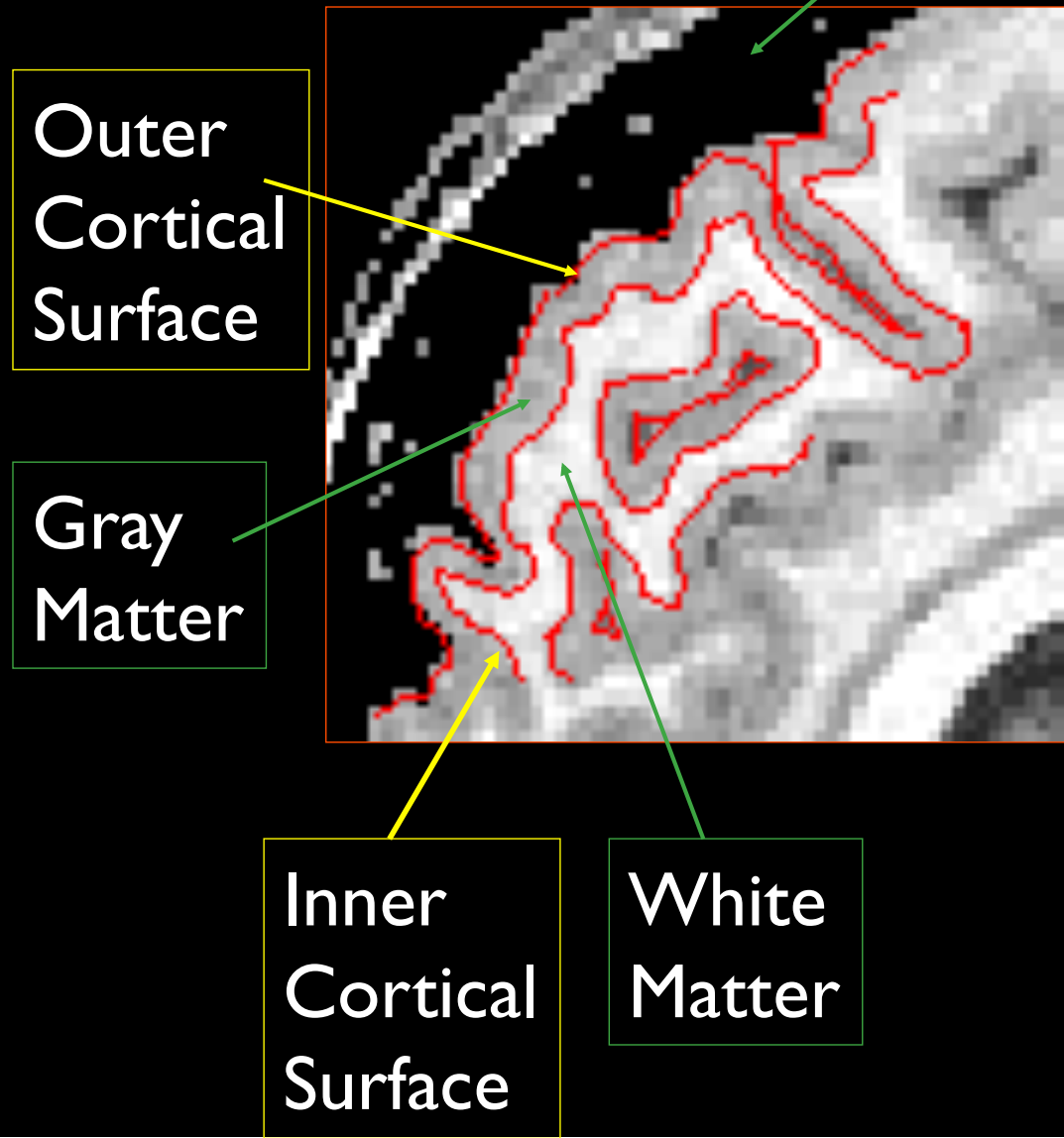


Corrected

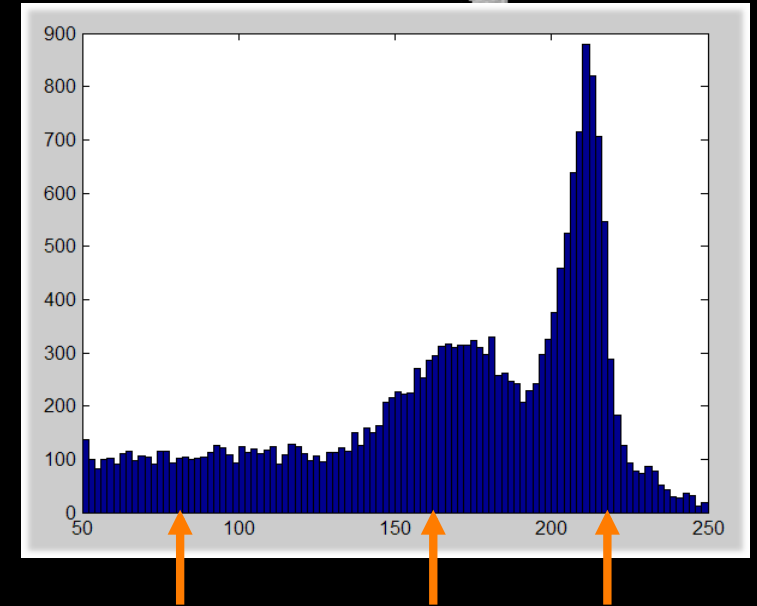


McConnell Brain Imaging Center, MNI

Cortical anatomy



Cerebral Spinal Fluid (CSF)



CSF

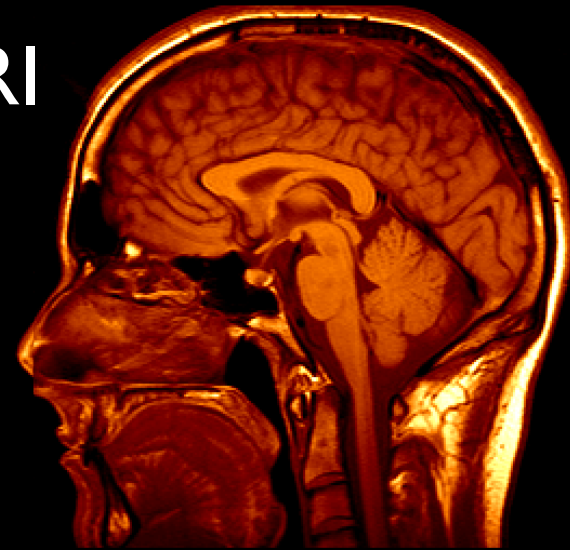
Gray White

Real brain

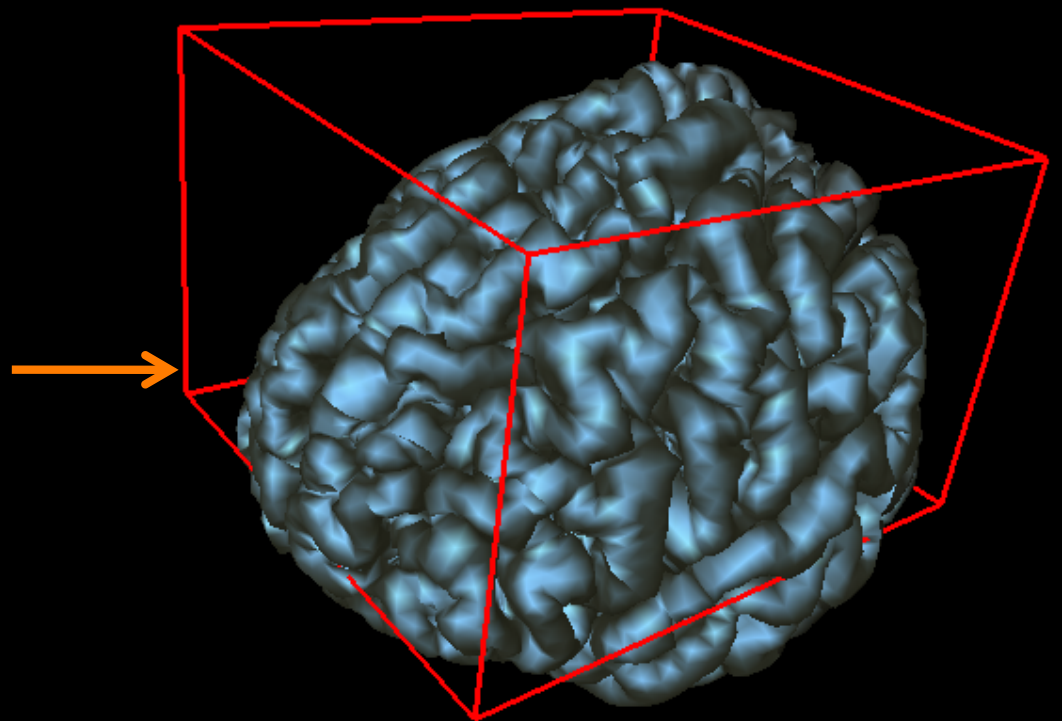
Image & structure segmentation



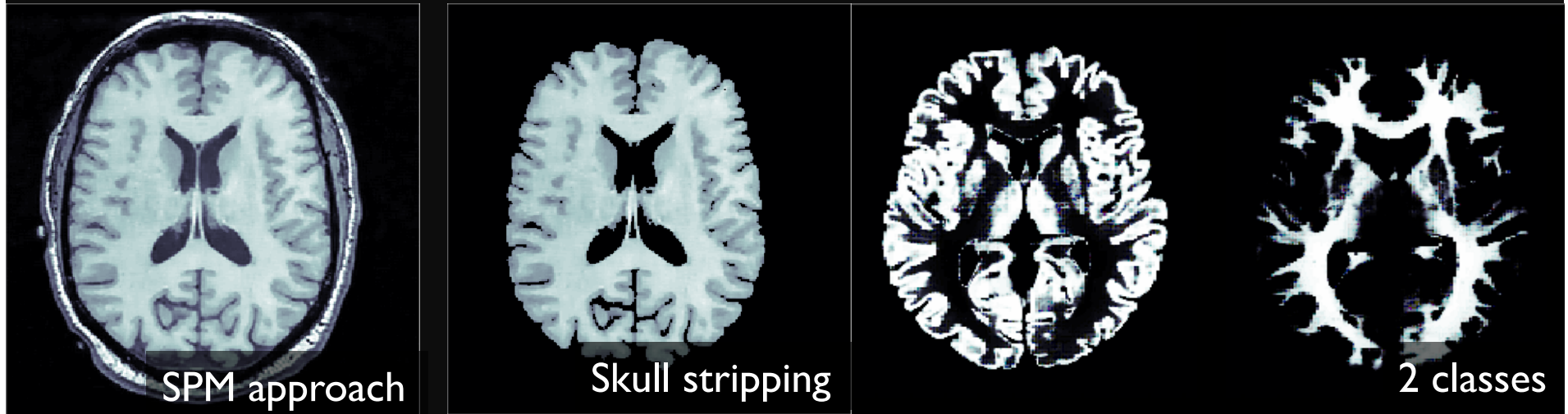
3T MRI



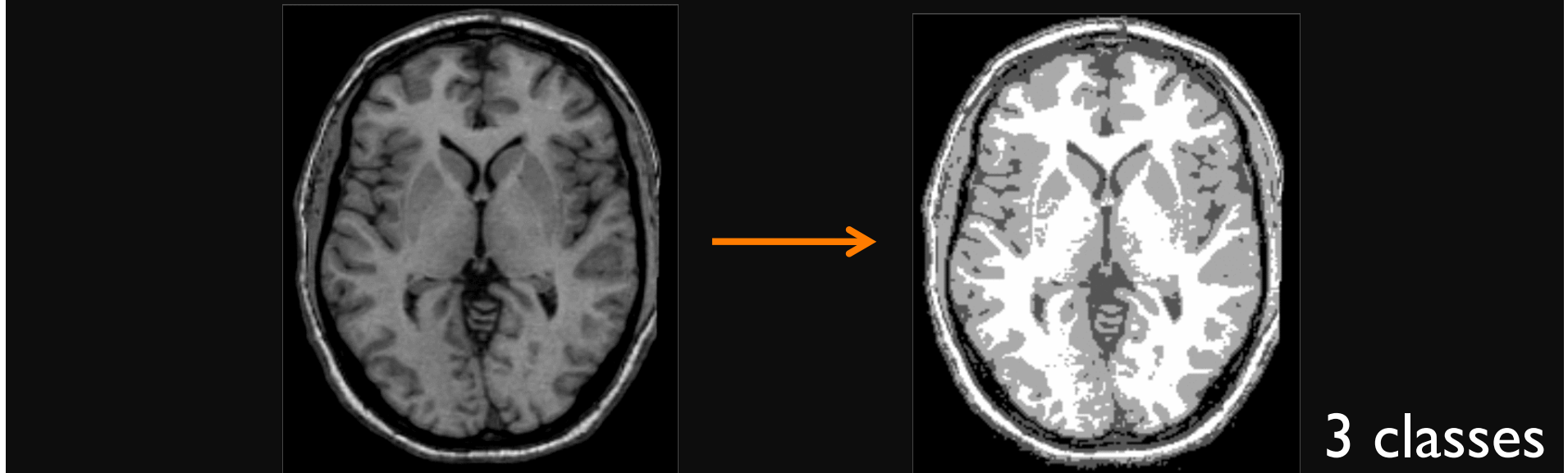
Cortical surface model

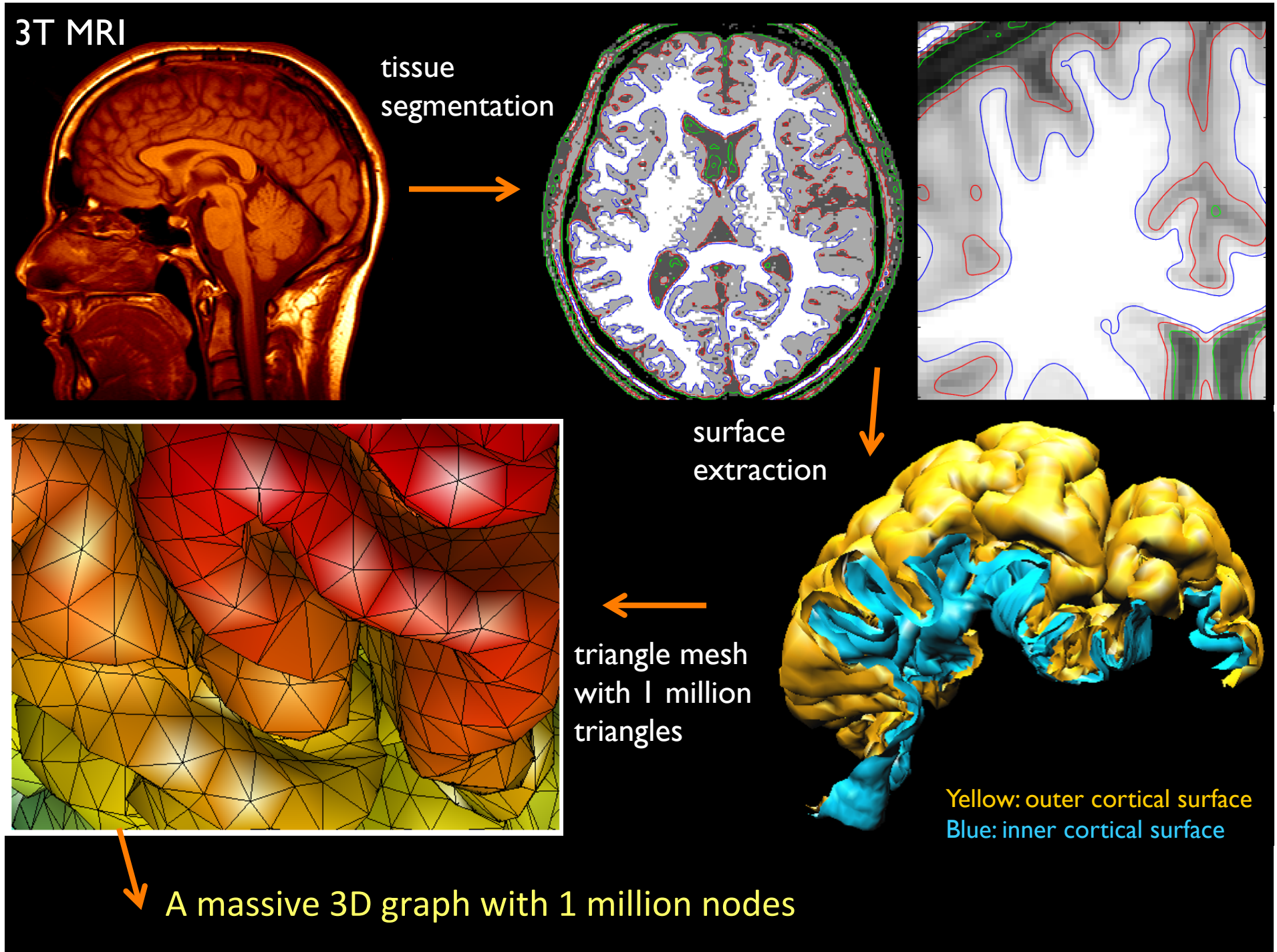


Gaussian mixture modeling

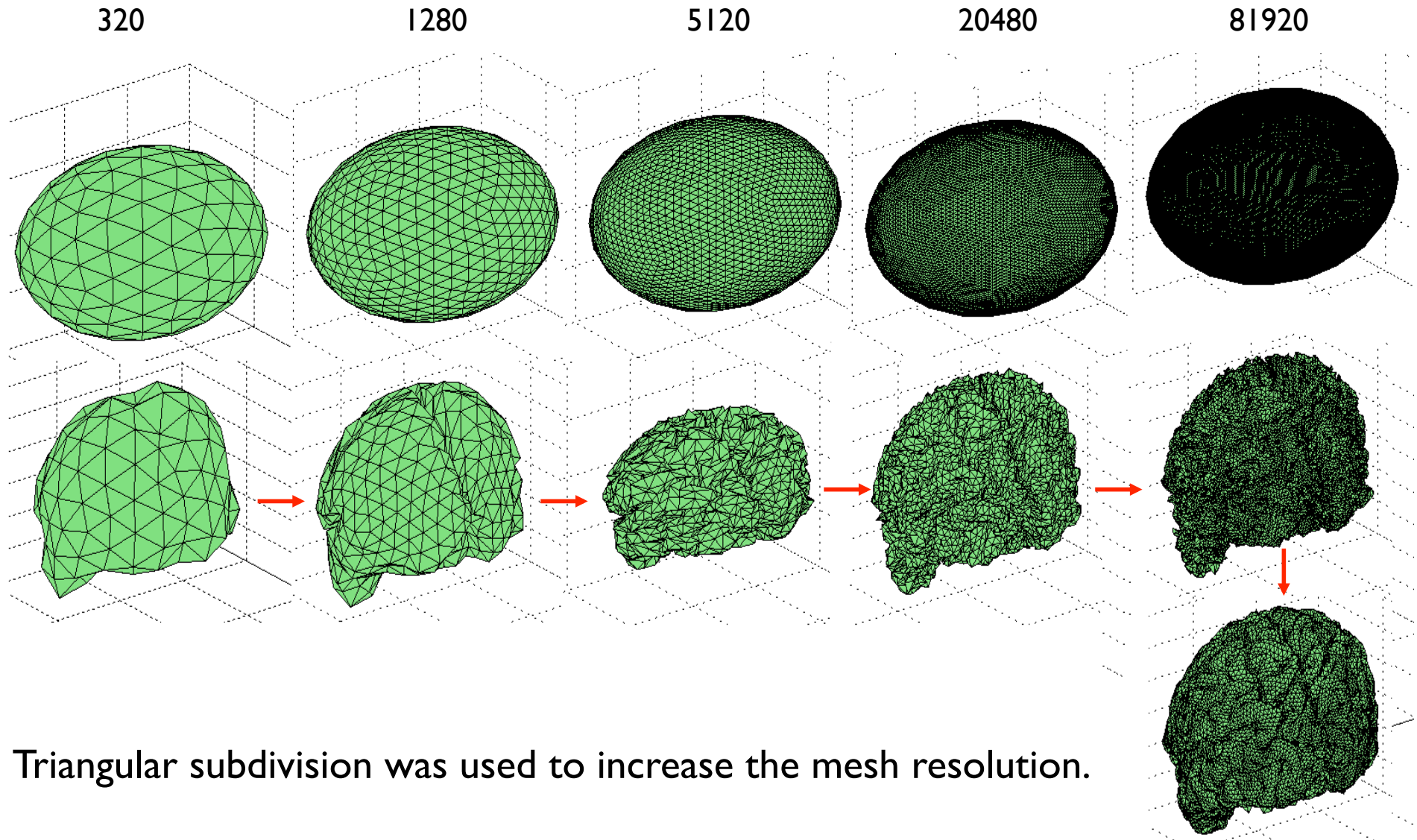


MNI Neural network classifier



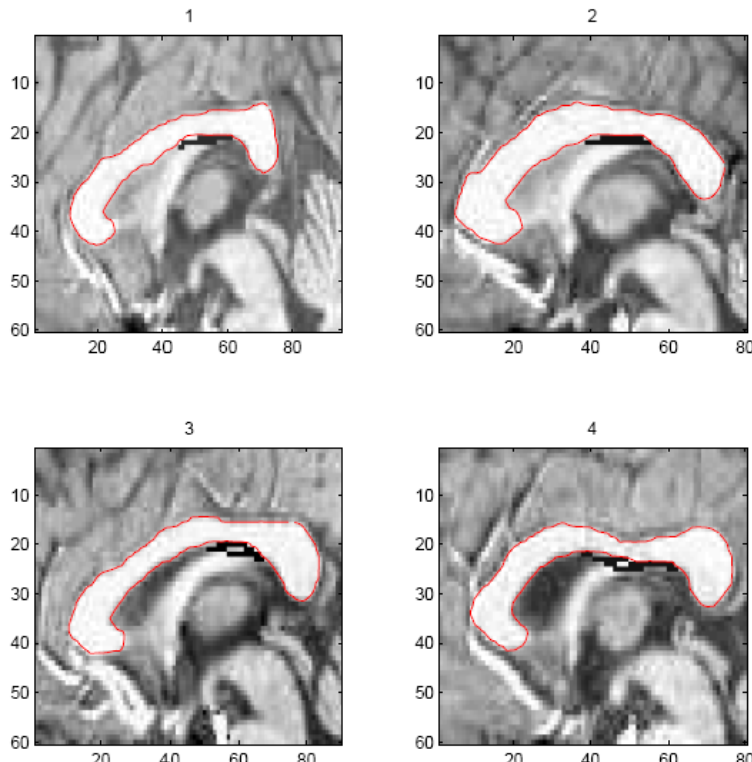


Deformable surface algorithm for cortical surfaces

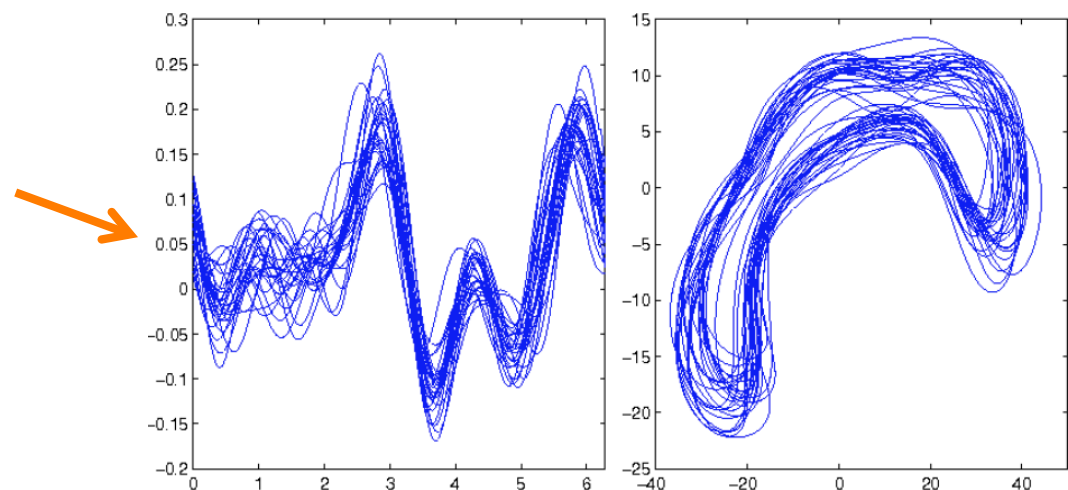


Triangular subdivision was used to increase the mesh resolution.

Active contour (snake) segmentation



Corpus callosum segmentation and modeling

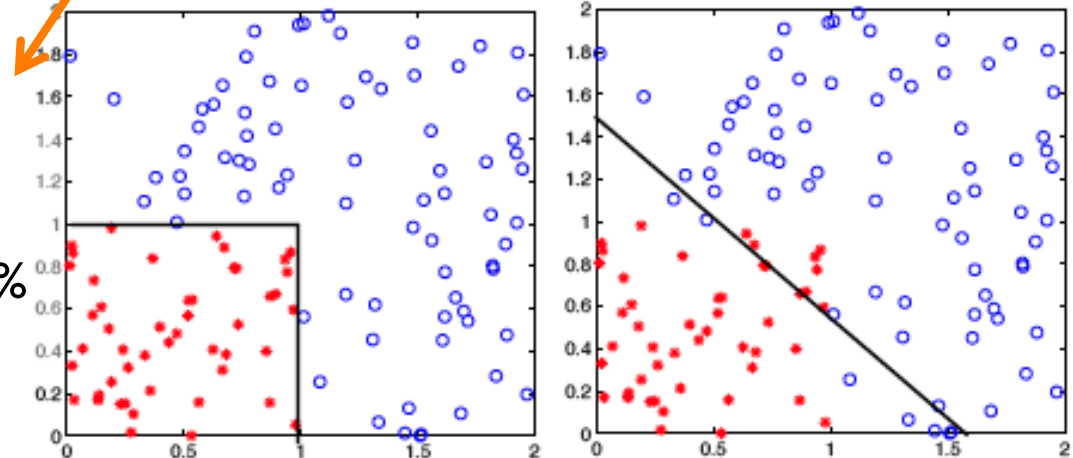


Active contour (snake) segmentation

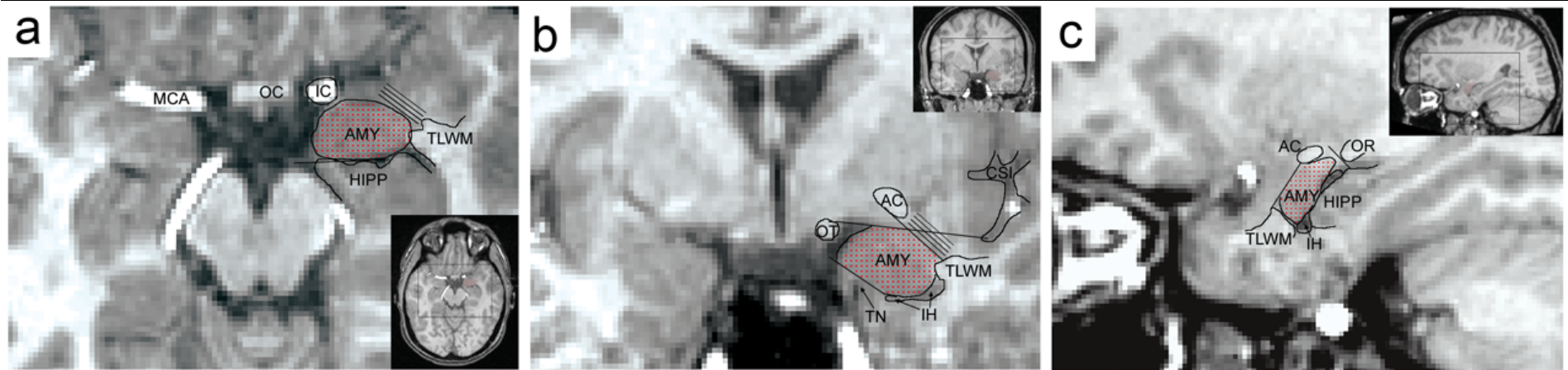
Classification result

Linear discriminant analysis (LDA) 75%

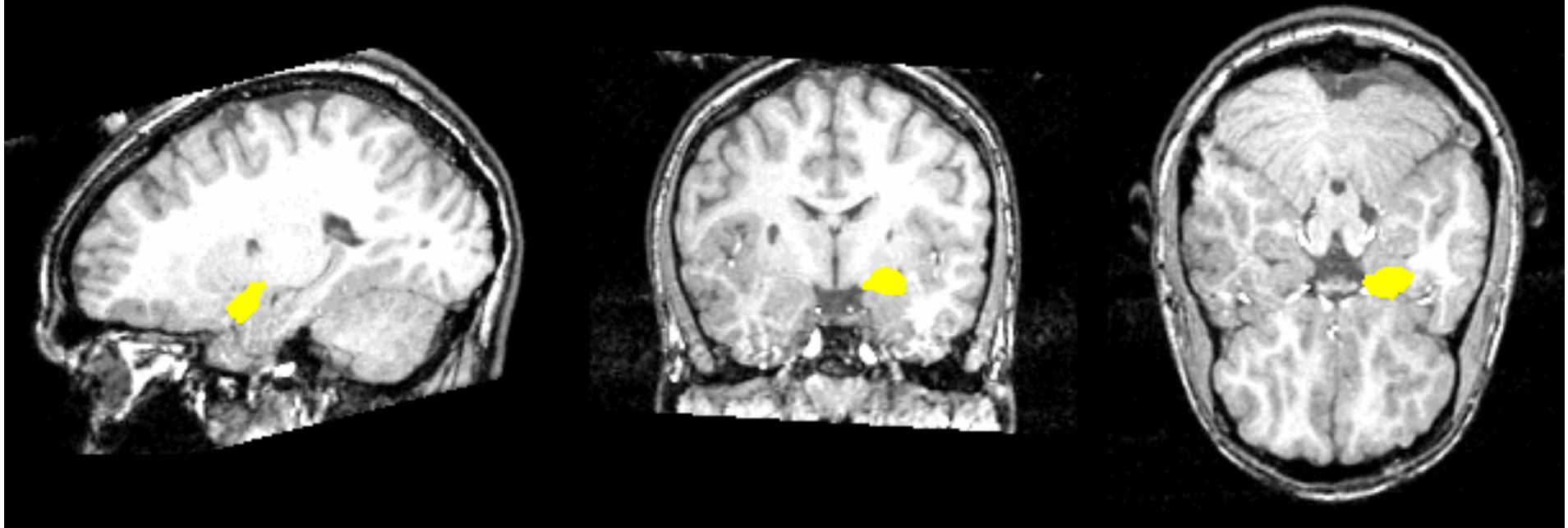
Regression tree 85%



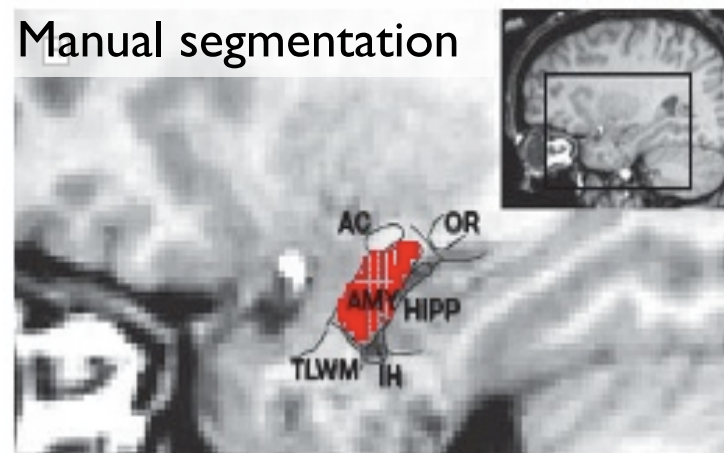
Manual segmentation



Left amygdala



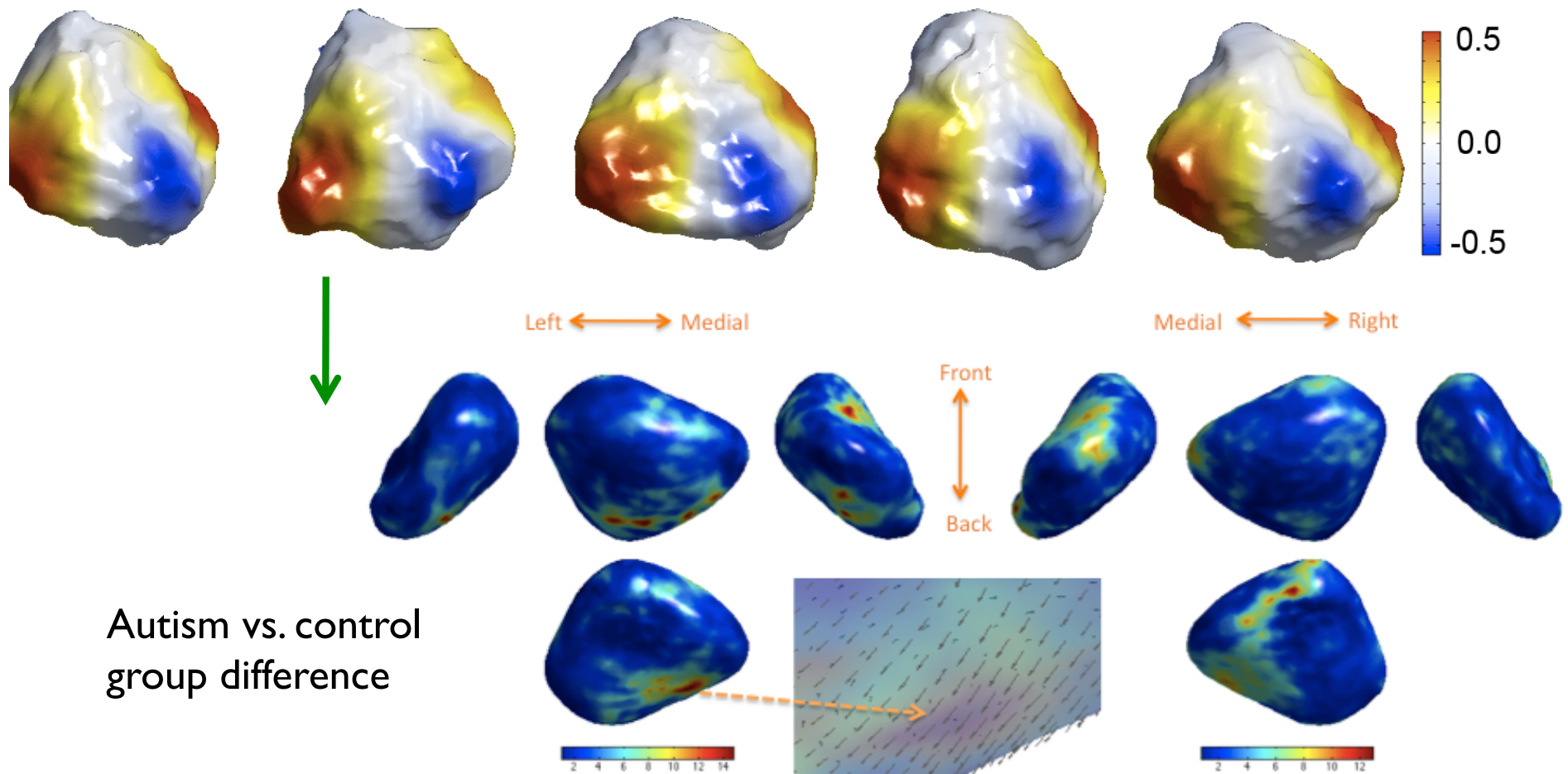
Manual segmentation



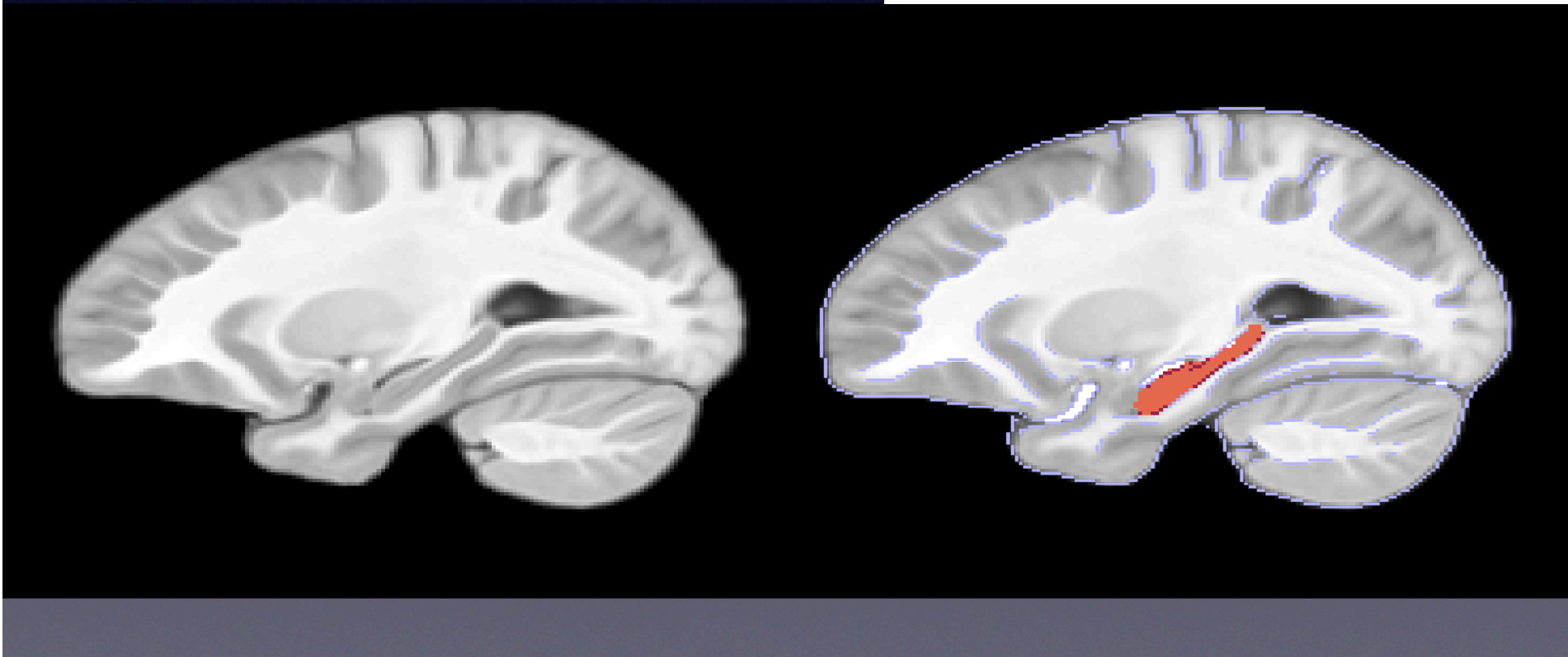
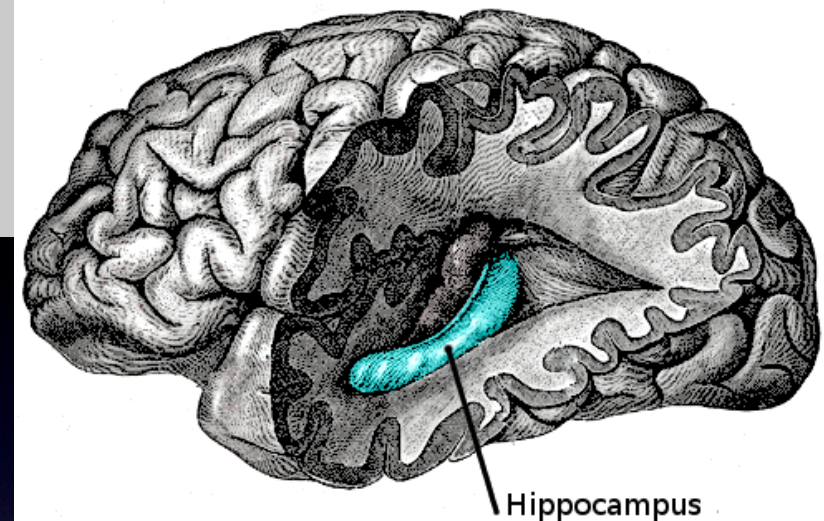
Amygdala shape modeling

Chung et al. 2010, *NeuroImage*

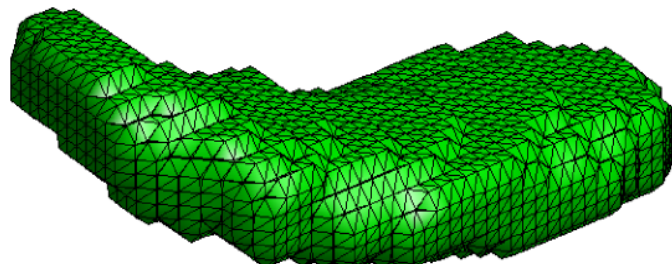
Amygdala registration via spherical harmonic representation



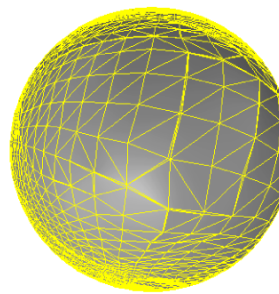
Manual hippocampus segmentation on MRI template



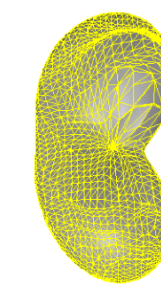
Hippocampus segmentation and modeling



Manual segmentation



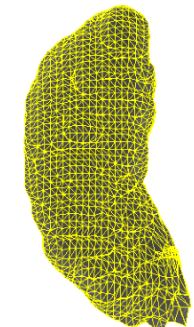
degree 1



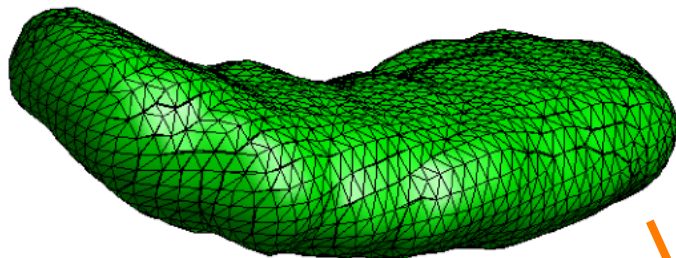
degree 5



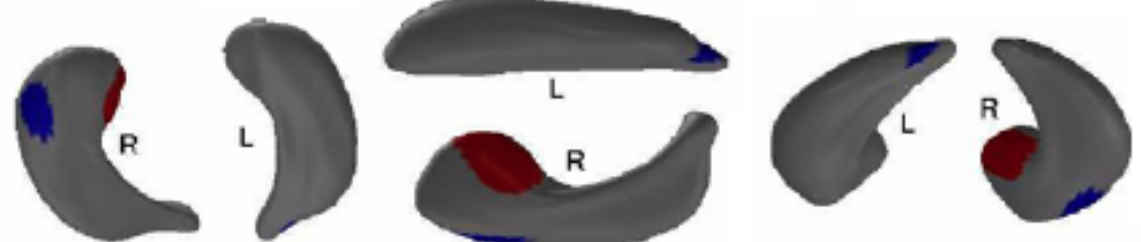
degree 10



degree 50



Parametric model

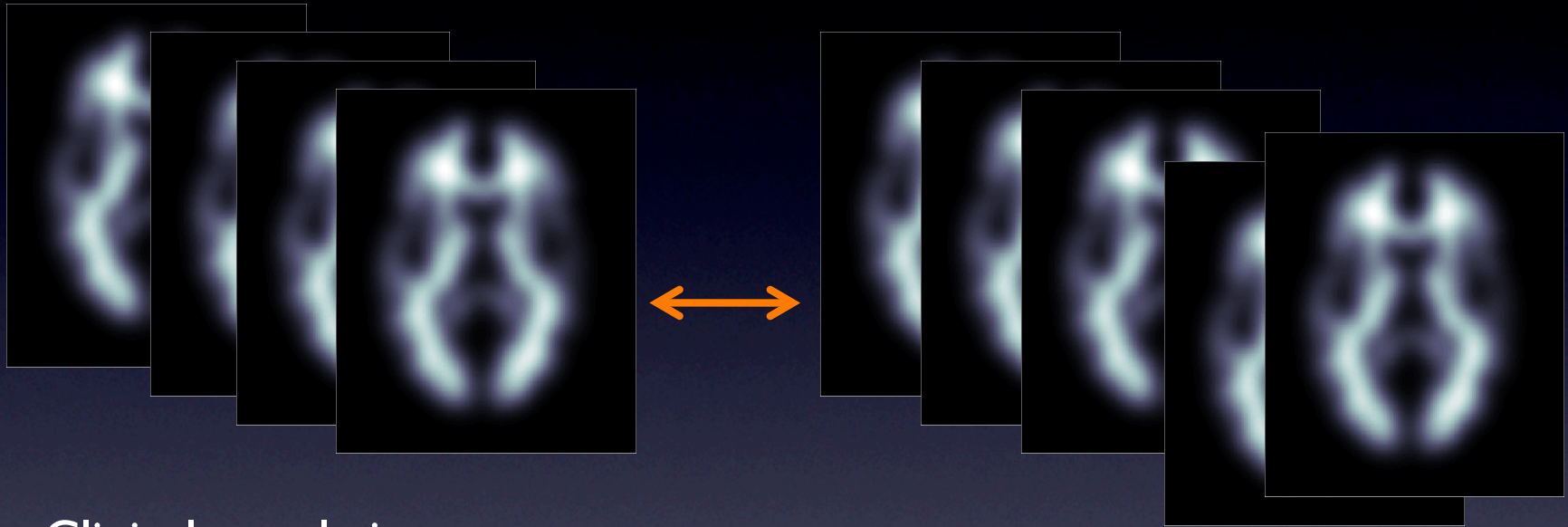


Mild cognition impairment (MCI) - control at $p=0.05$

Image registration

Typical question in computational neuroanatomy

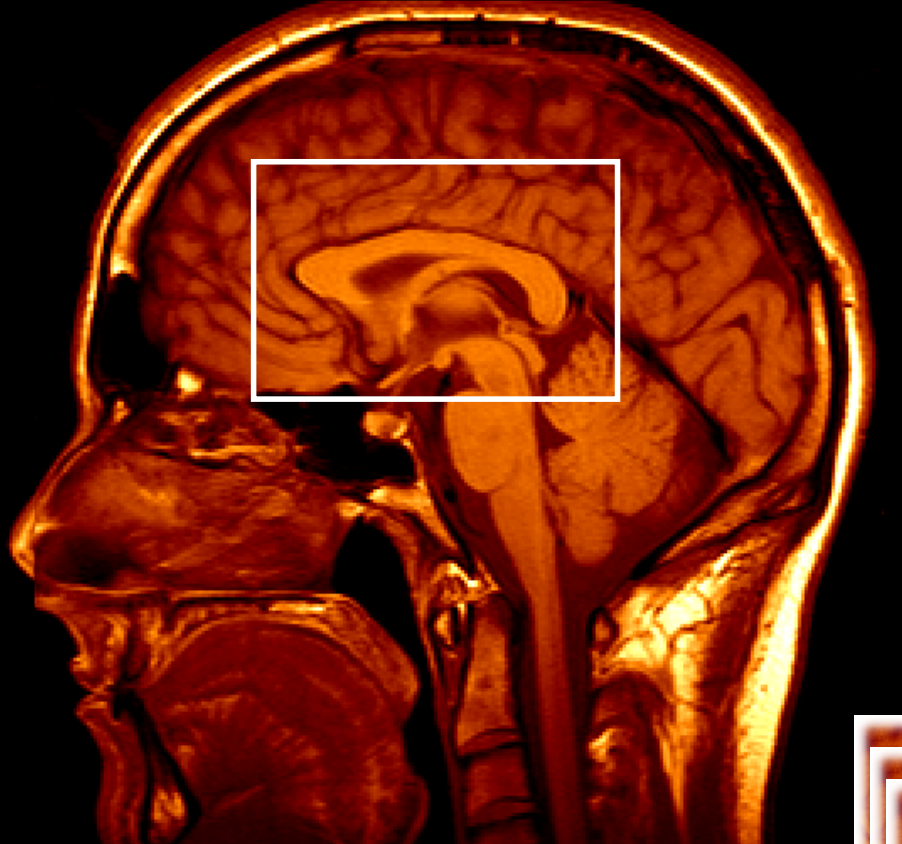
Given a collection of images



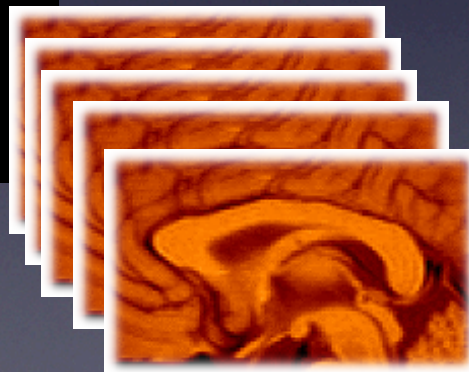
Clinical population:
autism, Parkinson's decease

Normal controls

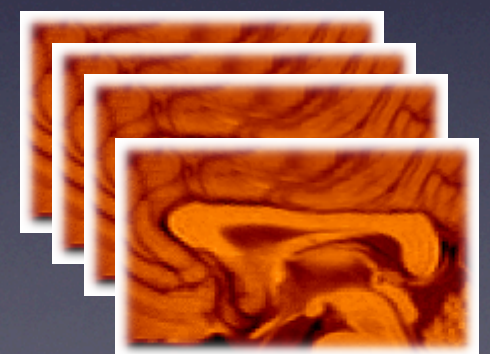
- I. Do brains differ in shape ?
2. How they differ?



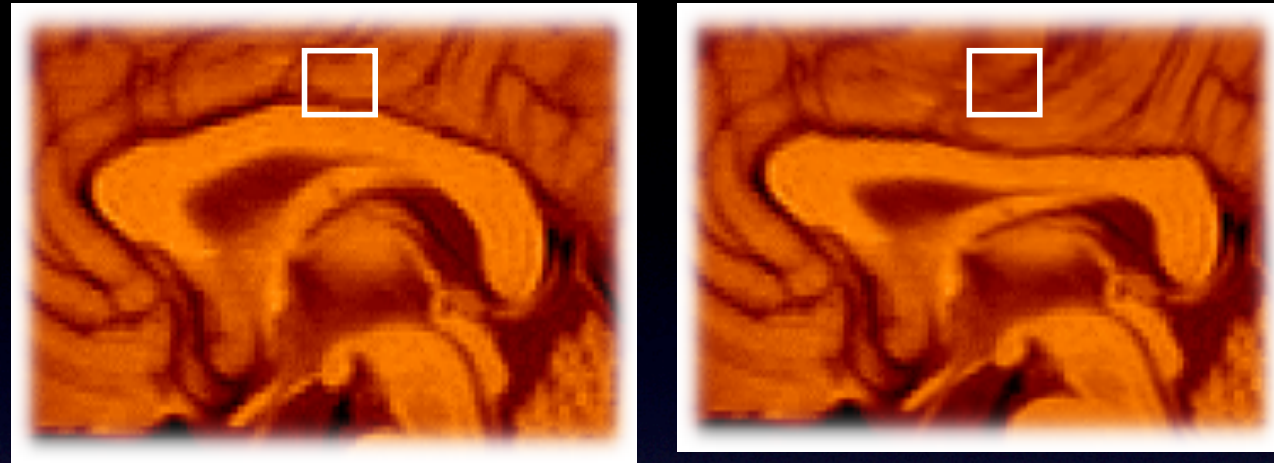
Each subject has different brain shape. So how do we compare shape difference across subjects?



Group 1



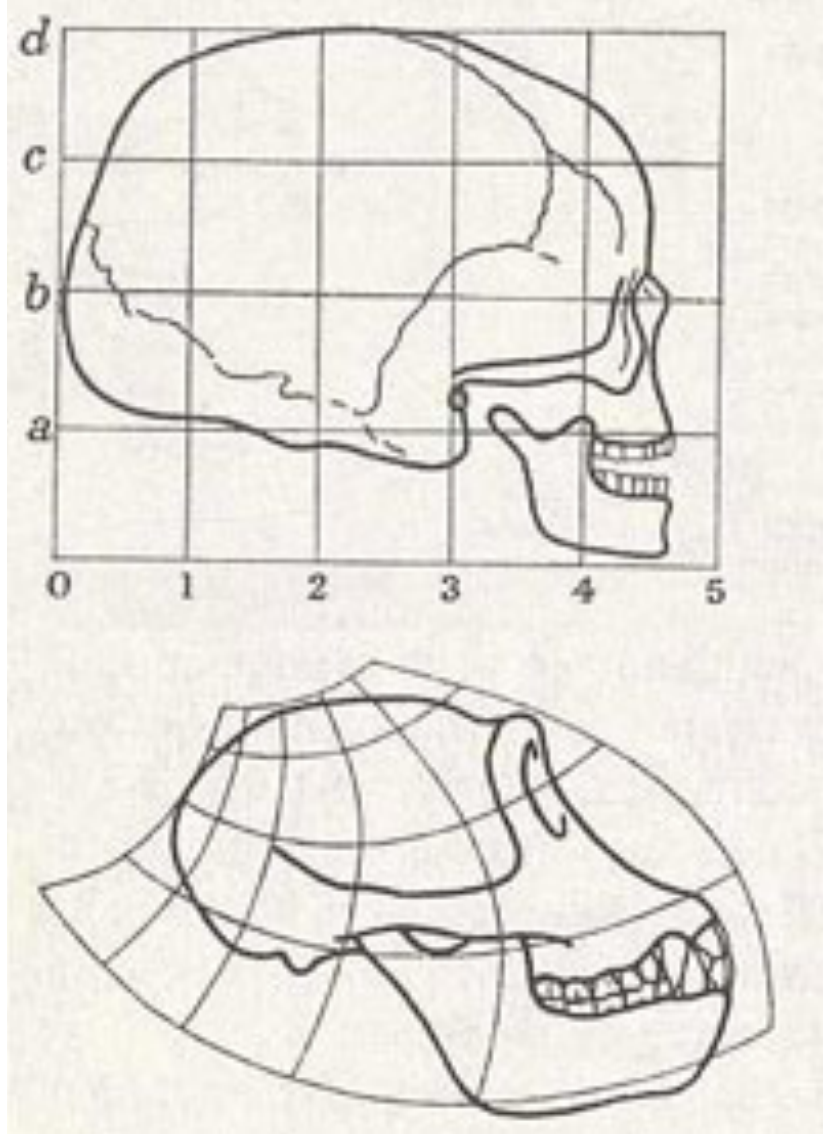
Group 2



Direct voxel-to-voxel comparison causes anatomical mismatching.

Image registration: The aim of image registration is to find a smooth one-to-one mapping that matches homologous anatomies together.

D'Arcy Thompson 1860-1948



figuratively speaking, the 'i

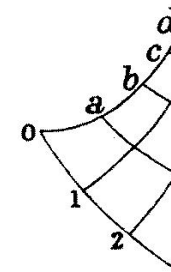


Fig. 178. Co-ordinates on the Cartesian

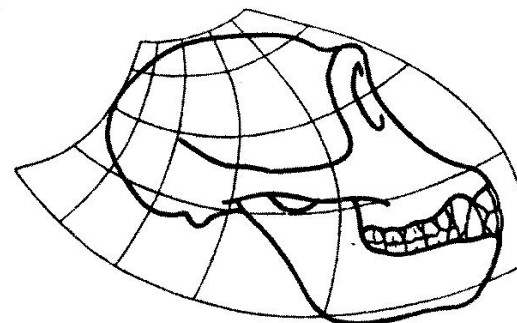
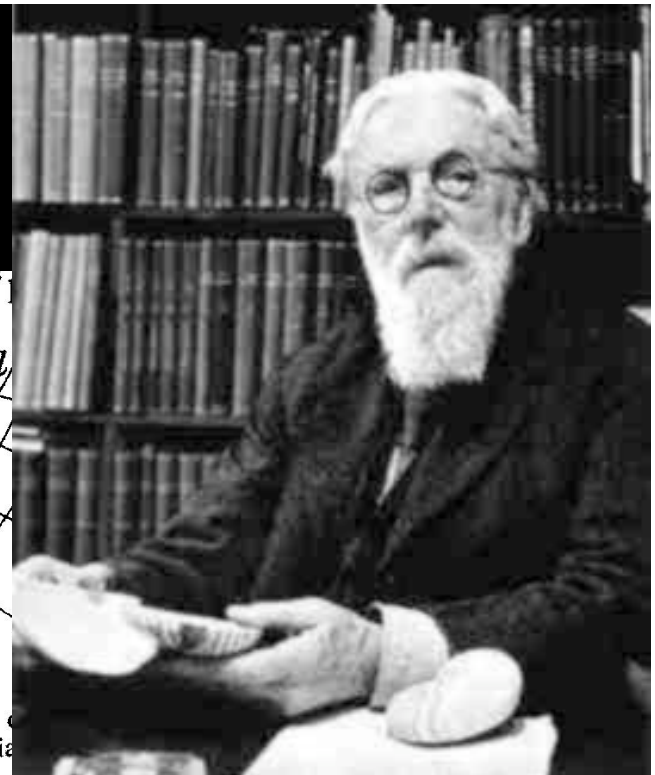


Fig. 179. Skull of chimpanzee.

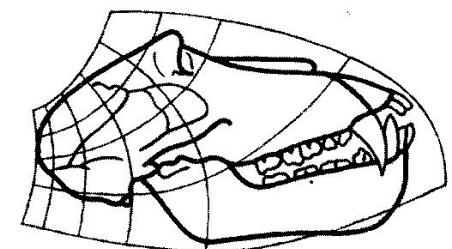


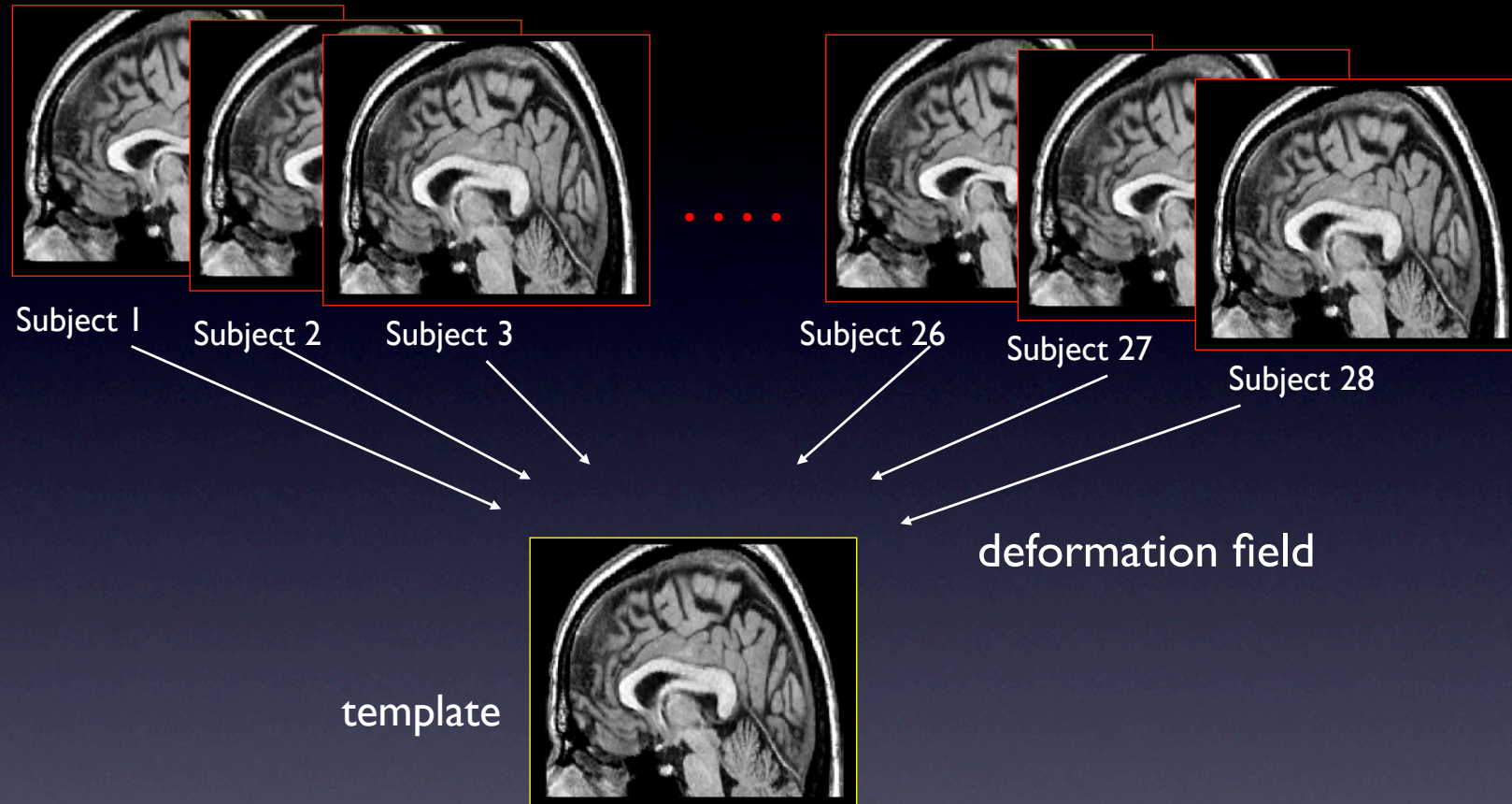
Fig. 180. Skull of baboon.

diagram
I have sh
is obviou
differs or
anthropo

On Growth and Form
D'Arcy Thompson

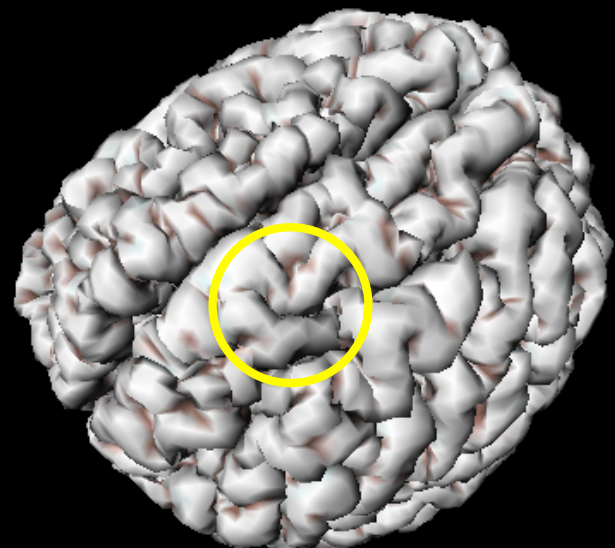
In Fig. 180
oon, and it
order, and
ion.¹ These
another by

Deformable template framework

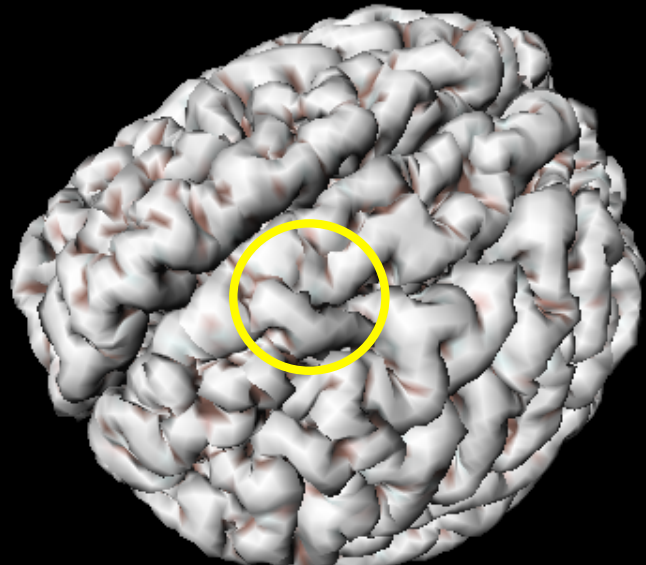


MRIs will be warped into a template and anatomical differences can be compared at a common reference frame.

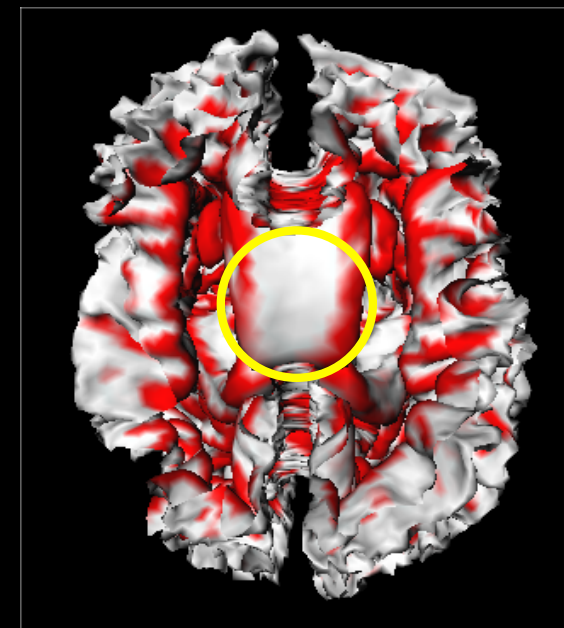
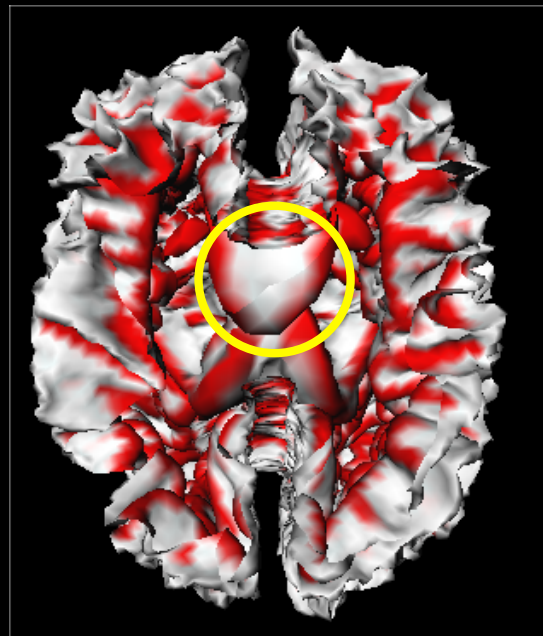
Motivation for 2D cortical surface matching



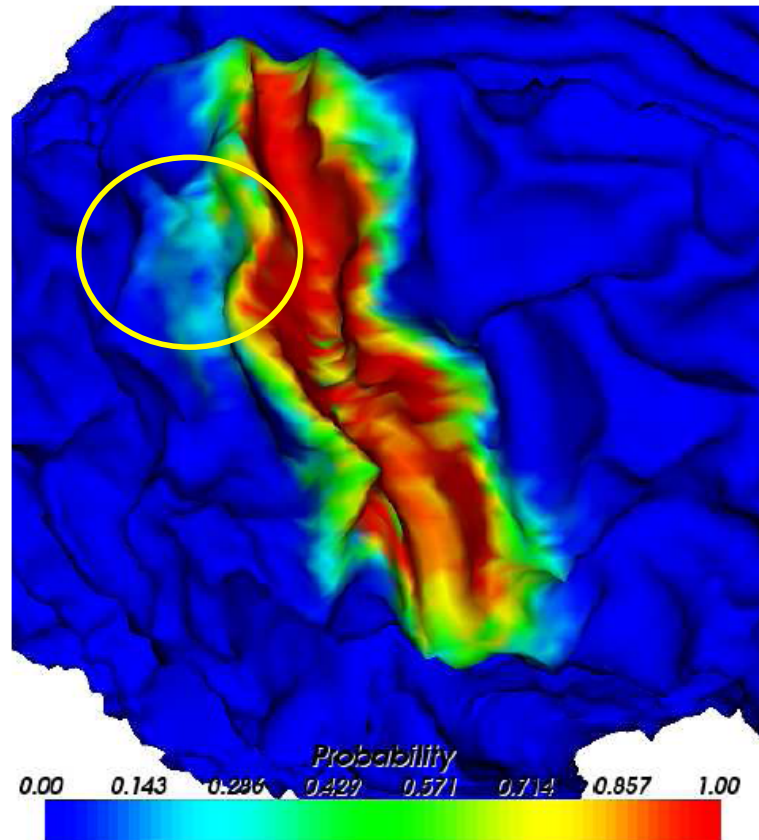
14 year old



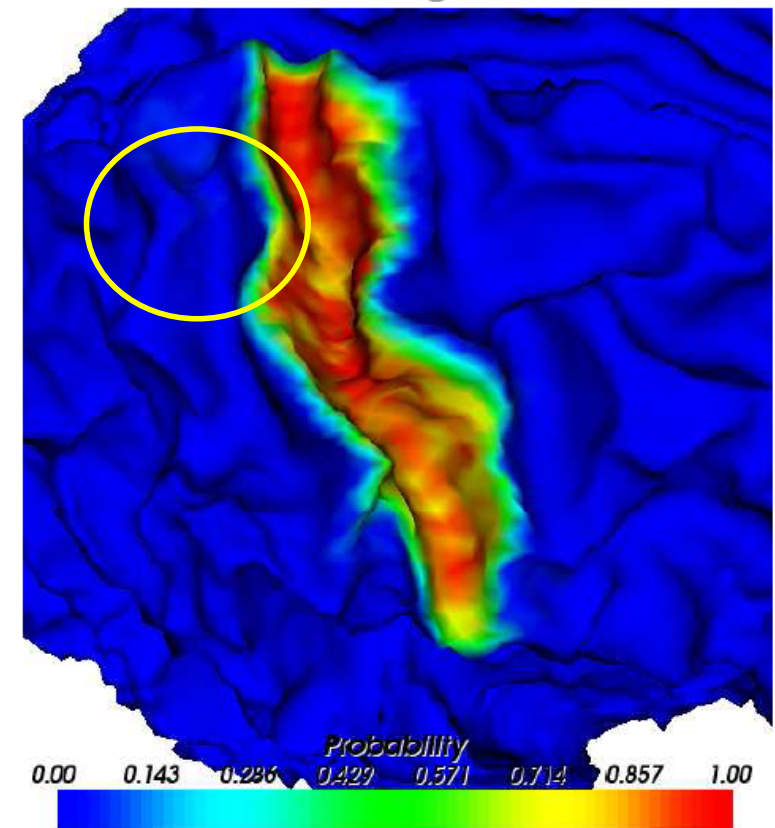
19 year old



Probability of matching in right central sulcus



3D volume registration

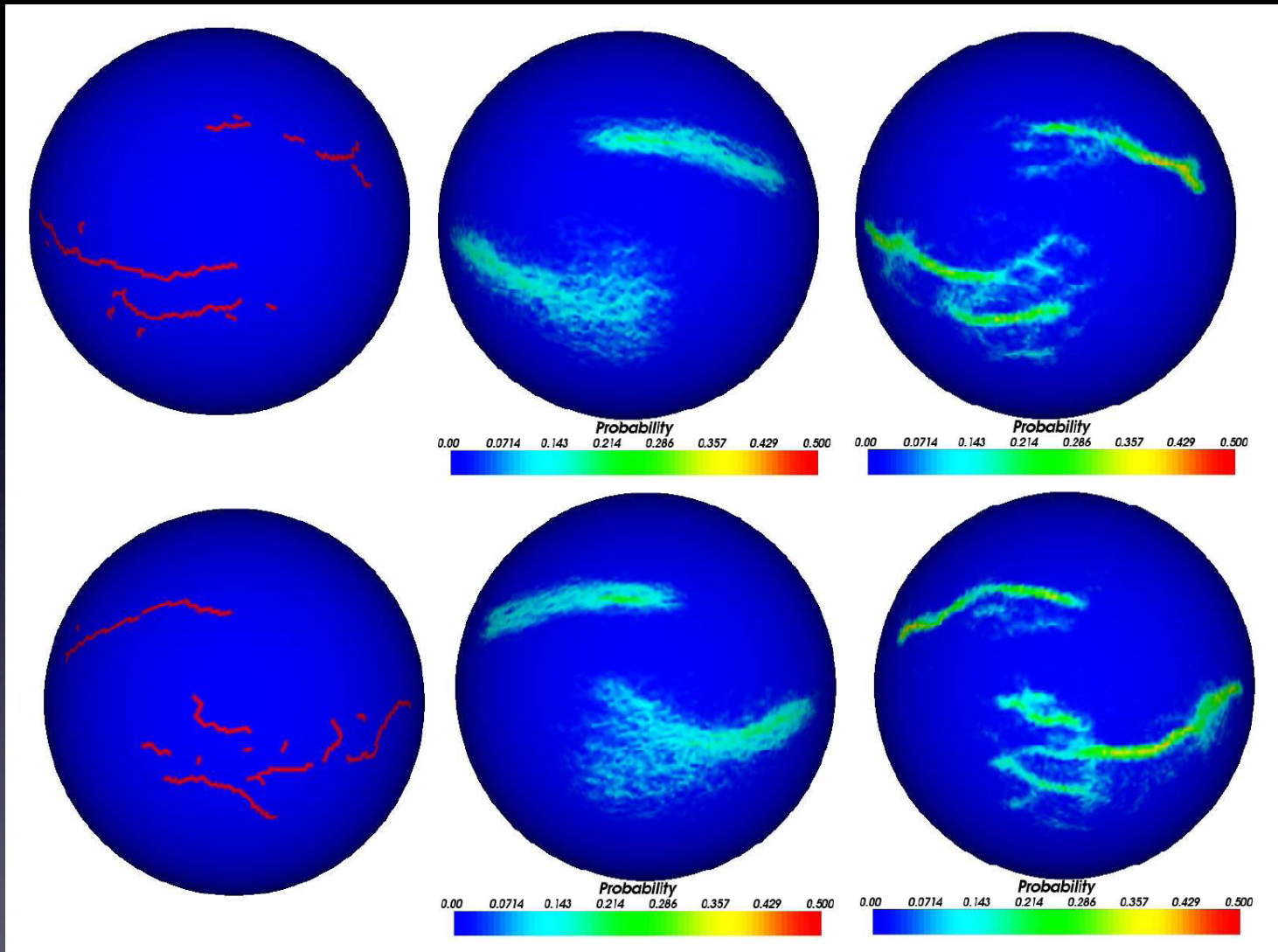


2D surface registration

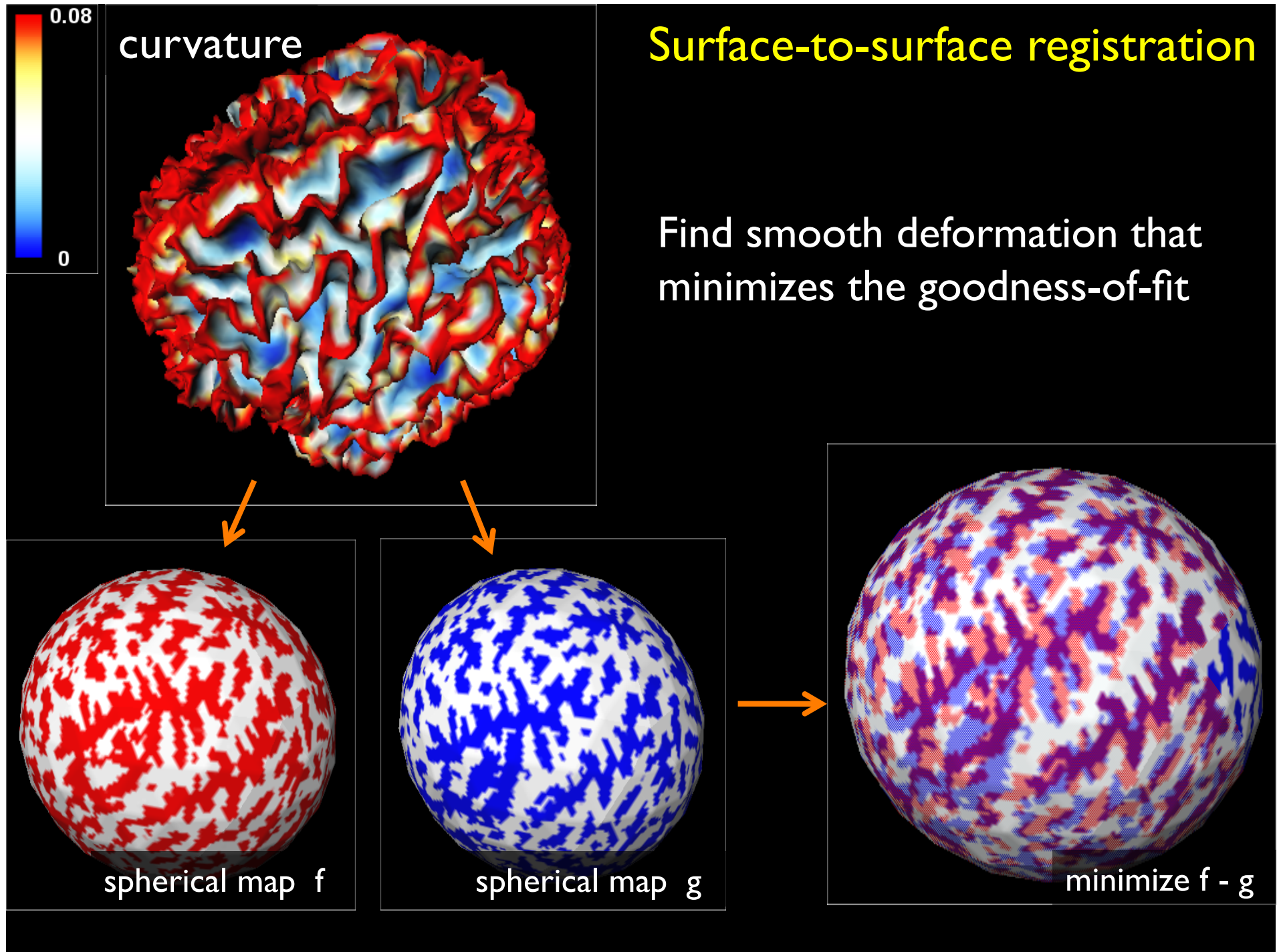
Chung et al., 2005 NeuroImage

Validation of surface registration (149 subjects)

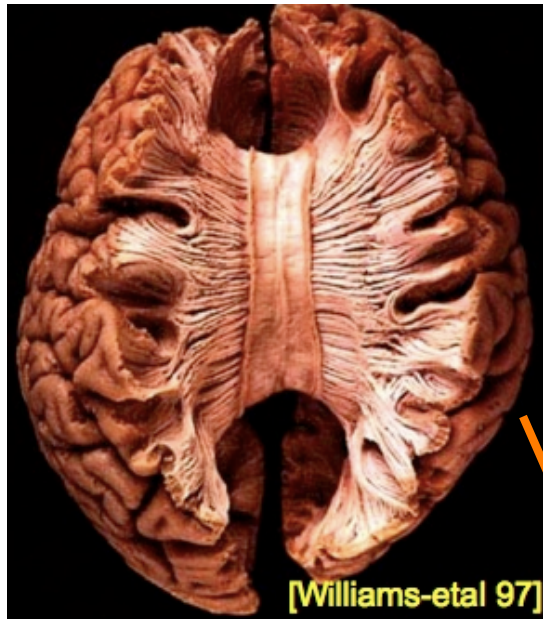
Central &
temporal
sulci



NeuroImage (2005)



Shape representation and modeling



DTI white matter fiber tracts

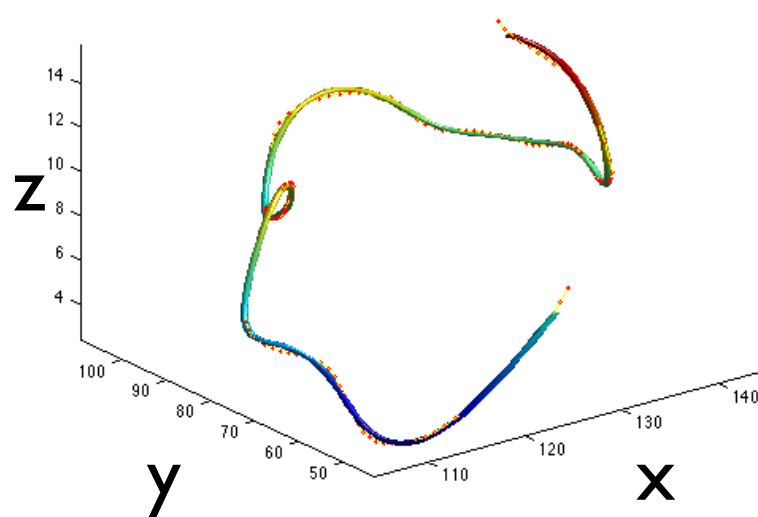
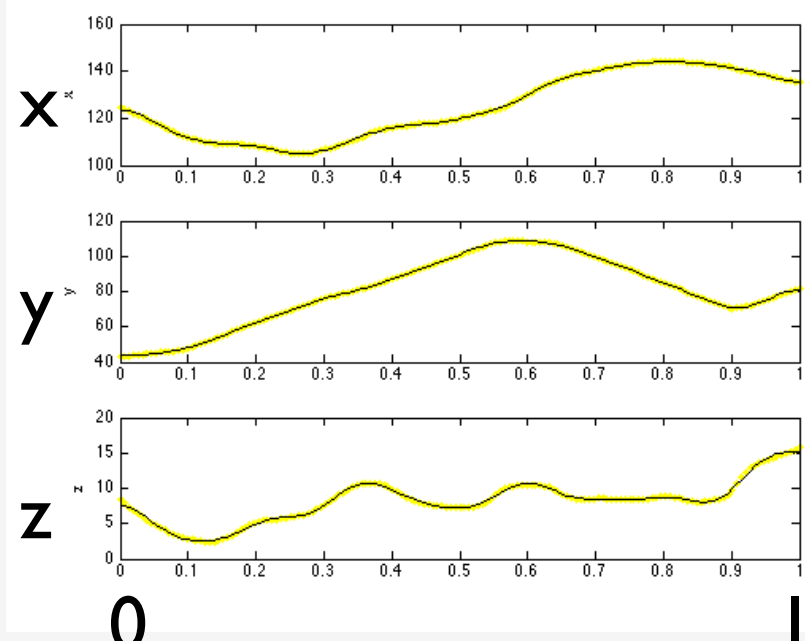
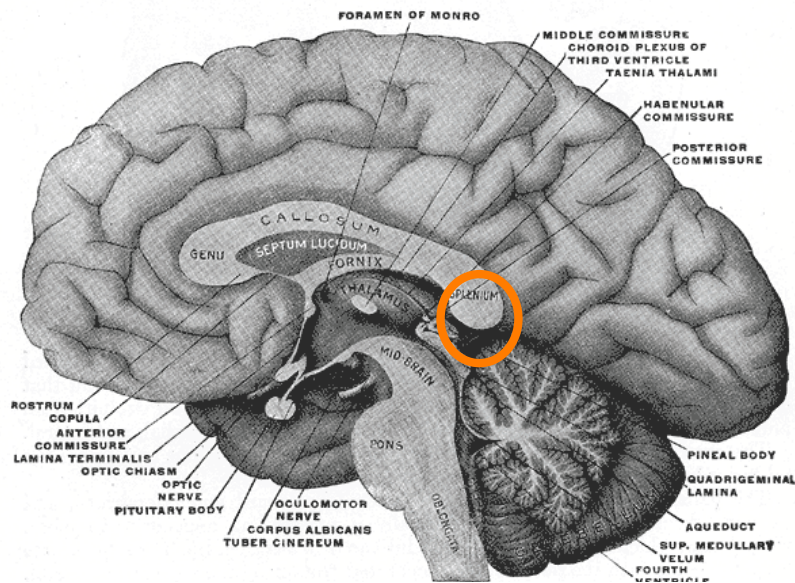


Image acquisition
& processing

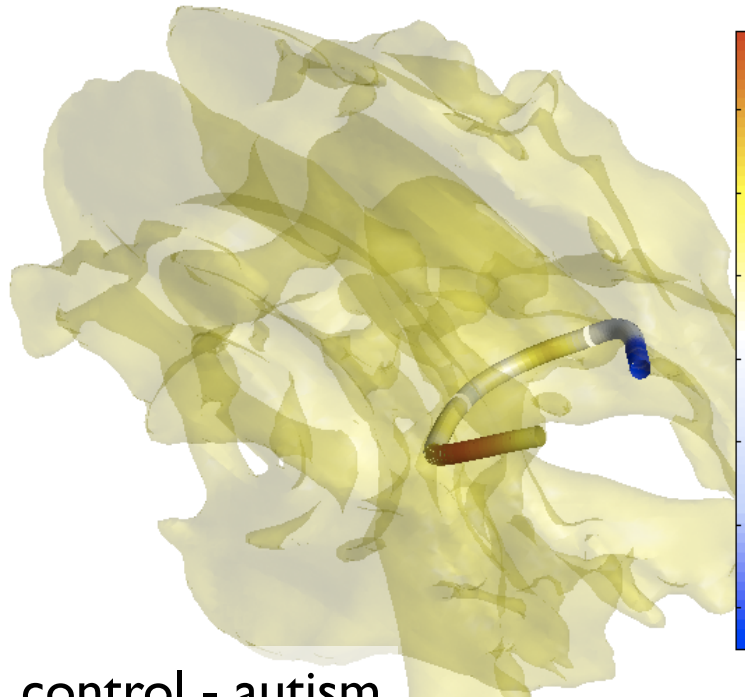


parameterization

Fiber concentration analysis in splenium



tracts passing through splenium



control - autism

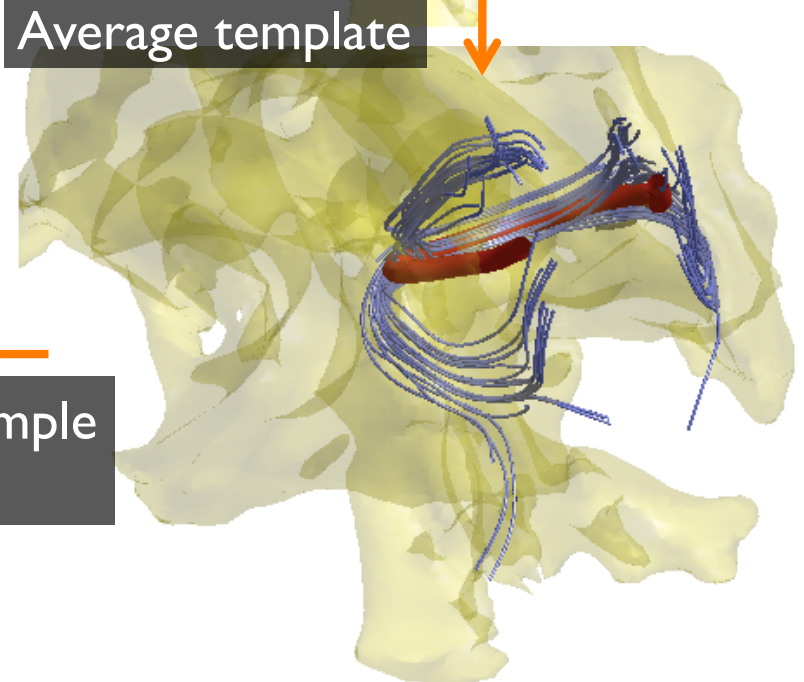
two sample t-test



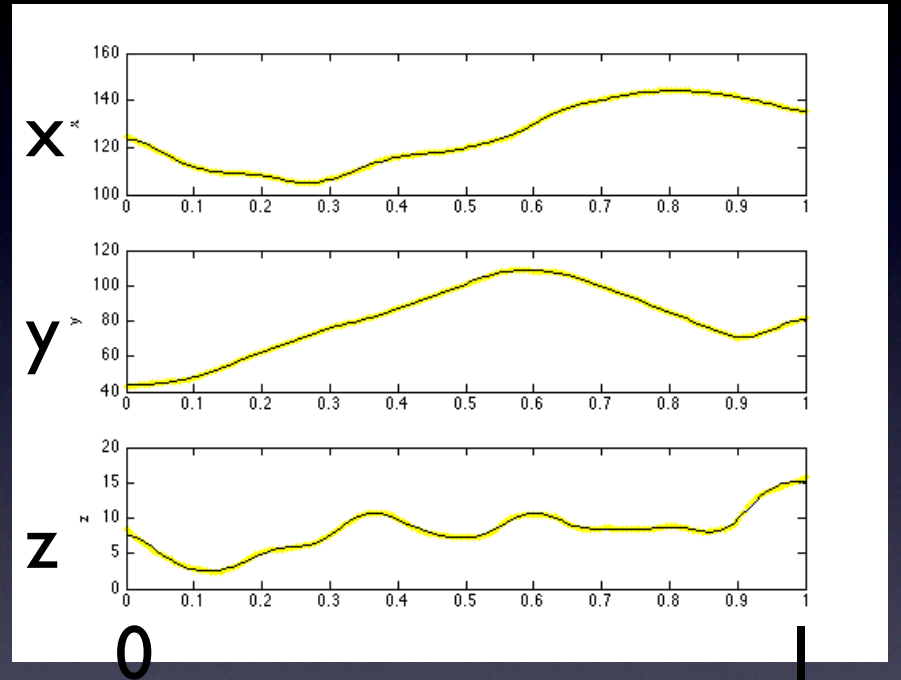
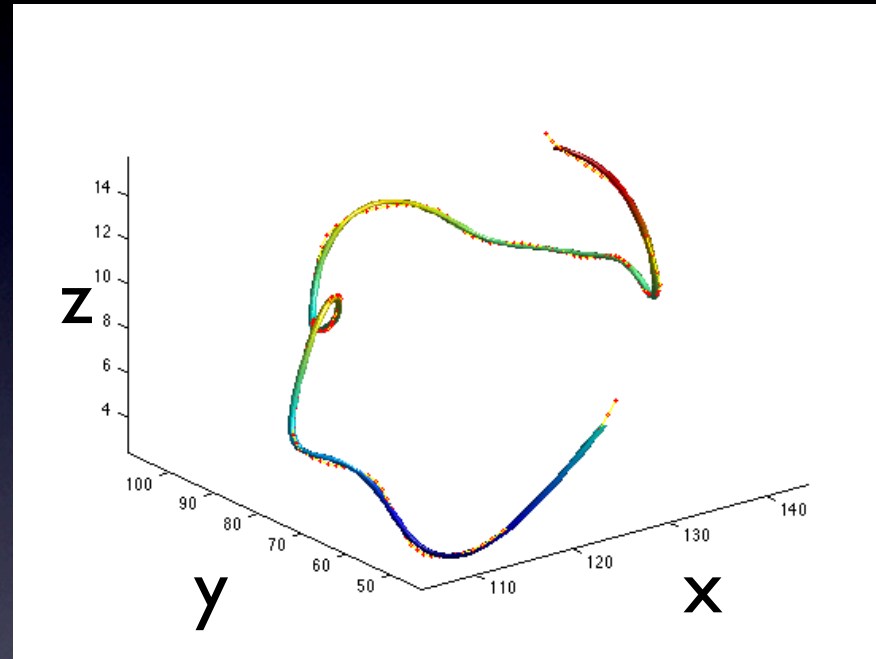
Average template



42 autistic & 32 control

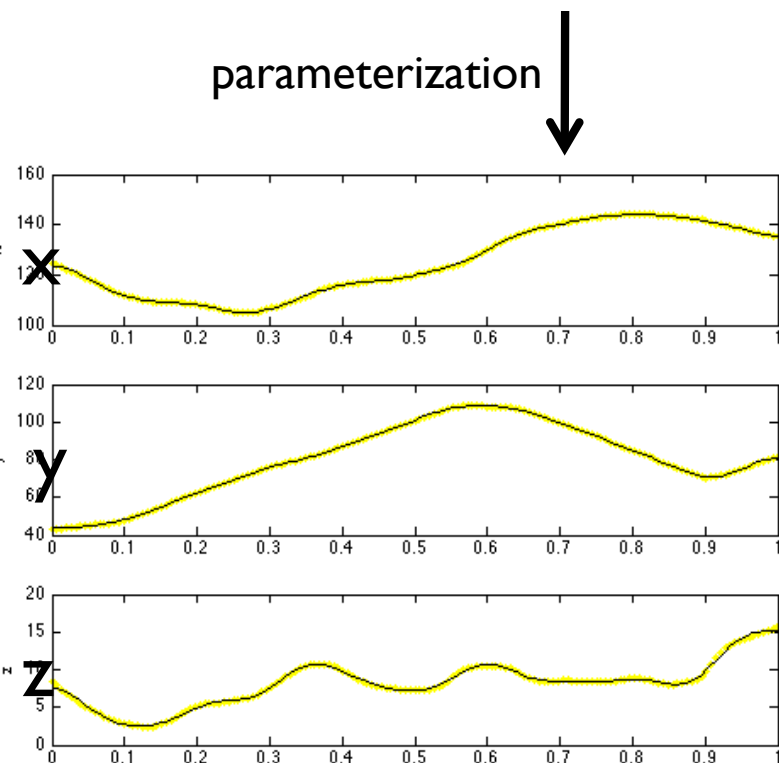
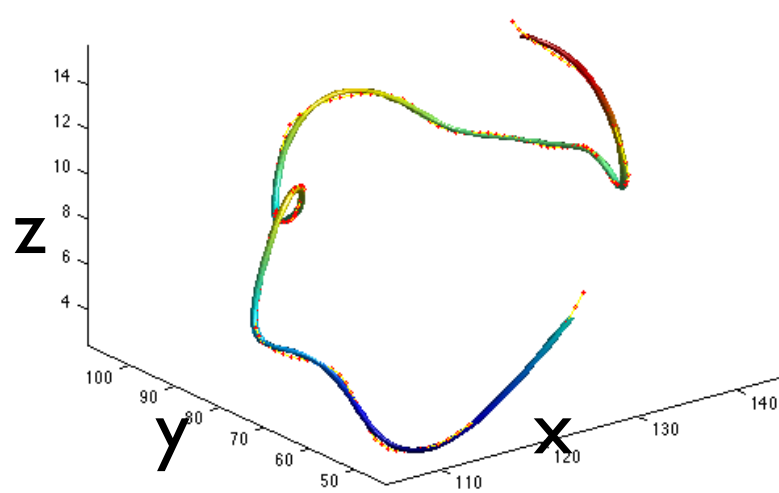


DTI Tract parameterization



x, y, z coordinate functions are mapped
onto a unit interval

Cosine series representation



88.1799	56.6336	5.7367
-12.4775	-11.2552	-2.0791
2.4336	-15.4428	-0.4021
4.3956	2.2733	-0.9354
-0.0106	-0.0674	0.6999
2.1773	-2.4194	-0.1176
0.5808	0.8390	1.2942
0.0615	-0.1893	0.1188
-0.2629	0.7524	0.1089
0.7909	-0.7276	-0.1901
0.5458	0.6236	0.6939
0.4295	-0.4337	0.2185
0.2150	0.4157	0.0254
0.1584	-0.1973	0.0762
-0.1557	0.2466	-0.1086
0.0632	-0.0978	-0.0208
0.0389	-0.0143	-0.0284
-0.0014	-0.1193	0.1970
0.0004	0.0129	-0.0198
0.1342	0.0002	0.0260

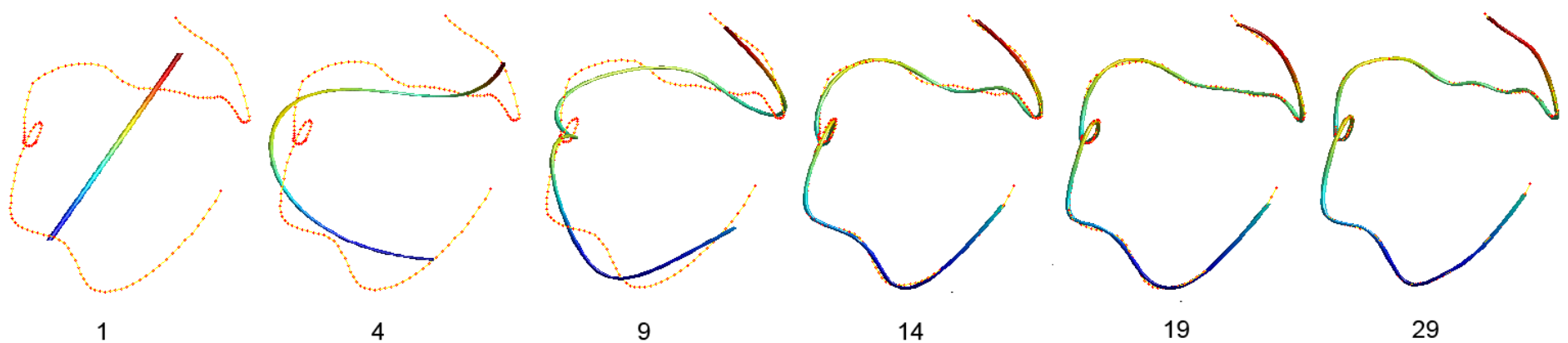
Any tract can be compactly parameterized with only 60 coefficients.

19

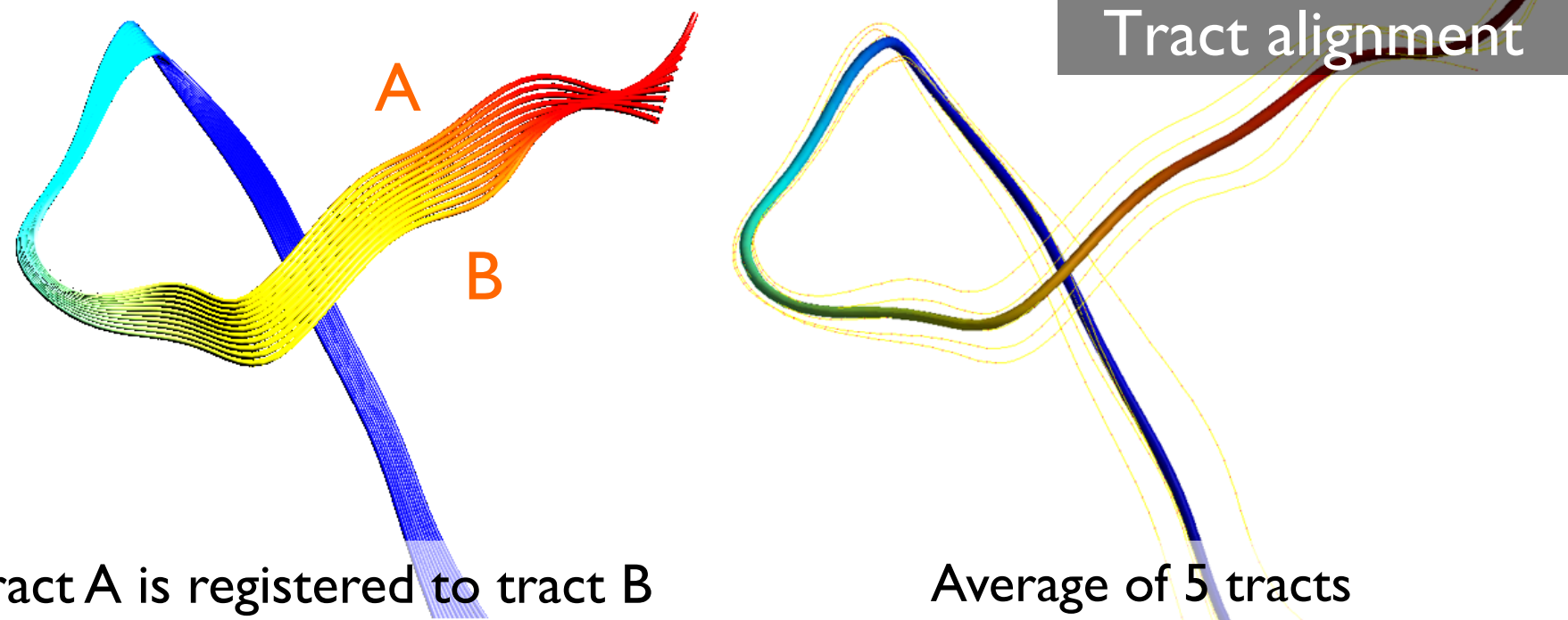
$$(x, y, z)' = \sum_{l=0}^{19} \beta_l \cos(l\pi t)$$

→ basis expansion

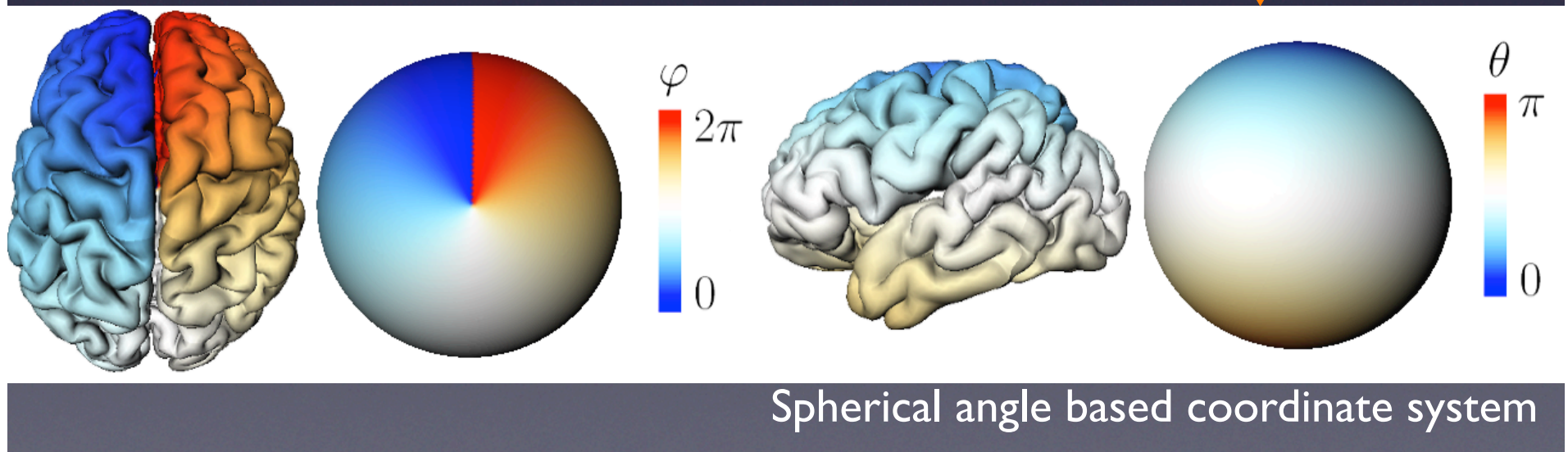
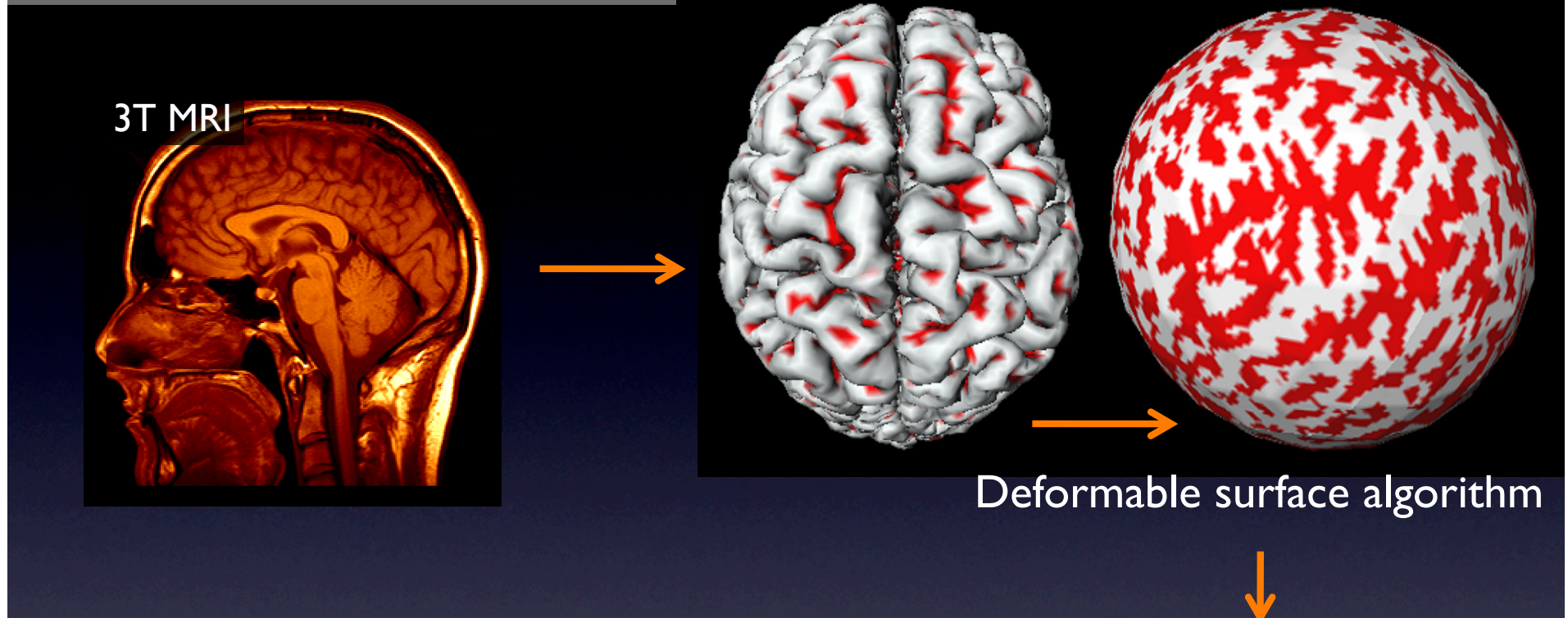
Cosine representation



Tract alignment

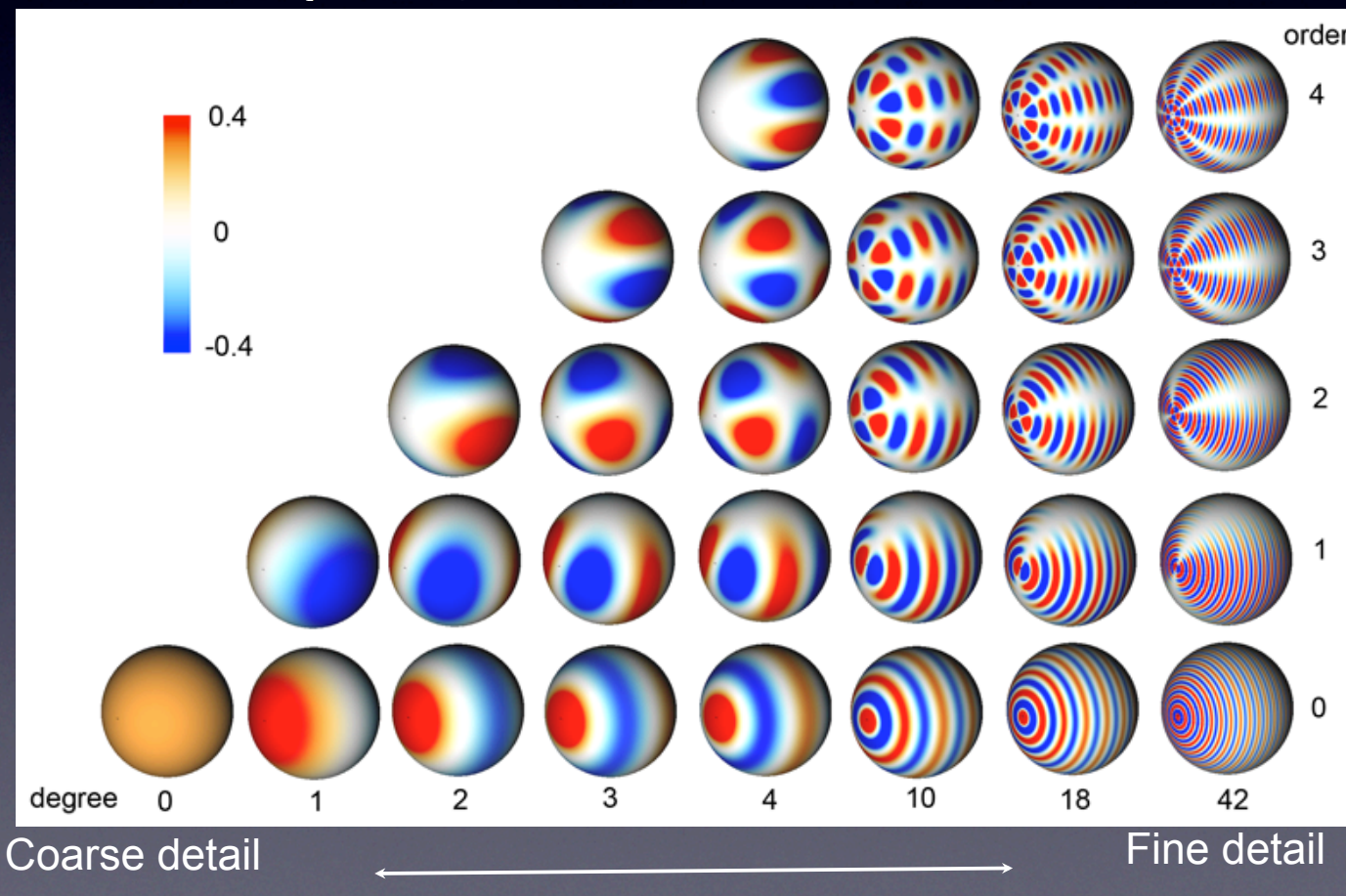


Cortical Surface Modeling

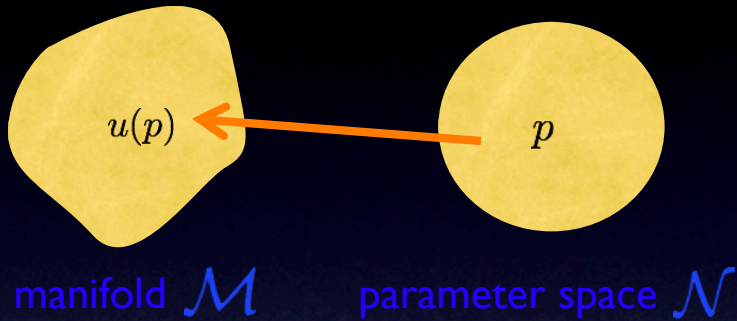


Spherical harmonic of degree l and order m

$$Y_{lm} = \begin{cases} c_{lm} P_l^{|m|}(\cos \theta) \sin(|m|\varphi), & -l \leq m \leq -1, \\ \frac{c_{lm}}{\sqrt{2}} P_l^0(\cos \theta), & m = 0, \\ c_{lm} P_l^{|m|}(\cos \theta) \cos(|m|\varphi), & 1 \leq m \leq l, \end{cases}$$



Cortical manifold and function defined on the manifold



Anatomical manifold $\mathcal{M} \in \mathbb{R}^d$
tracts, amygdala, hippocampus, cortical surface

↓ Flattening/
parameterization

Parameter space $\mathcal{N} \in \mathbb{R}^m$

Hilbert space $L^2(\mathcal{N})$ with inner product

$$\langle g_1, g_2 \rangle = \int_{\mathcal{N}} g_1(p)g_2(p)\mu(p)$$

Self-adjoint operator \mathcal{L}

$$\langle \mathcal{L}g_1, g_2 \rangle = \langle g_1, \mathcal{L}g_2 \rangle$$

Basis function

$$\mathcal{L}\psi_j = \lambda_j\psi_j$$

Weighted Fourier Analysis

t = scale, bandwidth, diffusion time

Input signal

$$\text{PDE: } \partial_t g + \mathcal{L}g = 0, g(p, t=0) = f(p)$$

Analytic solution

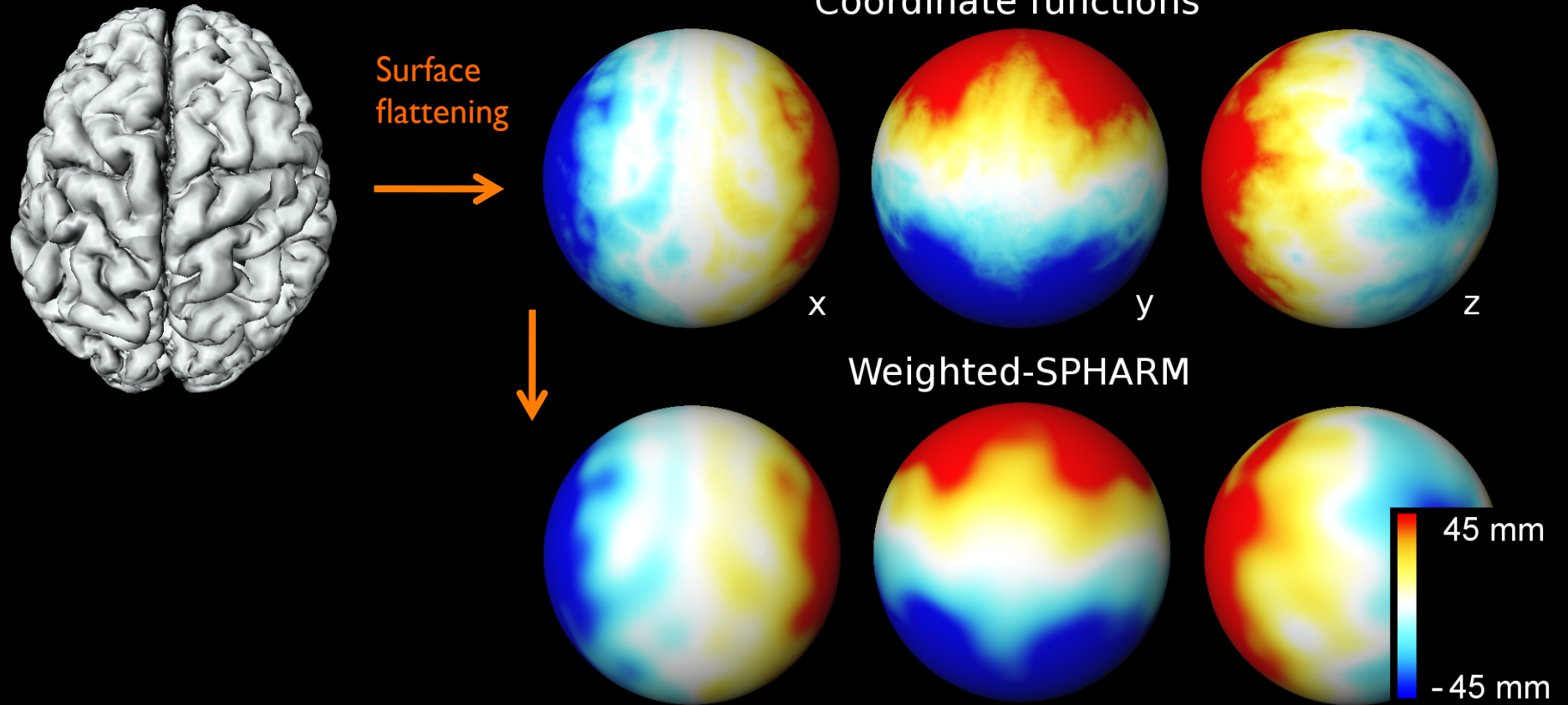
Weighted Fourier series

$$g(p, t) = \sum_{j=0}^{\infty} e^{-\lambda_j t} \langle f, \psi_j \rangle \psi_j(p)$$

Kernel smoothing

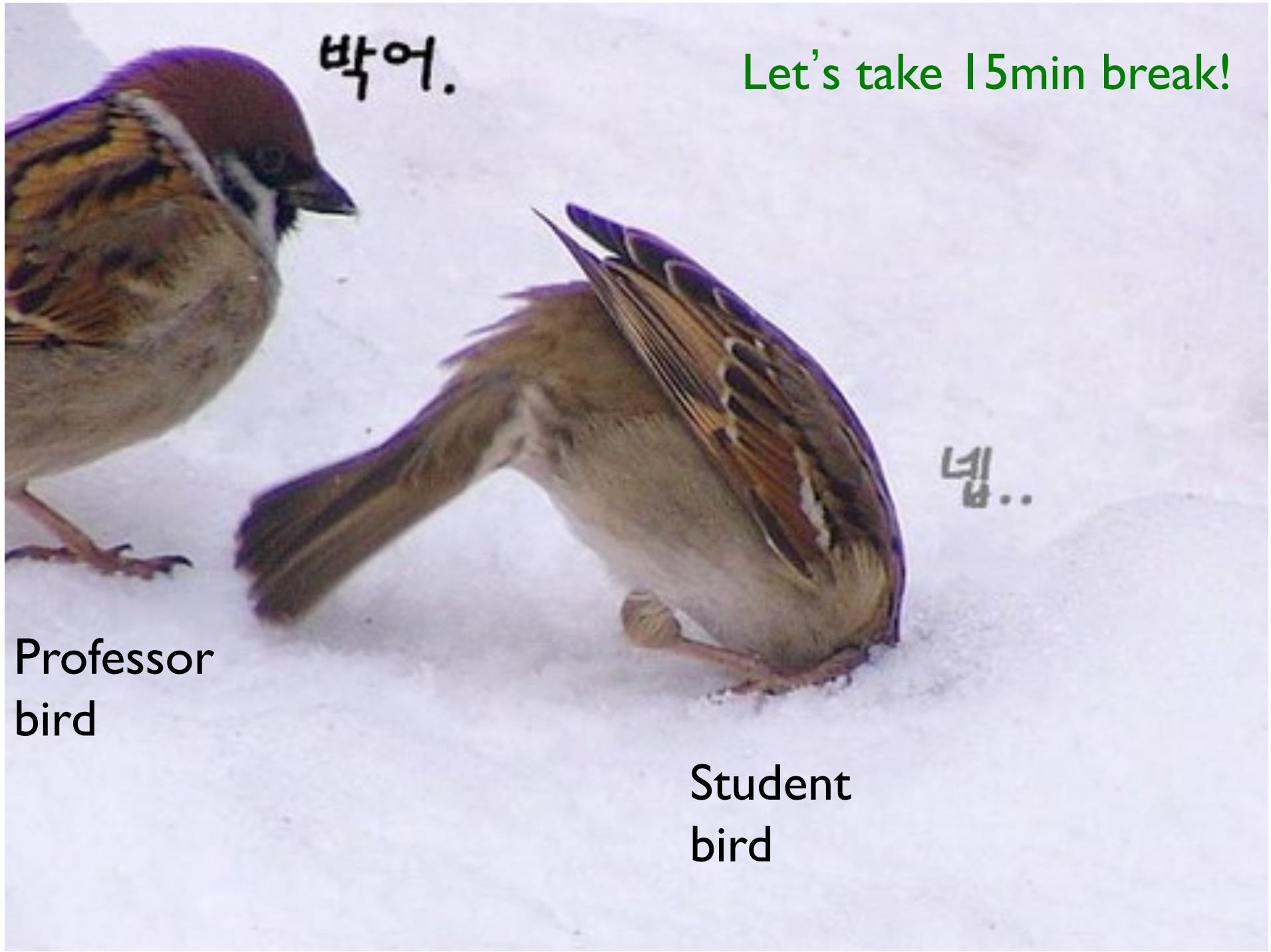
$$= \int_{\mathcal{N}} K_t(p, q) f(q) d\mu(q)$$

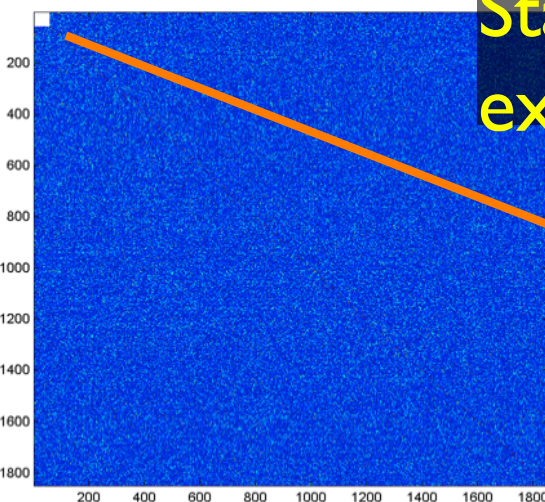
Spherical harmonic representation



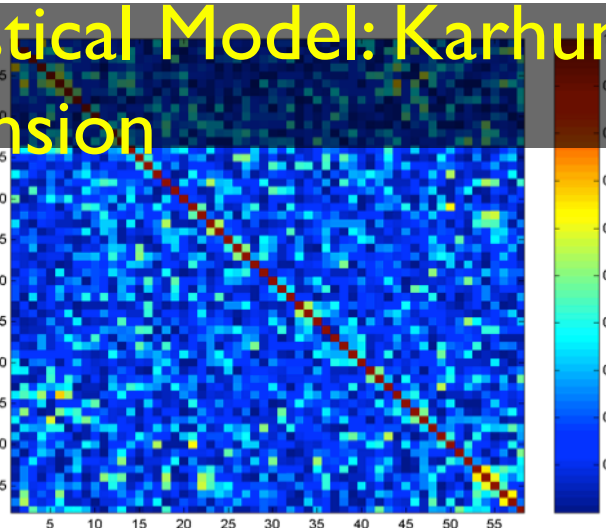
Coordinates are represented
in a functional form:

$$\sum_{l=0}^k \sum_{m=-l}^l e^{-l(l+1)t} \langle f, Y_{lm} \rangle Y_{lm}(\theta, \varphi)$$

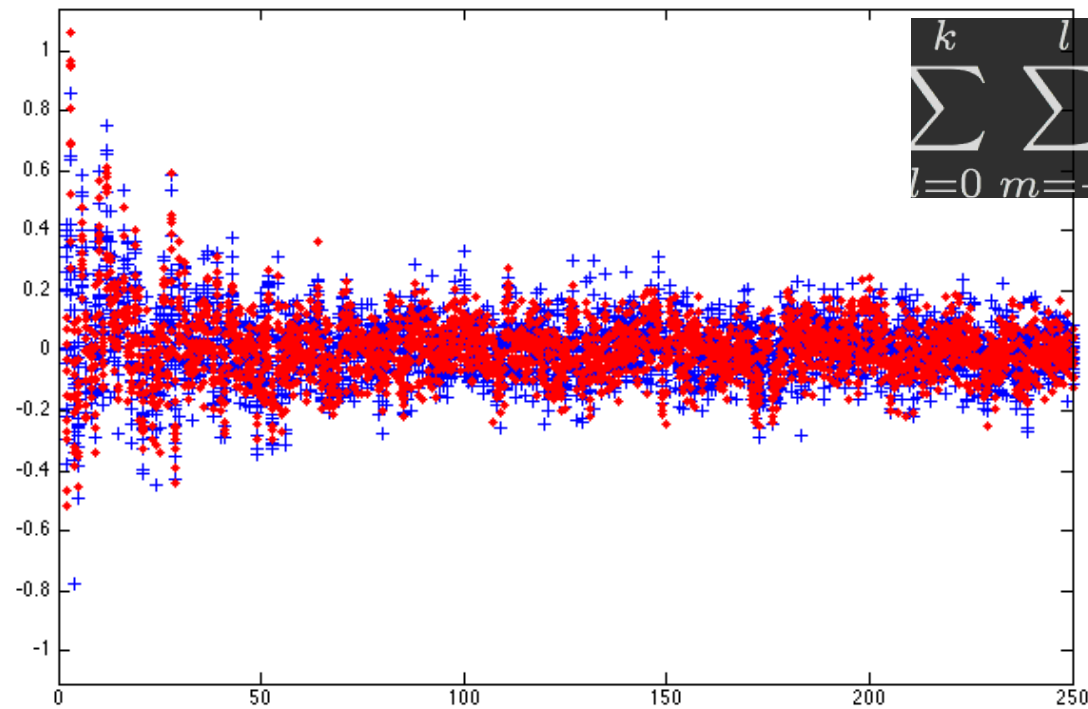




Statistical Model: Karhunen-Loeve
expansion

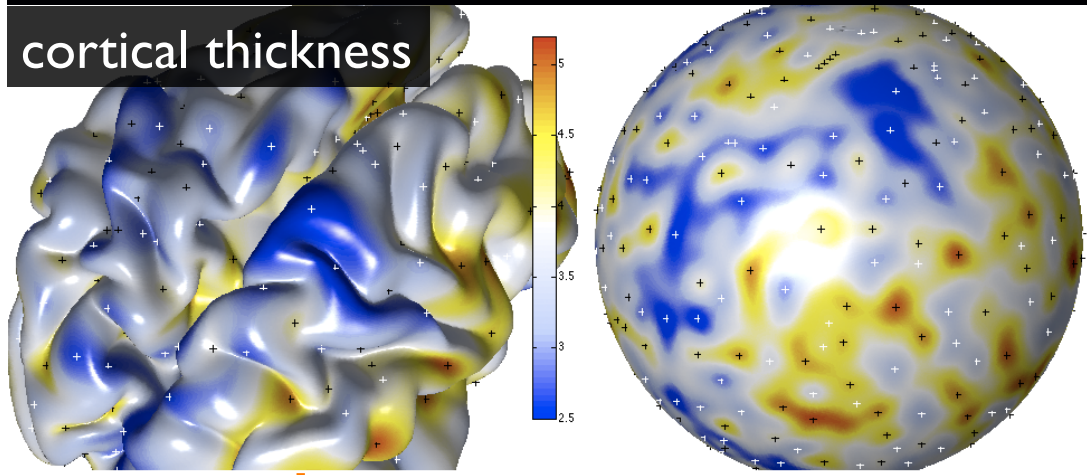
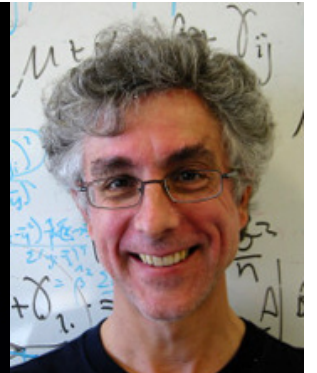


uncorrelated normal



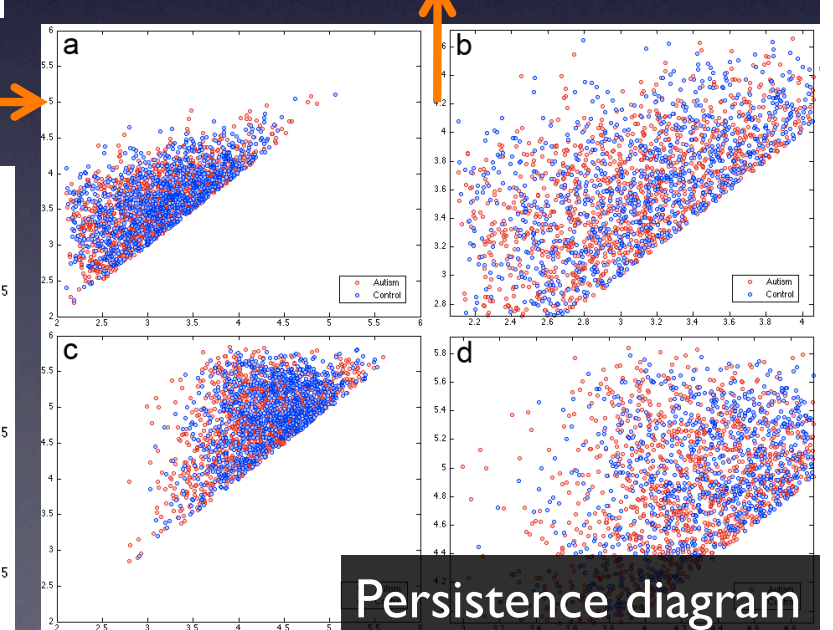
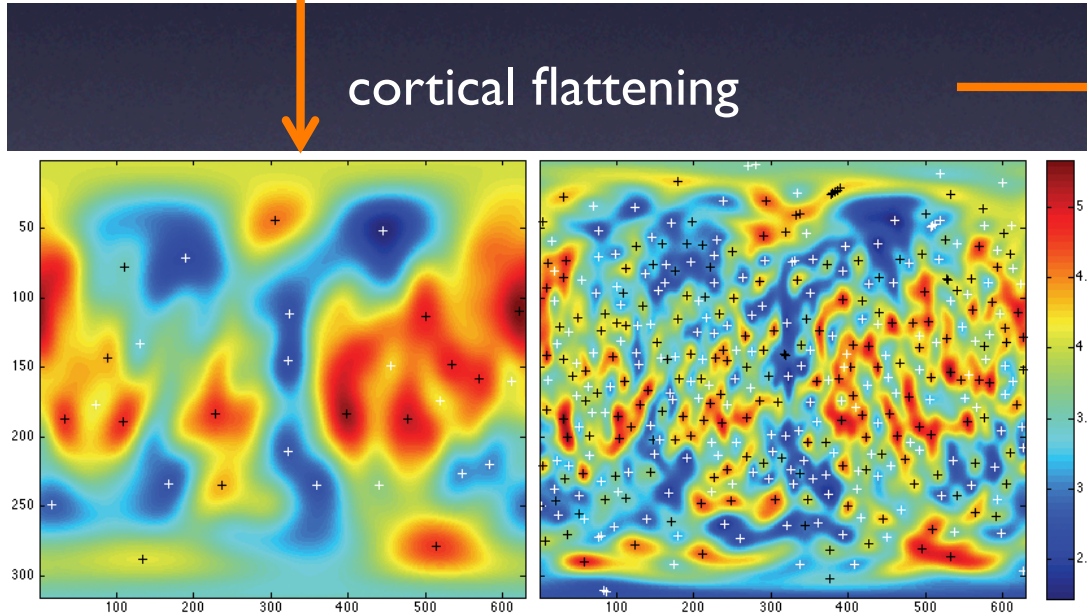
Classification ?

Persistent homology based signal detection (IPMI, 2009)
concept coming from algebraic topology, related to Euler characteristic, Betti numbers, Morse functions, Worsley's random field theory.

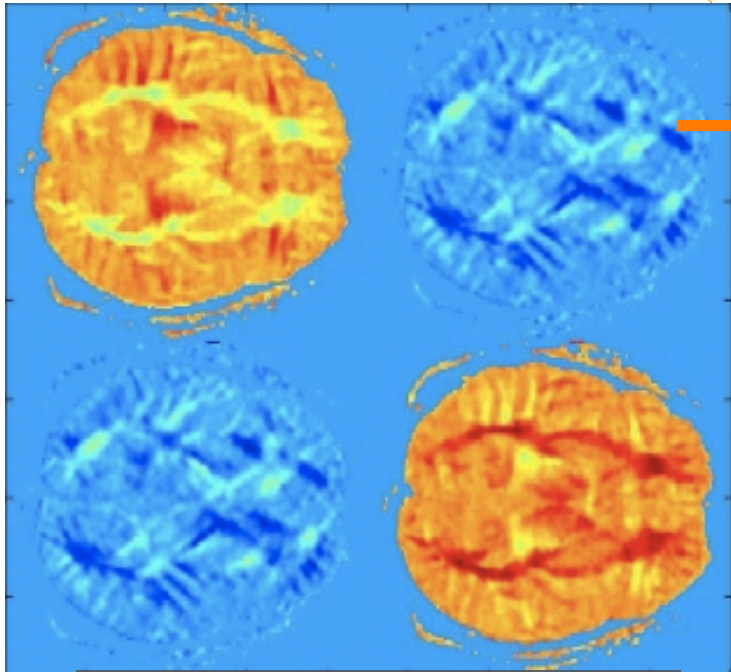


Classification accuracy of 96%
using a simple support vector
machine

Best available thickness analysis technique with Ada-boost 90%

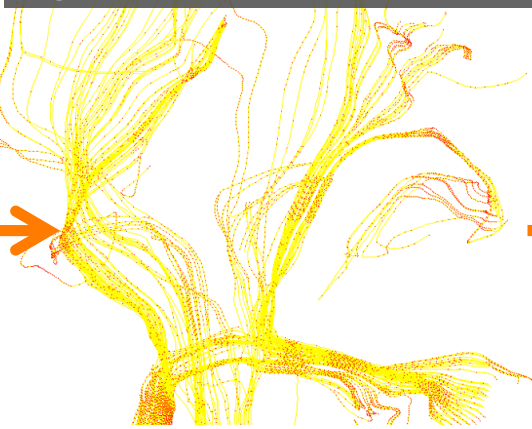


DTI connectivity model

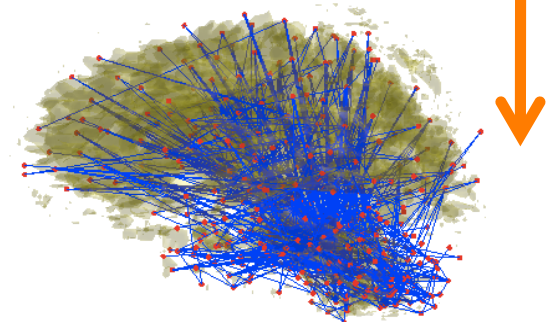
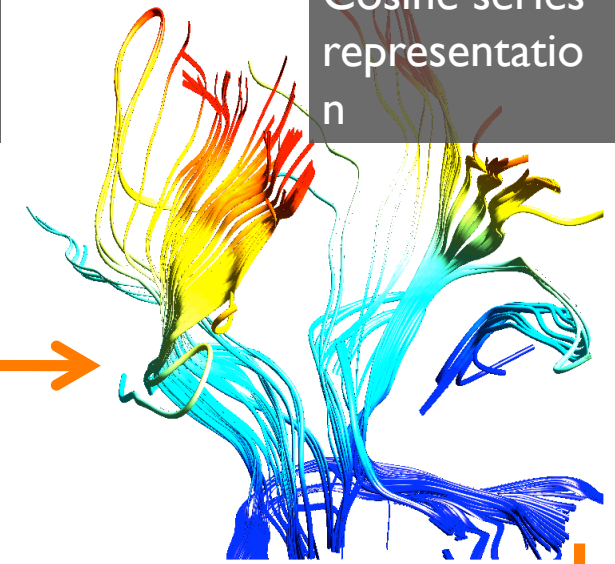


Diffusion tensor imaging
(DTI)

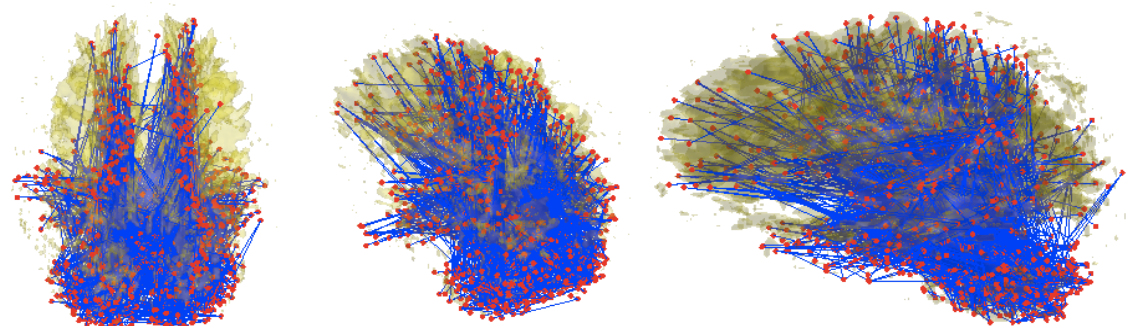
Second order Runge-Kutta streamline algorithm



Cosine series representation

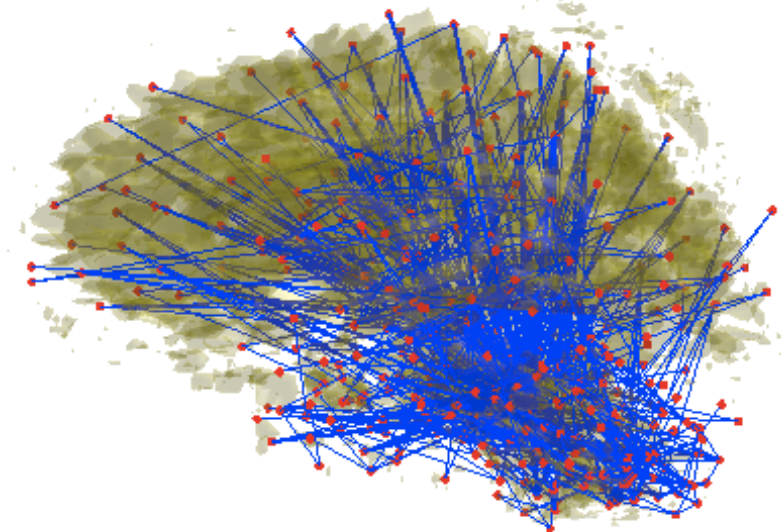
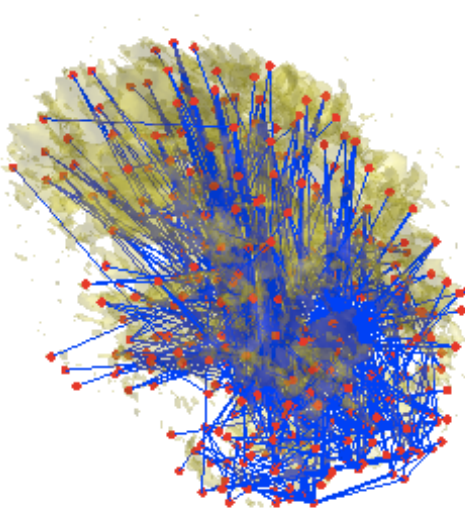
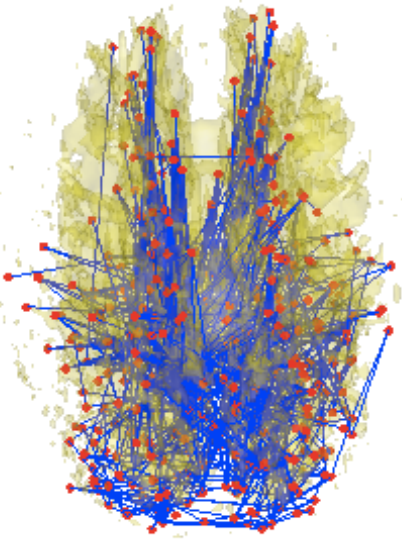


10 mm resolution 405 node network

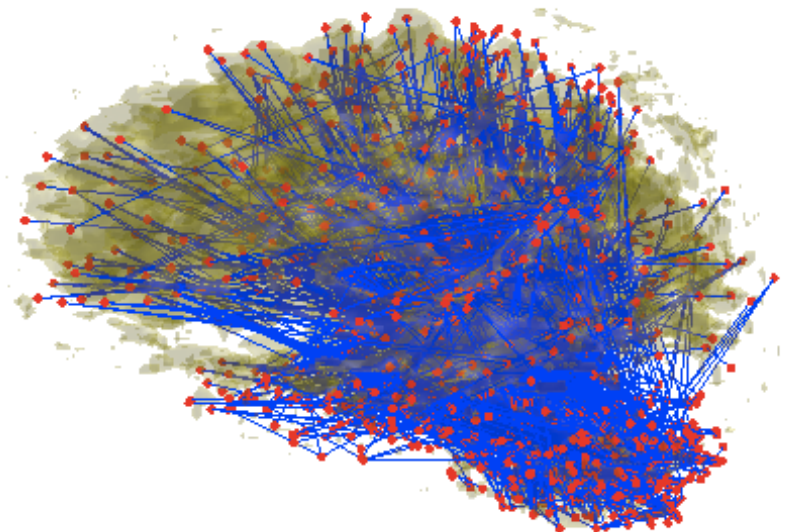
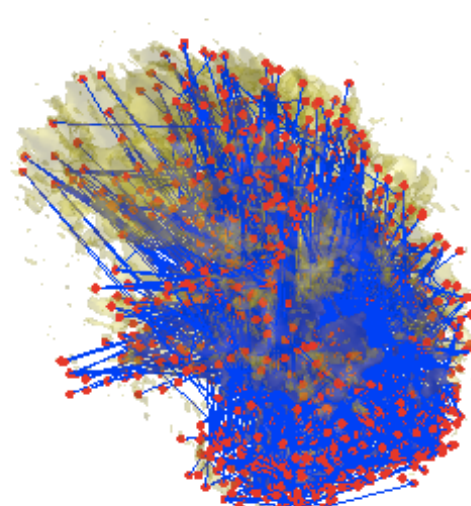
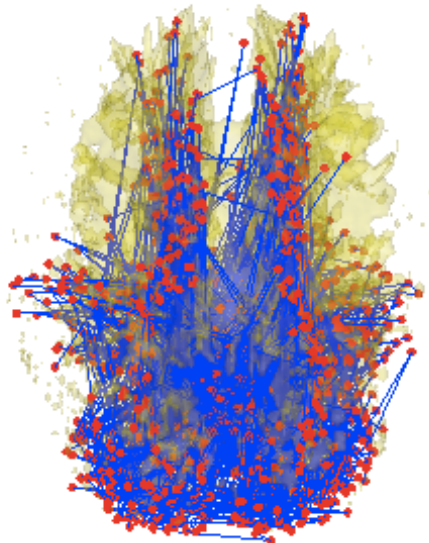


5 mm resolution 1502 node network

Multiscale
3D graph



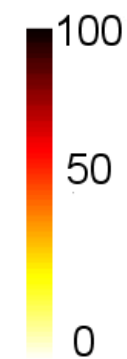
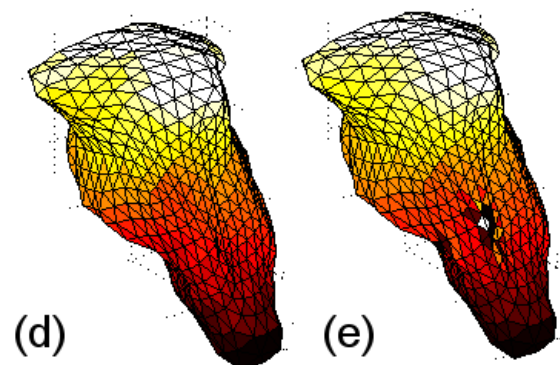
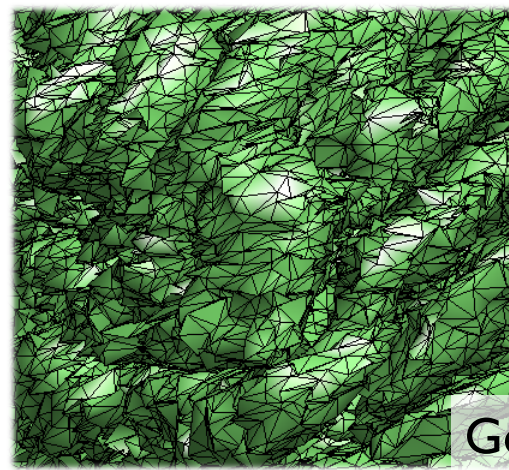
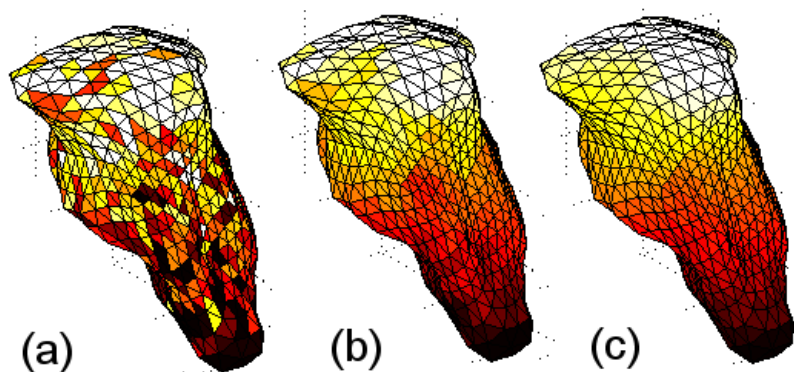
10 mm resolution 405 node network



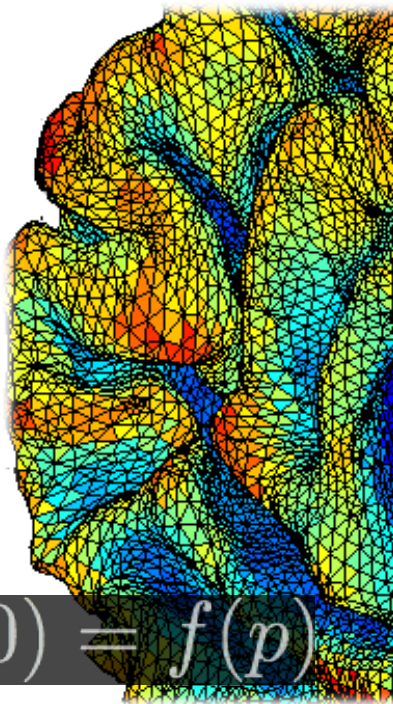
5 mm resolution 1502 node network

Image smoothing

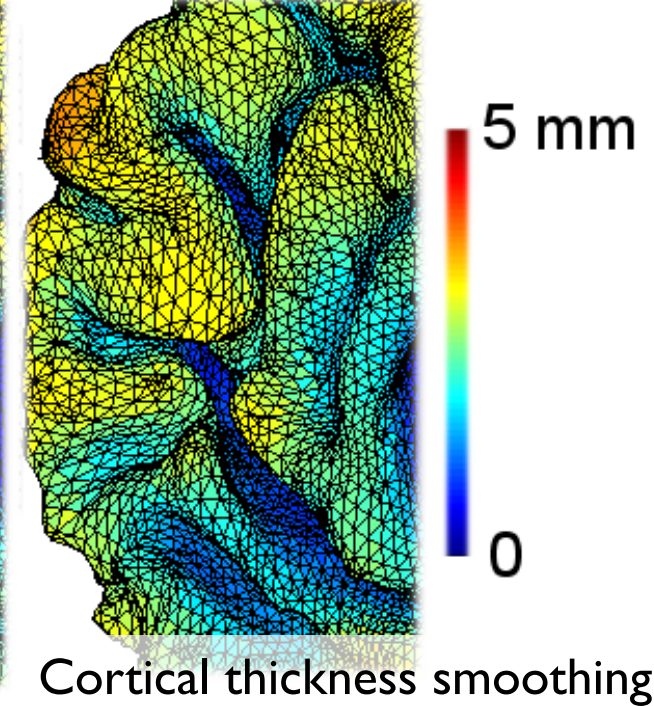
Smoothing on anatomical boundary



Diffusion smoothing on brain stem



$$\partial_t g + \mathcal{L}g = 0, g(p, t=0) = f(p)$$



3D Gaussian kernel smoothing
will blur measurements
between A and B in
different hemisphere

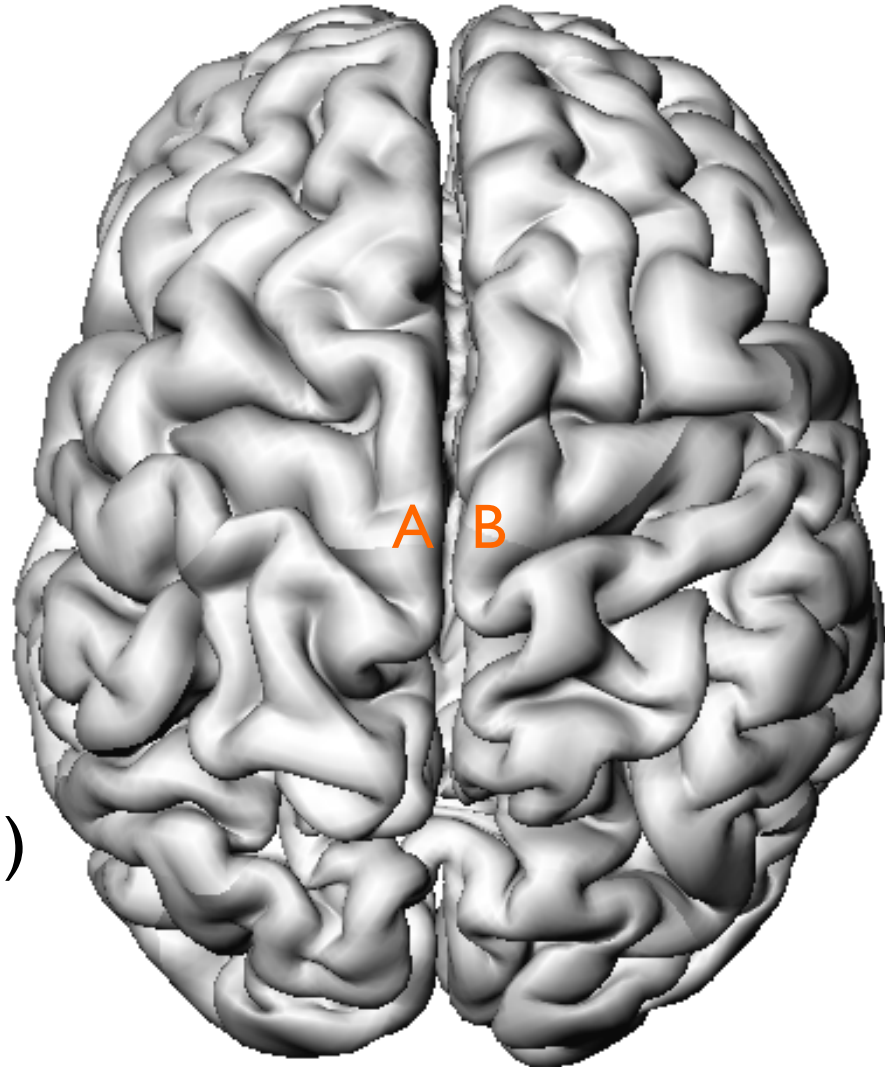


Need to smooth along the
surface

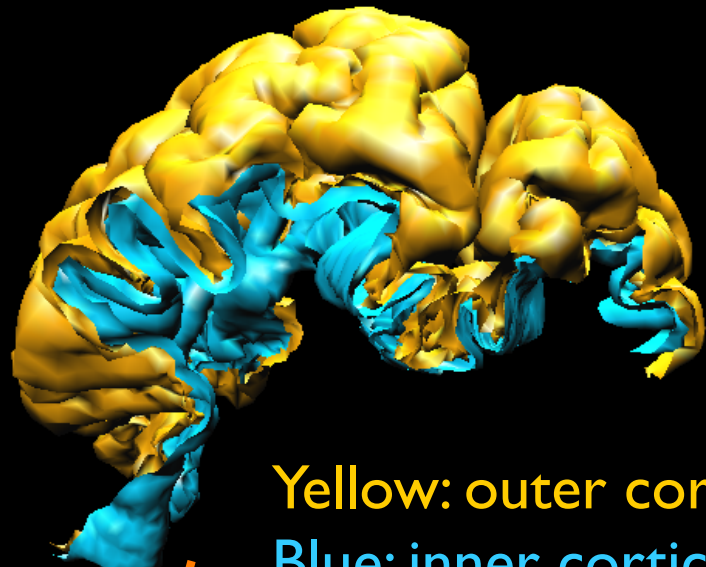


Diffusion smoothing (2001, 2003)
Heat kernel smoothing (2005)

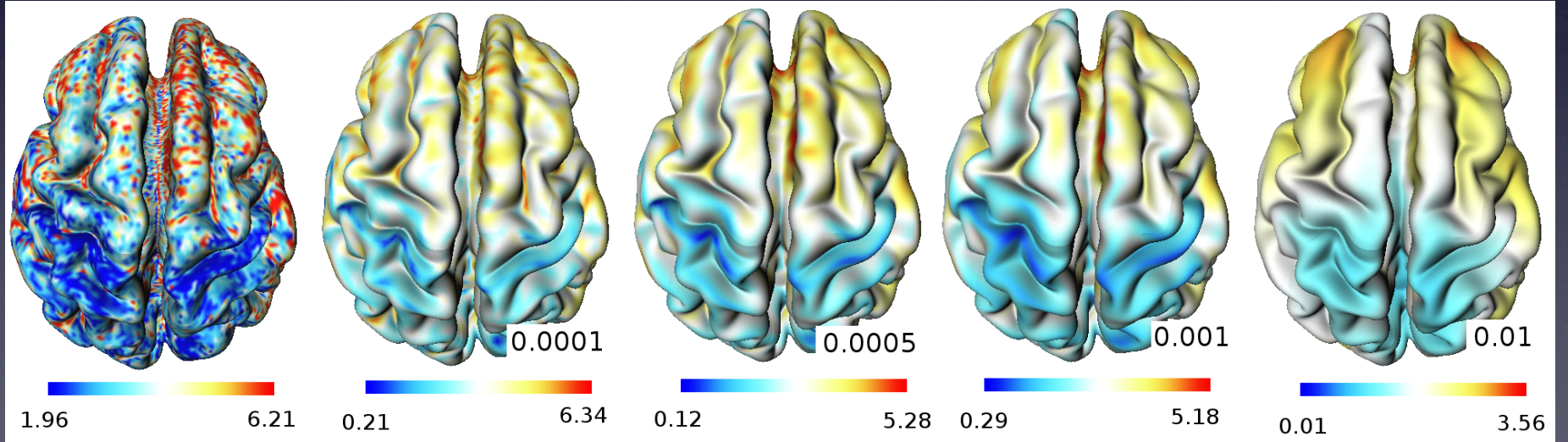
Most widely used cortical
smoothing techniques



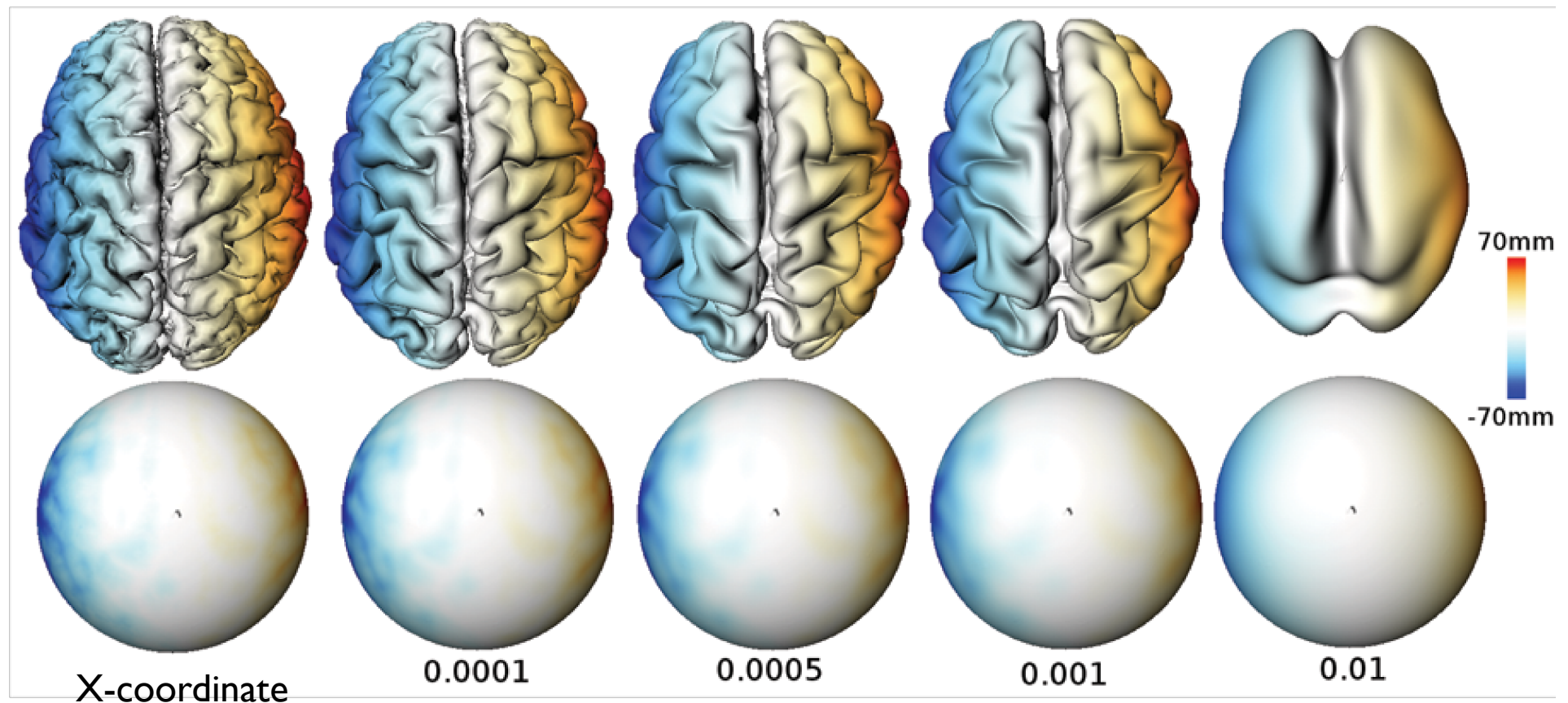
Weighted Fourier representation of cortical thickness



Yellow: outer cortical surface
Blue: inner cortical surface



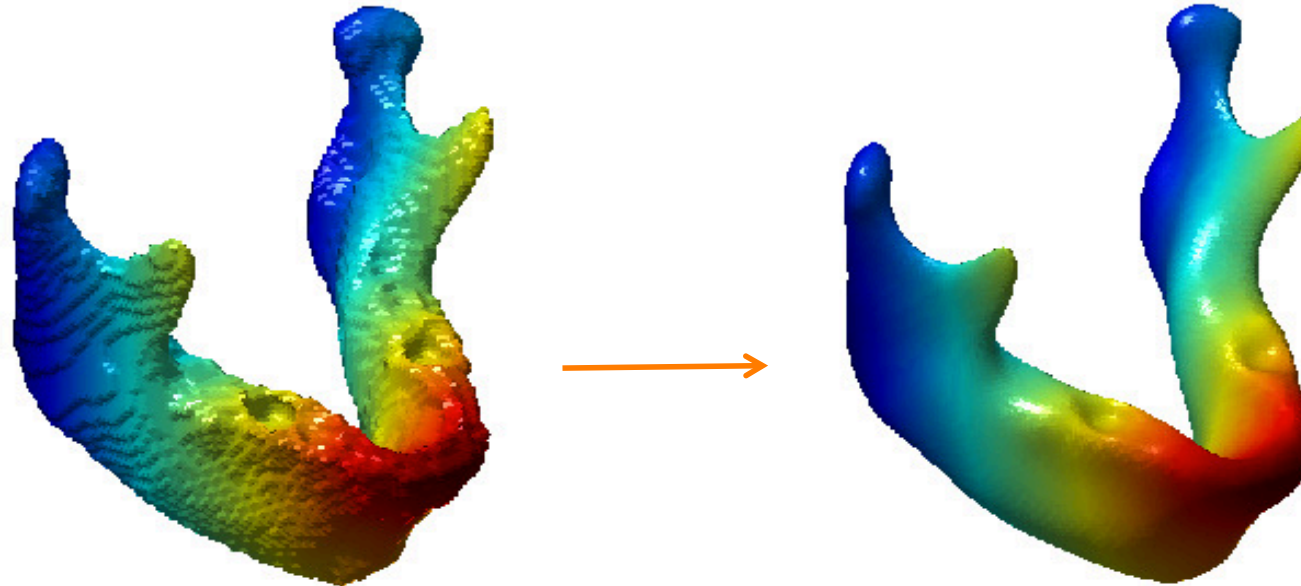
Multiscale representation of anatomy via weighted-SPHARM



Heat kernel smoothing on surface

Heat kernel:
$$K_t(p, q) = \sum_{i=0}^{\infty} e^{-\lambda_i t} \psi_i(p) \psi_i(q)$$

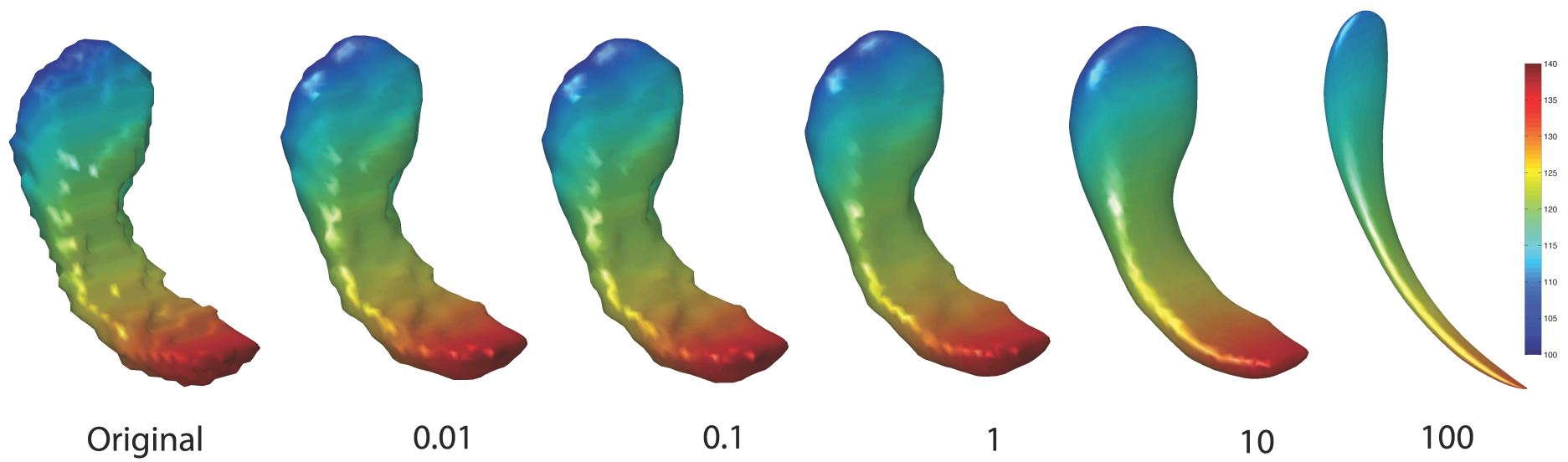
$$K_t * f = \int_{\mathcal{M}} K_t(p, q) f(q) dq$$



X-coordinate on
mandible surface

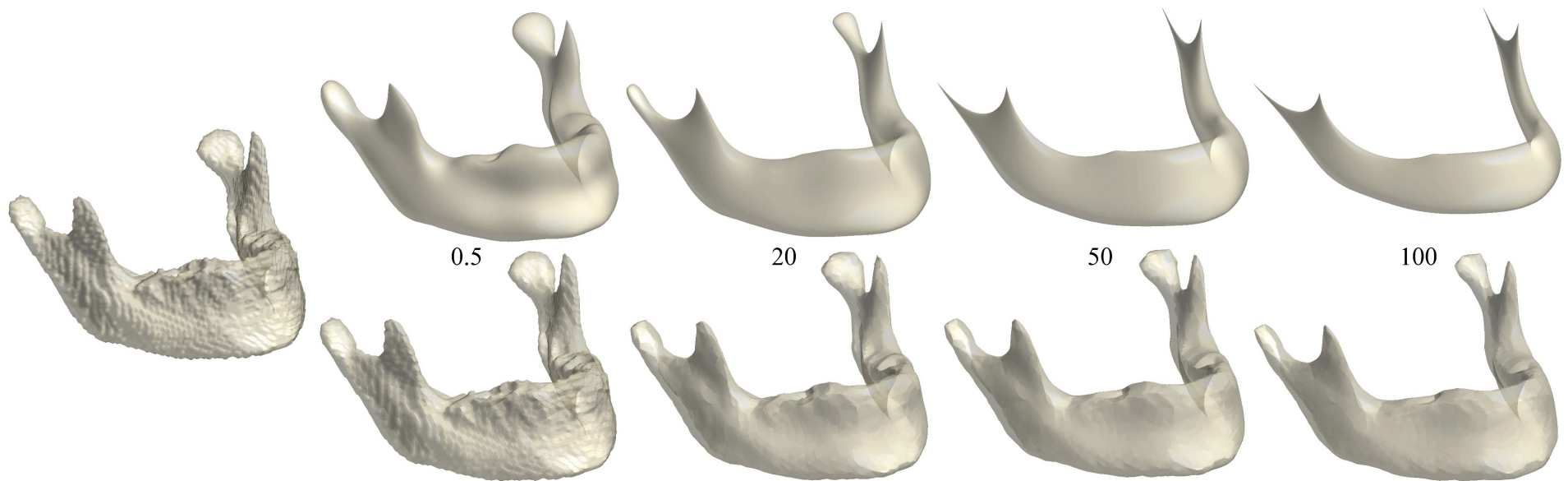
smoothed with bandwidth
10 and 1269 eigenfunctions

Heat kernel smoothing of hippocampus



Heat kernel smoothing on mandible shape

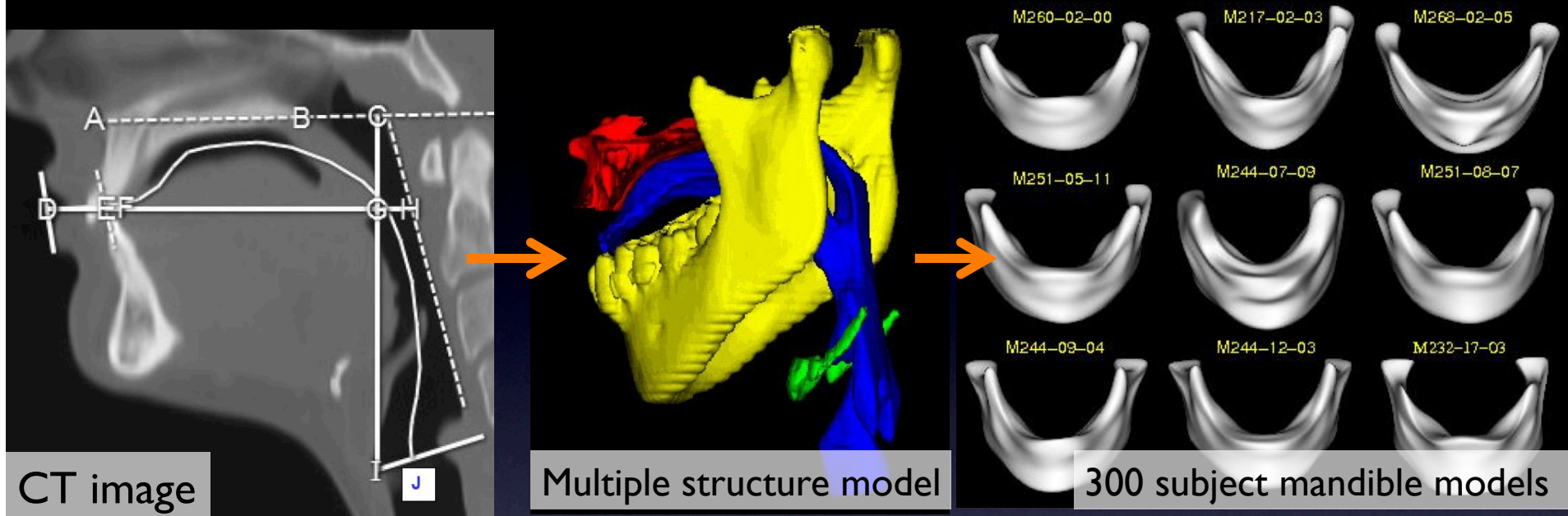
Heat kernel smoothing (Seo et al., 2010 MICCAI)



Iterated kernel smoothing (Chung et al., 2005 NeuroImage)

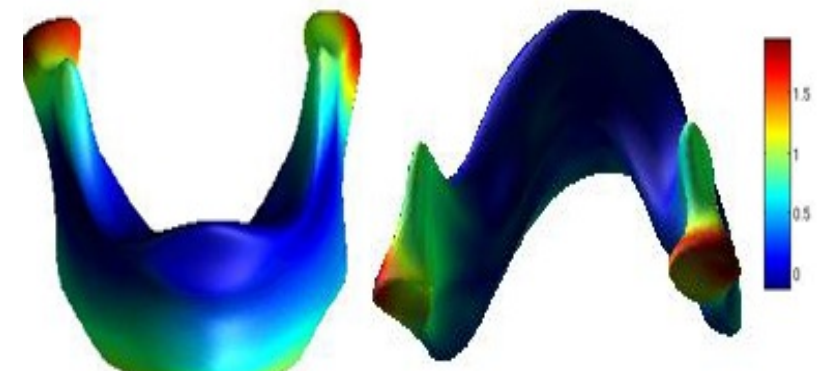
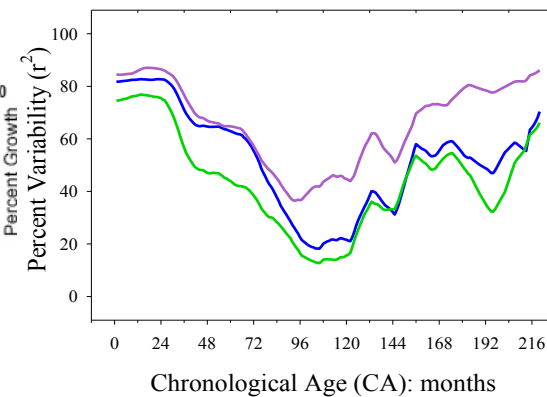
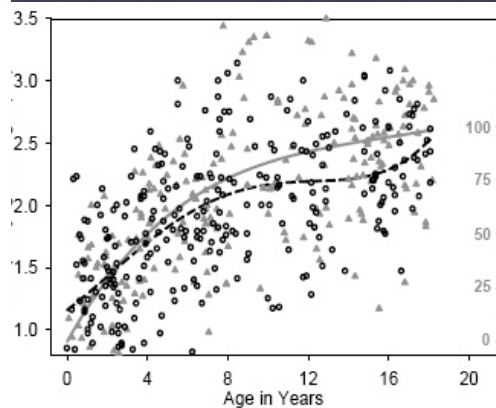
Statistical models

Longitudinal growth modeling on mandible CT images



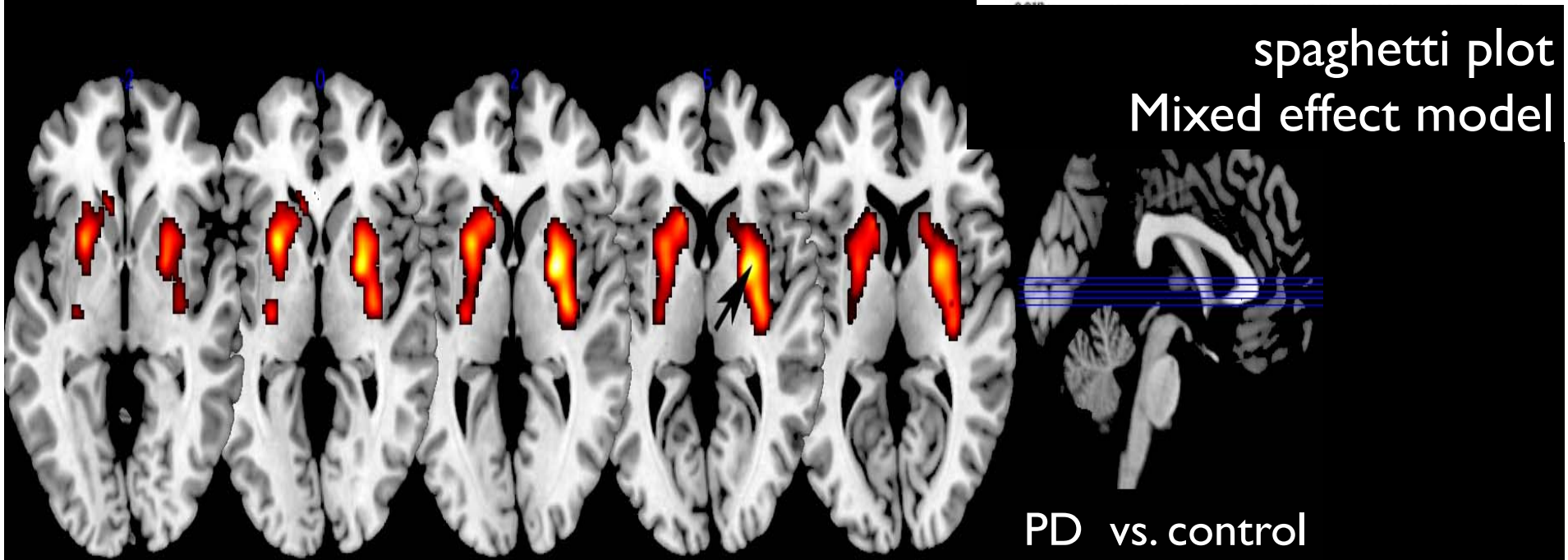
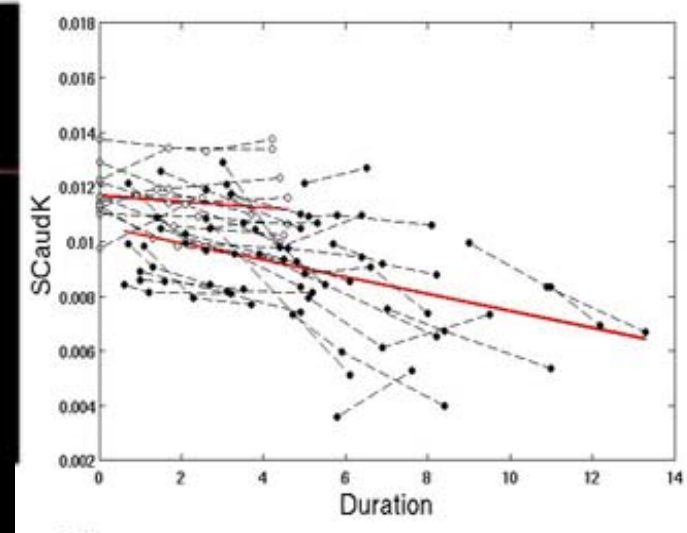
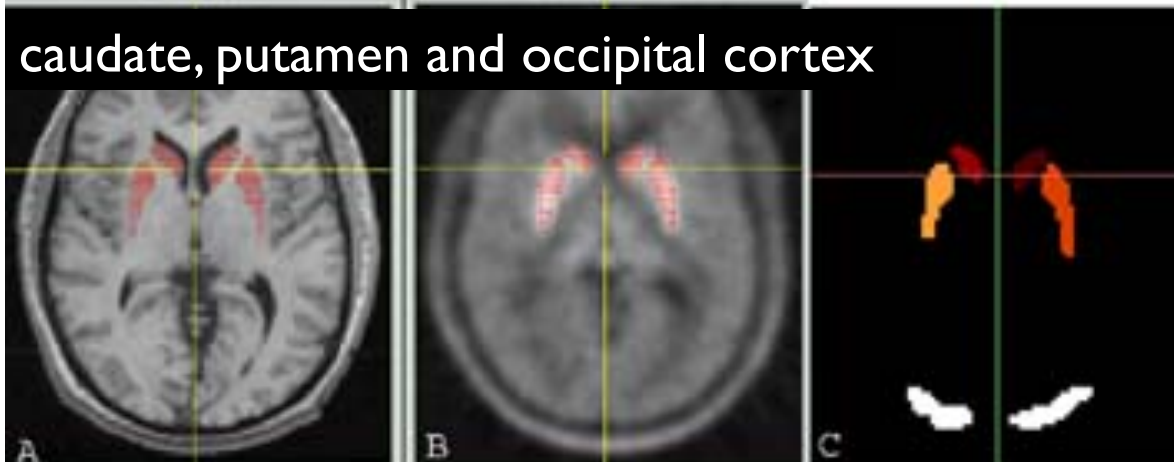
Longitudinal modeling

Growth
↓ rate analysis

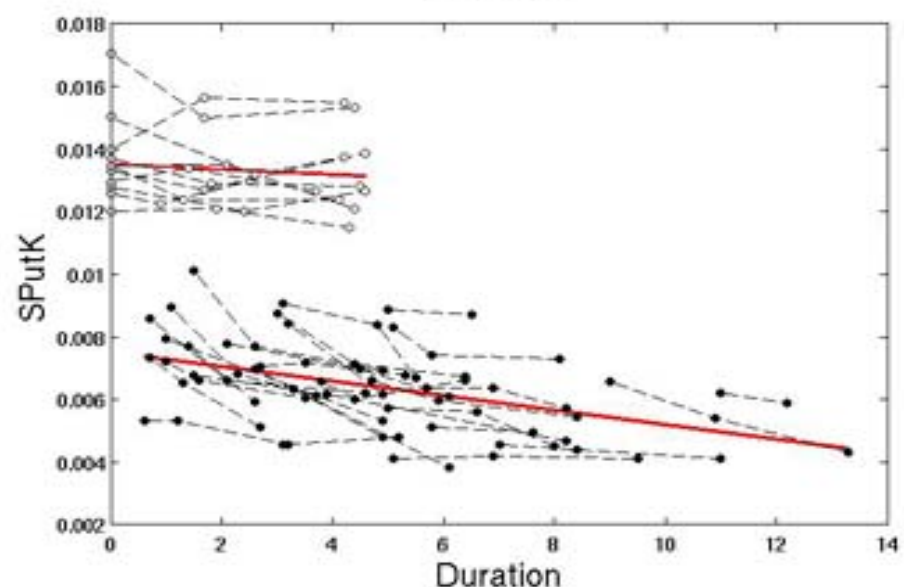
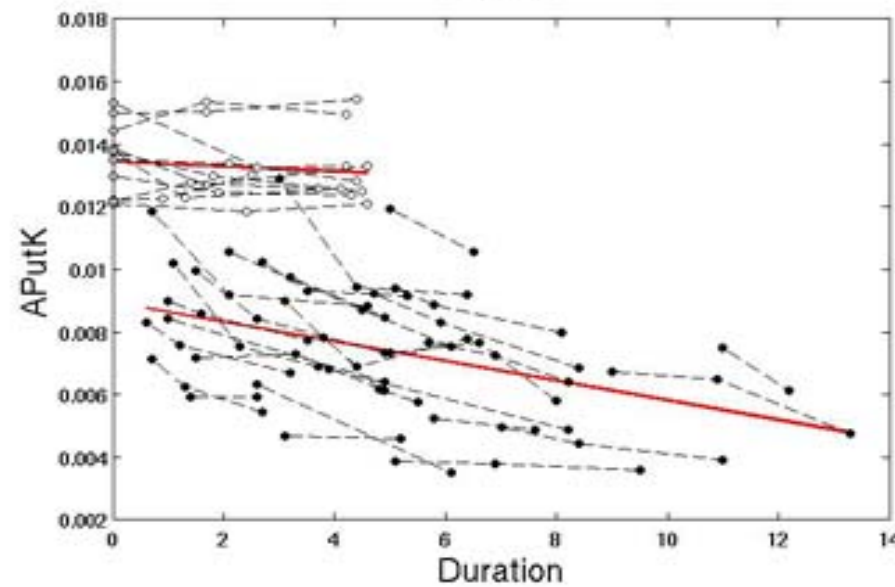
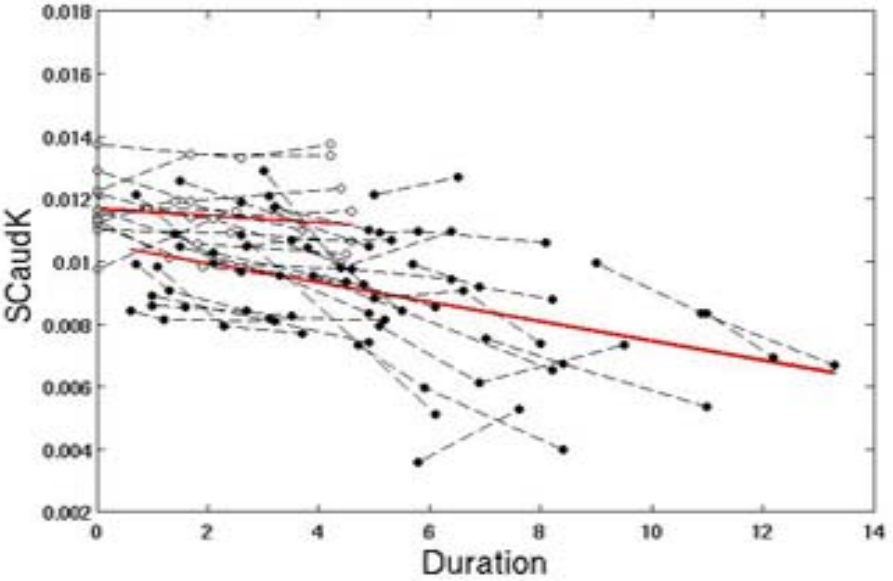
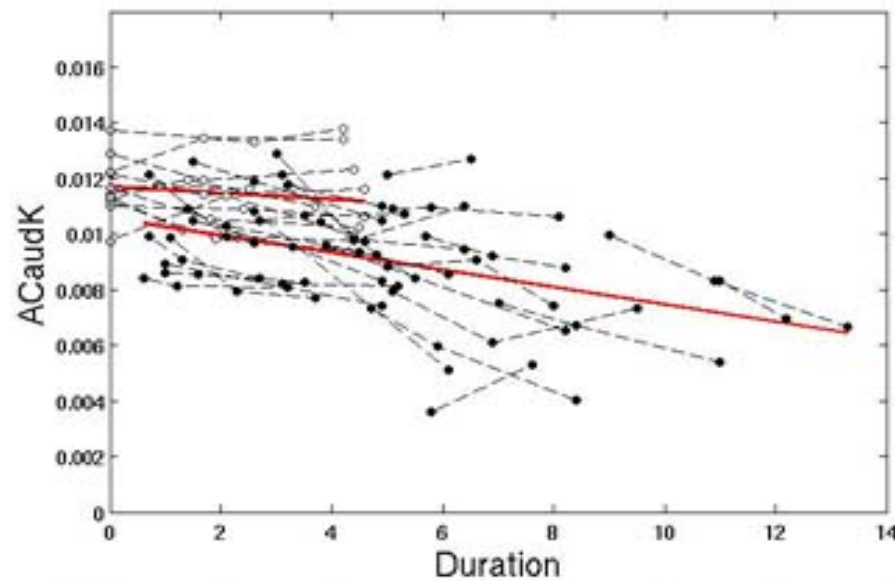


A longitudinal study of regional differences in the rate of striatal FDOPA uptake decline in Parkinson disease (PD)

caudate, putamen and occipital cortex

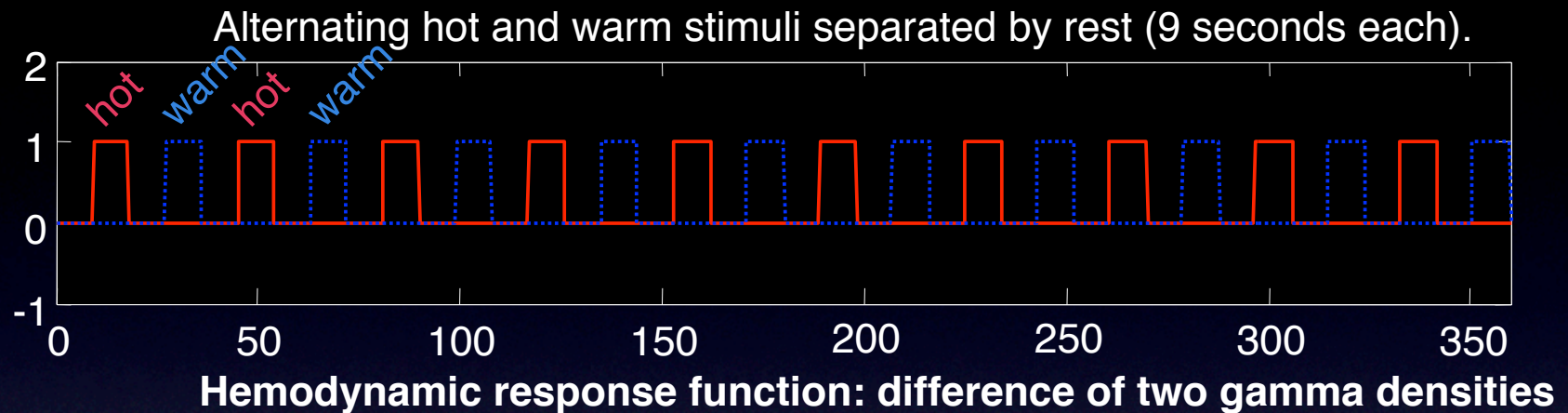


Asymtomatic putamen, symptomatic caudate uptake

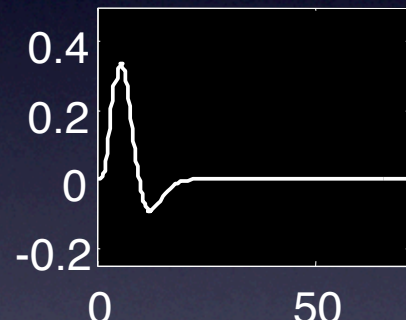


Pain perception fMRI study

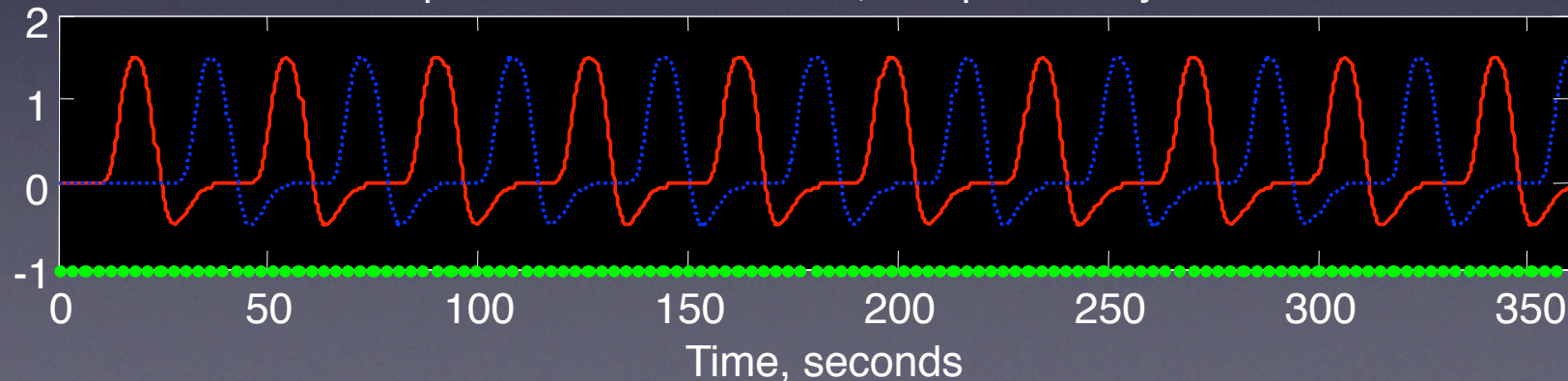
Keith Worsley



Hemodynamic response function: difference of two gamma densities

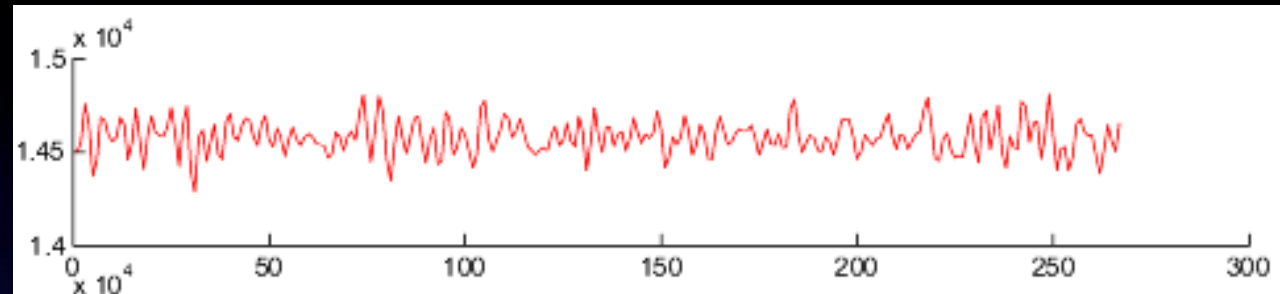


Responses = stimuli * HRF, sampled every 3 seconds

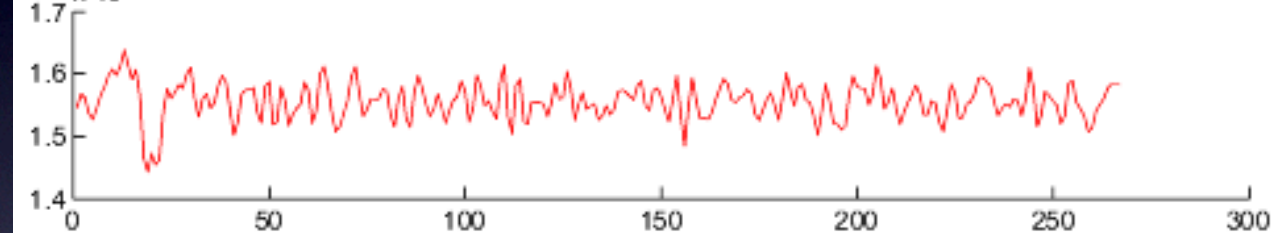


Event-related fMRI design of fear response in amygdala

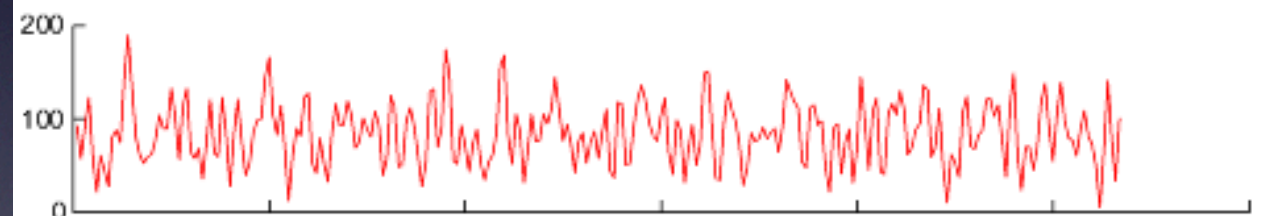
Right Amygdala



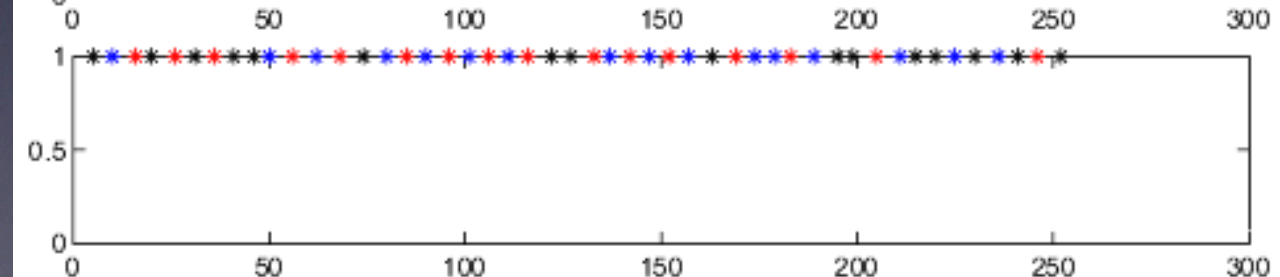
Left Amygdala

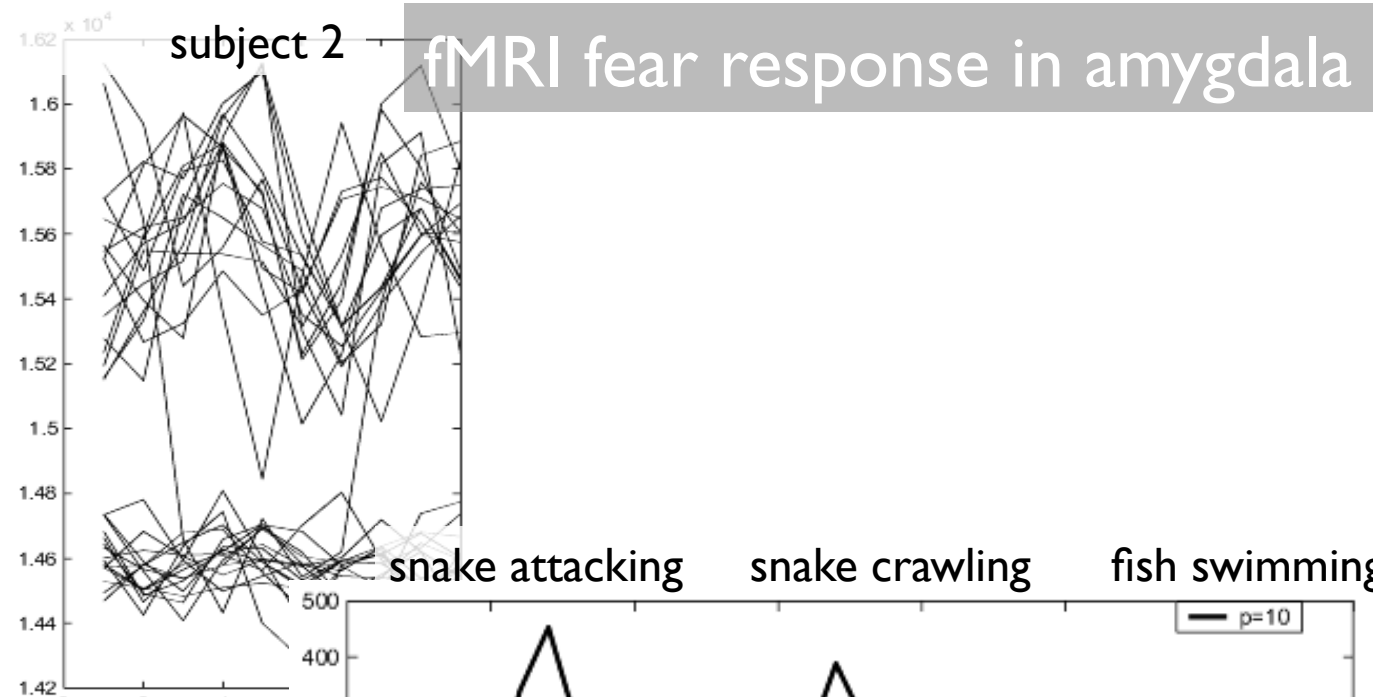
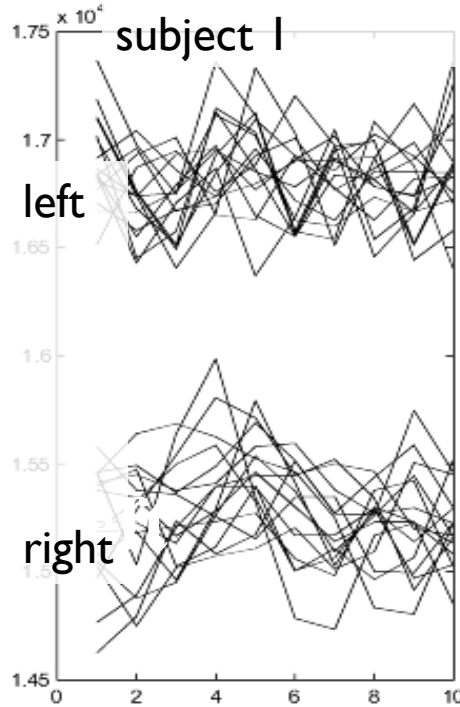


Background Noise



Stimuli



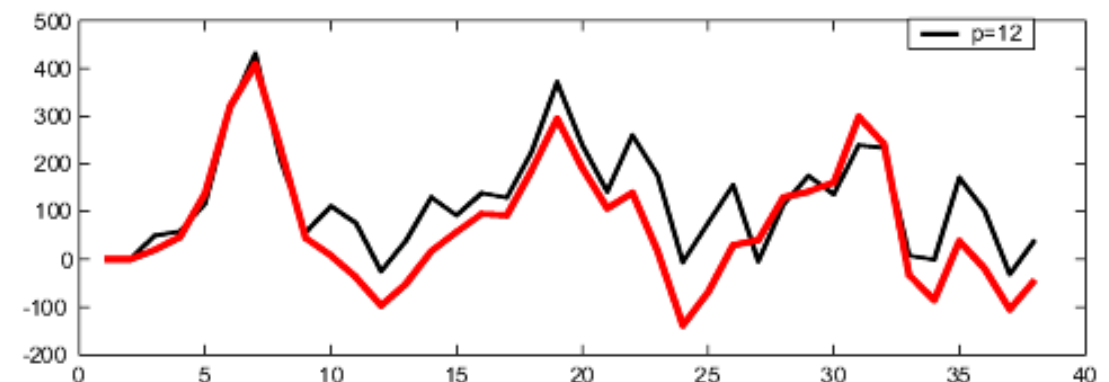


Hemodynamic response modeling

$$y(t) = \int_0^t H(t-s) f(s) ds + e(t)$$

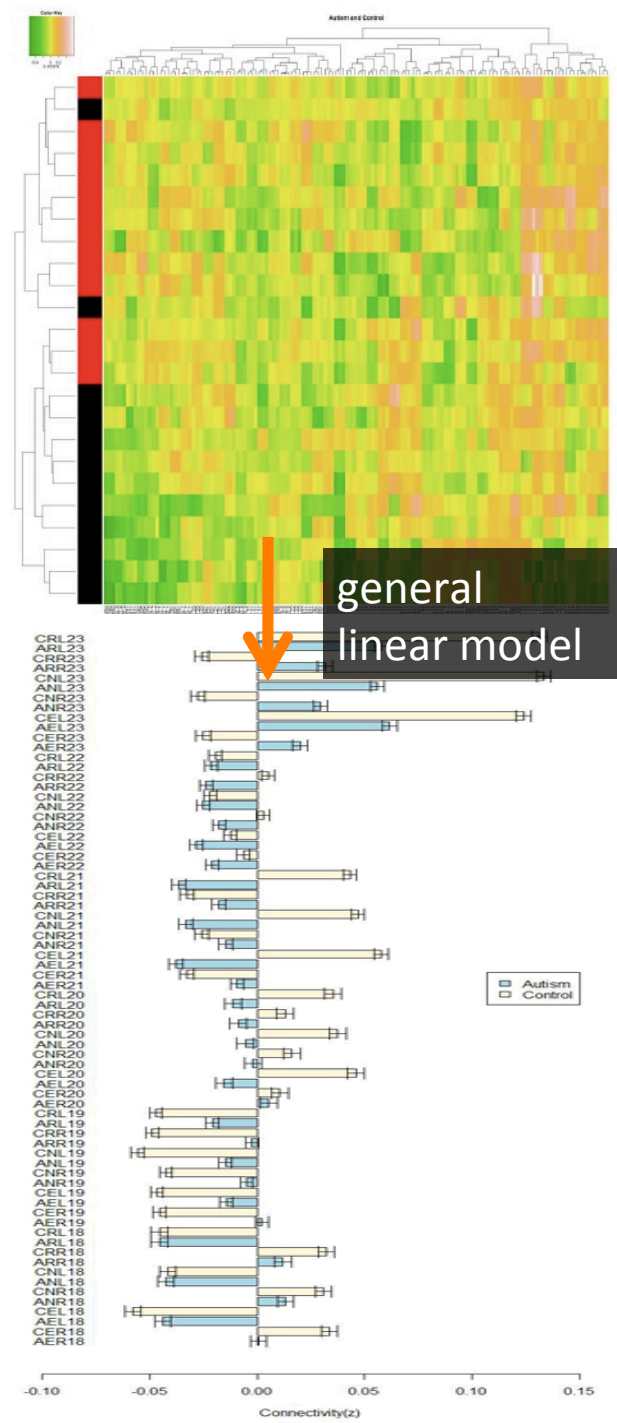
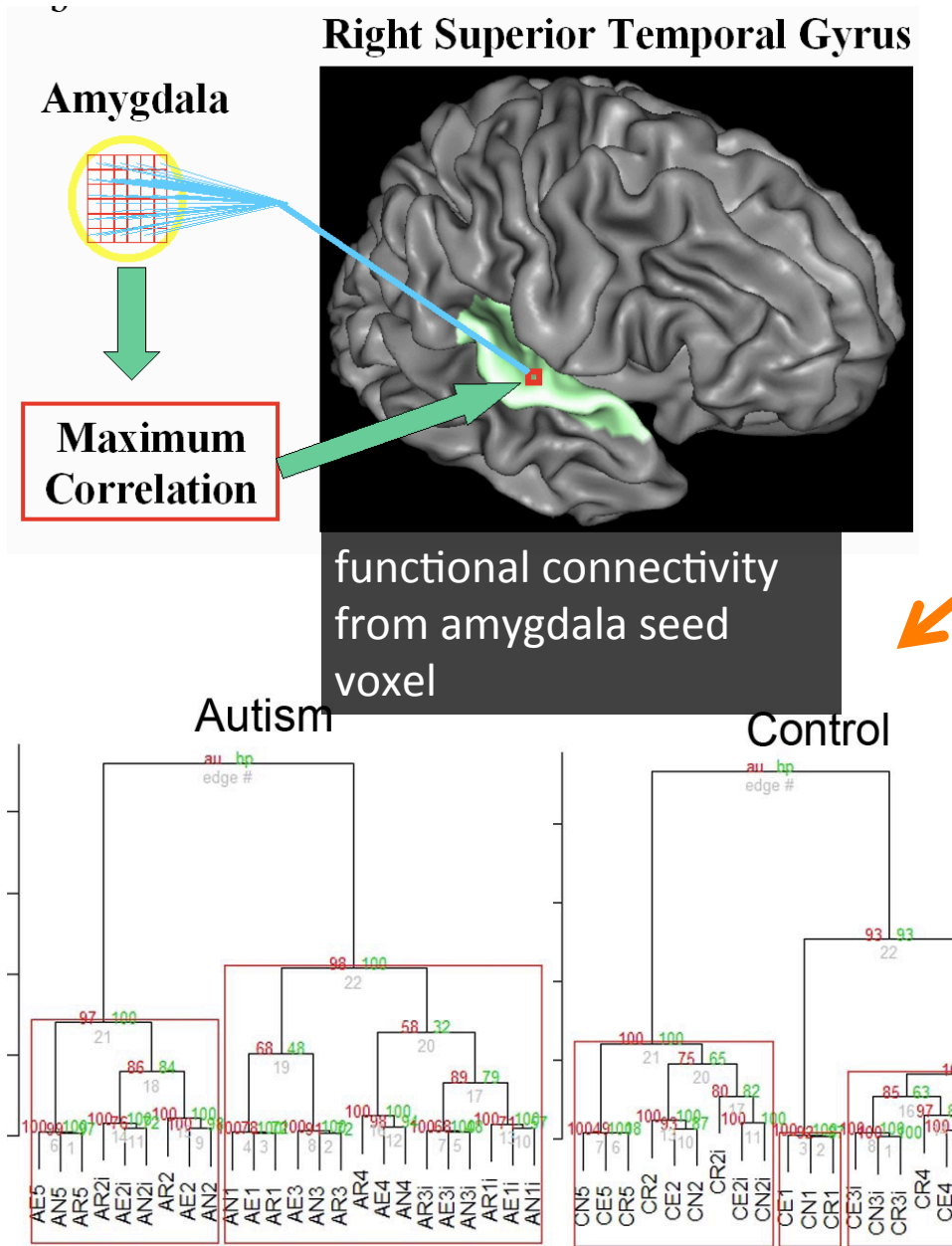


Weighted least squares
Least squares



Effective fMRI connectivity

D.J. Kelley



Inside fMRI scanner

Input:

24 emotional faces

16 neutral faces

Output:

Response time

2 (Emotion) \times 2 (Orientation)

Neutral

Emotional



Straight-ahead

Quarter-turned

nature
neuroscience

Gaze fixation and the neural circuitry of face processing in autism

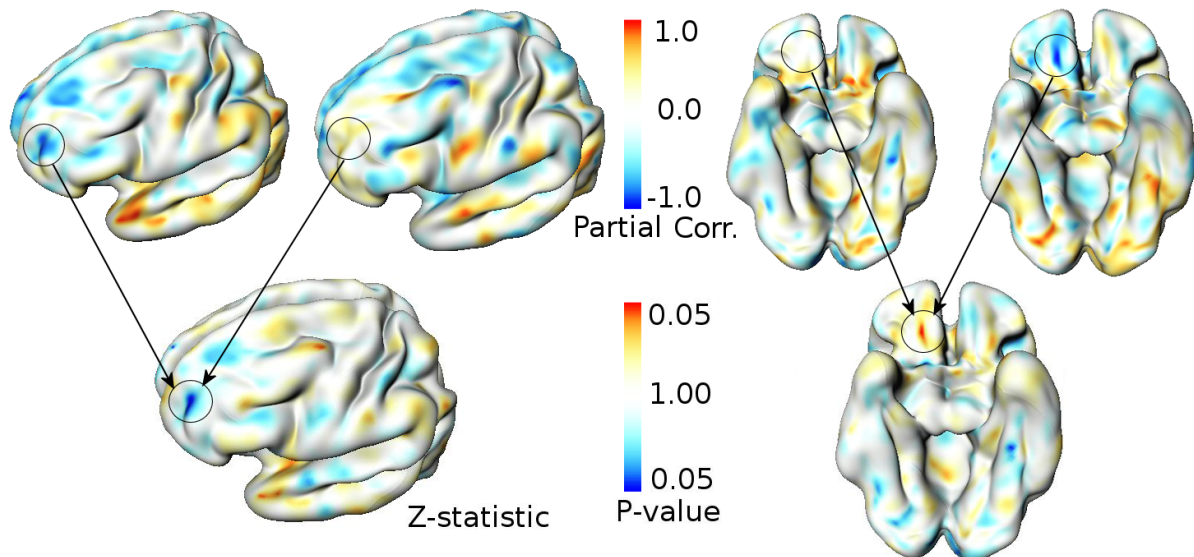
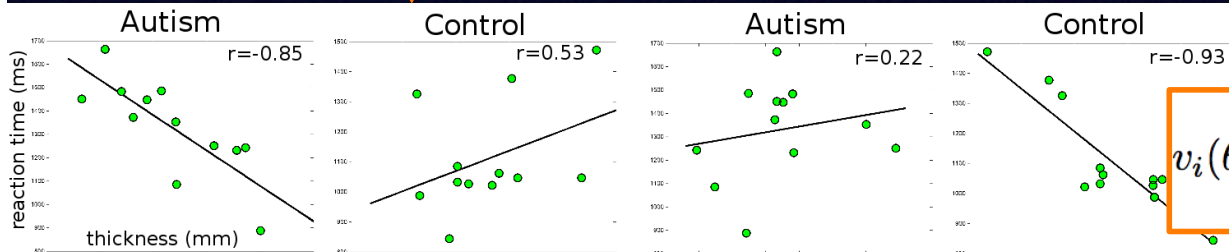
Kim M Dalton^{1,2}, Brendon M Nacewicz², Tom Johnstone², Hillary S Schaefer², Morton Ann Gernsbacher^{1,3}, H H Goldsmith^{1,3}, Andrew L Alexander^{1,2,4} & Richard J Davidson¹⁻⁴

Partial correlation mapping

Eye tracking data



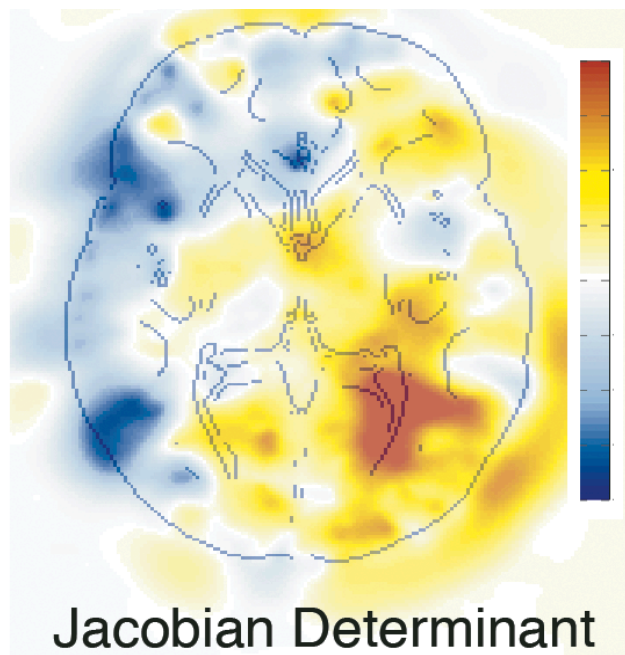
↓ Partial correlation analysis



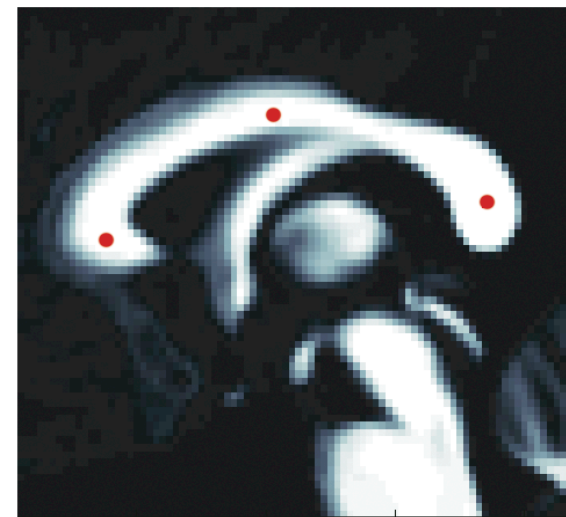
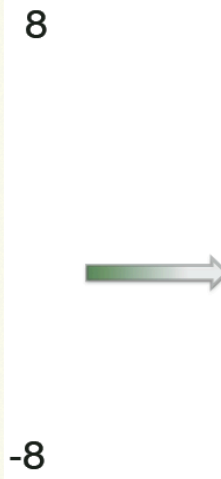
↓ Weighted Fourier representation

$$v_i(\theta, \varphi) = \sum_{l=0}^k \sum_{m=-l}^l e^{-il(l+1)\sigma} f_{lm}^i Y_{lm}(\theta, \varphi)$$

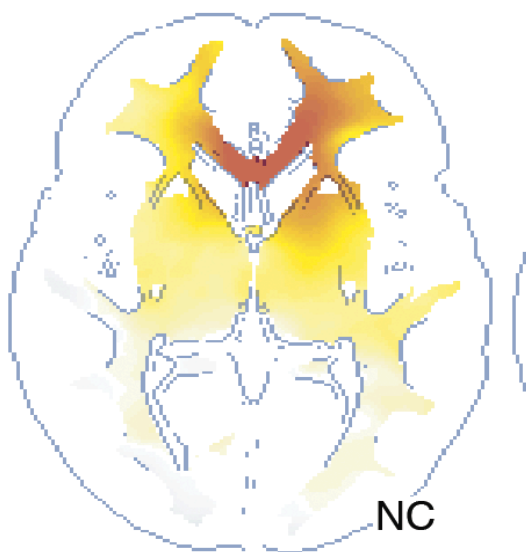
88.1799	56.6336	5.7367
-12.4775	-11.2552	-2.0791
2.4336	-15.4428	-0.4021
4.3956	2.2733	-0.9354
-0.0106	-0.0674	0.6999
2.1773	-2.4194	-0.1176
0.5808	0.8390	1.2942
0.0615	-0.1893	0.1188
-0.2629	0.7524	0.1089
0.7909	-0.7276	-0.1901
0.5458	0.6236	0.6939
.....		



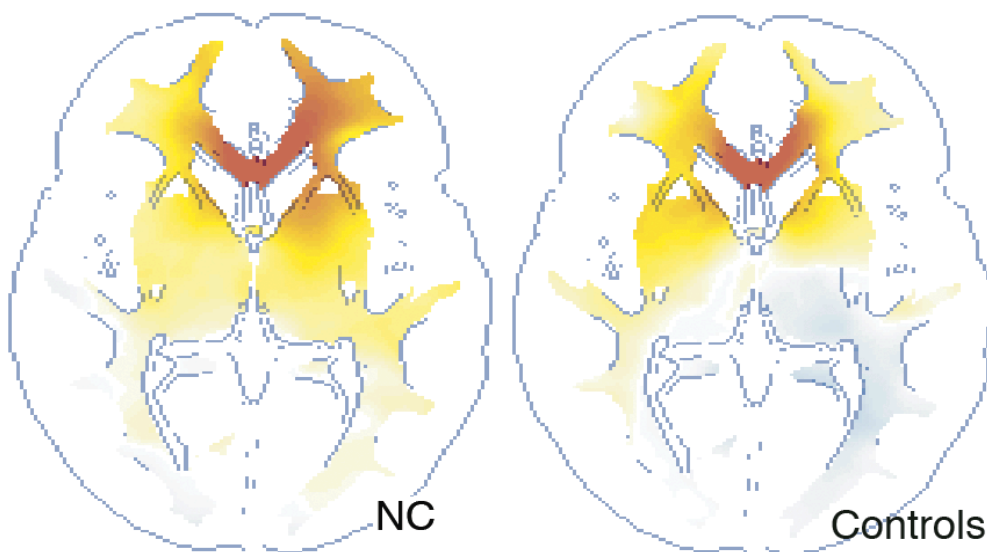
Jacobian Determinant



Seed voxels

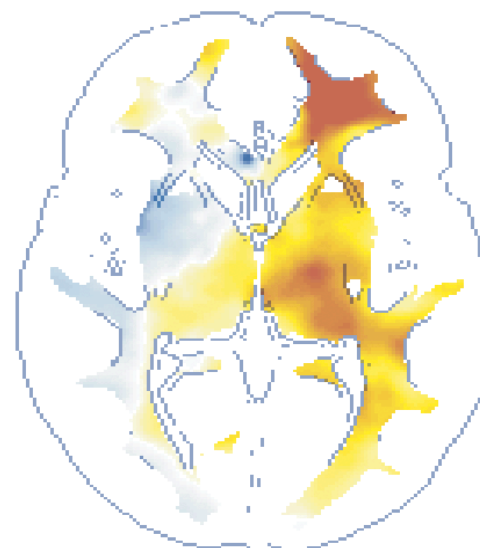


NC



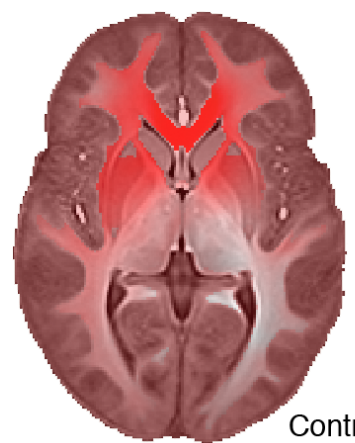
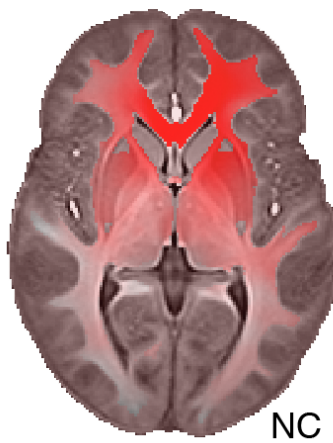
Controls

Connectivity Maps

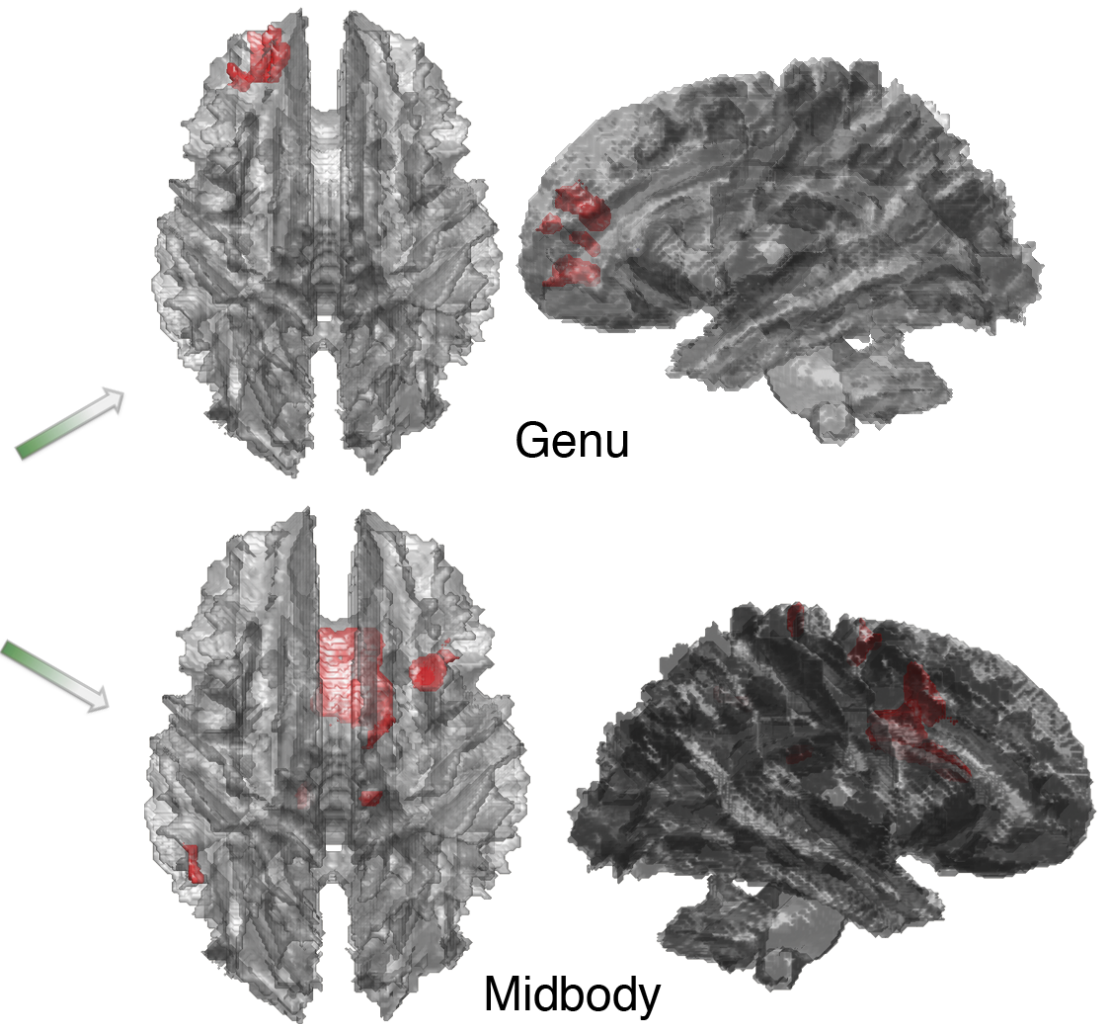


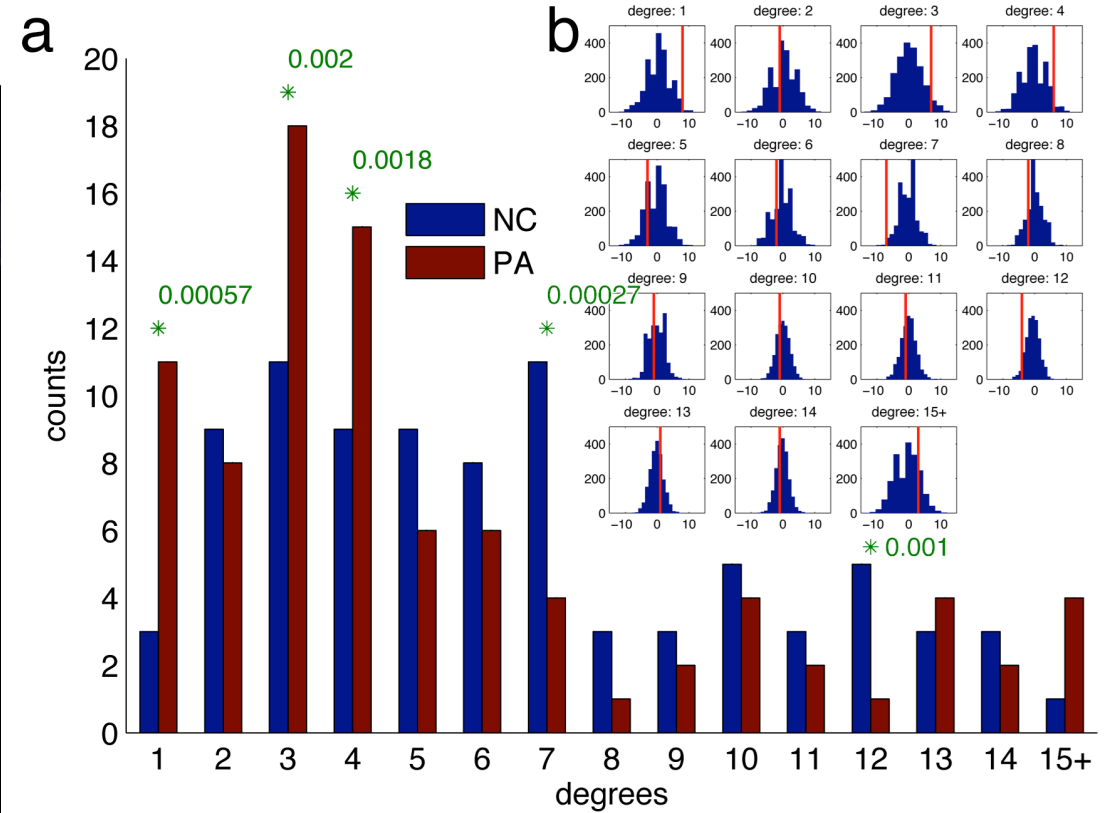
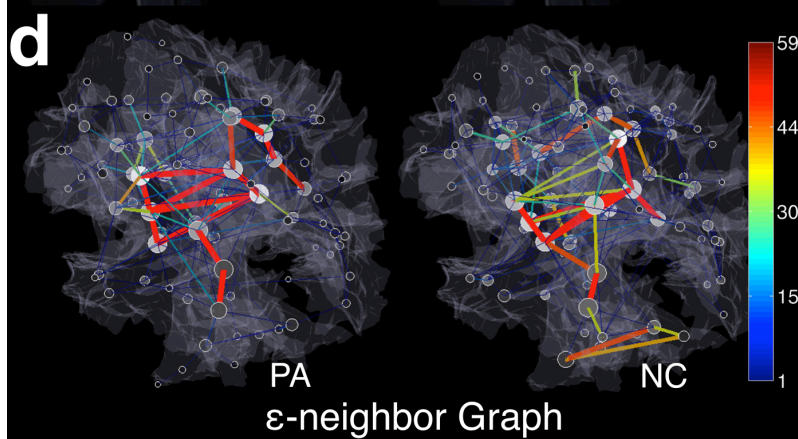
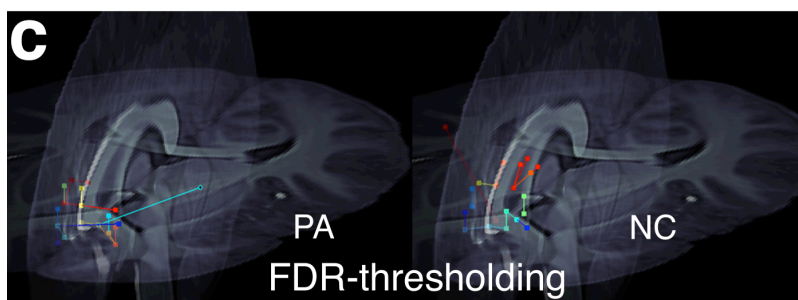
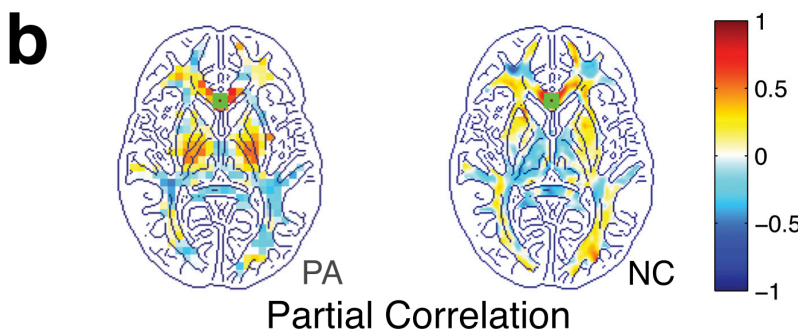
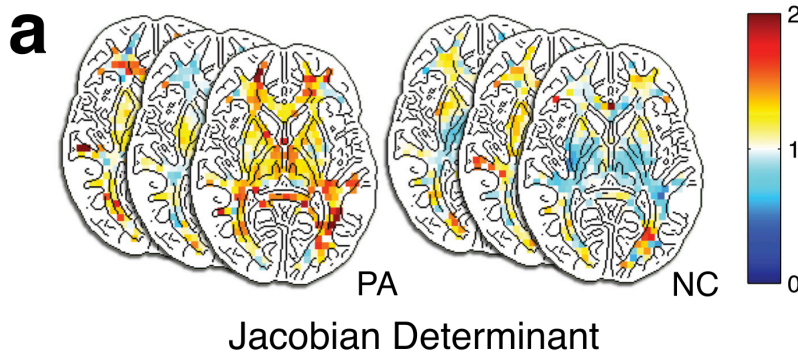
Z-statistic



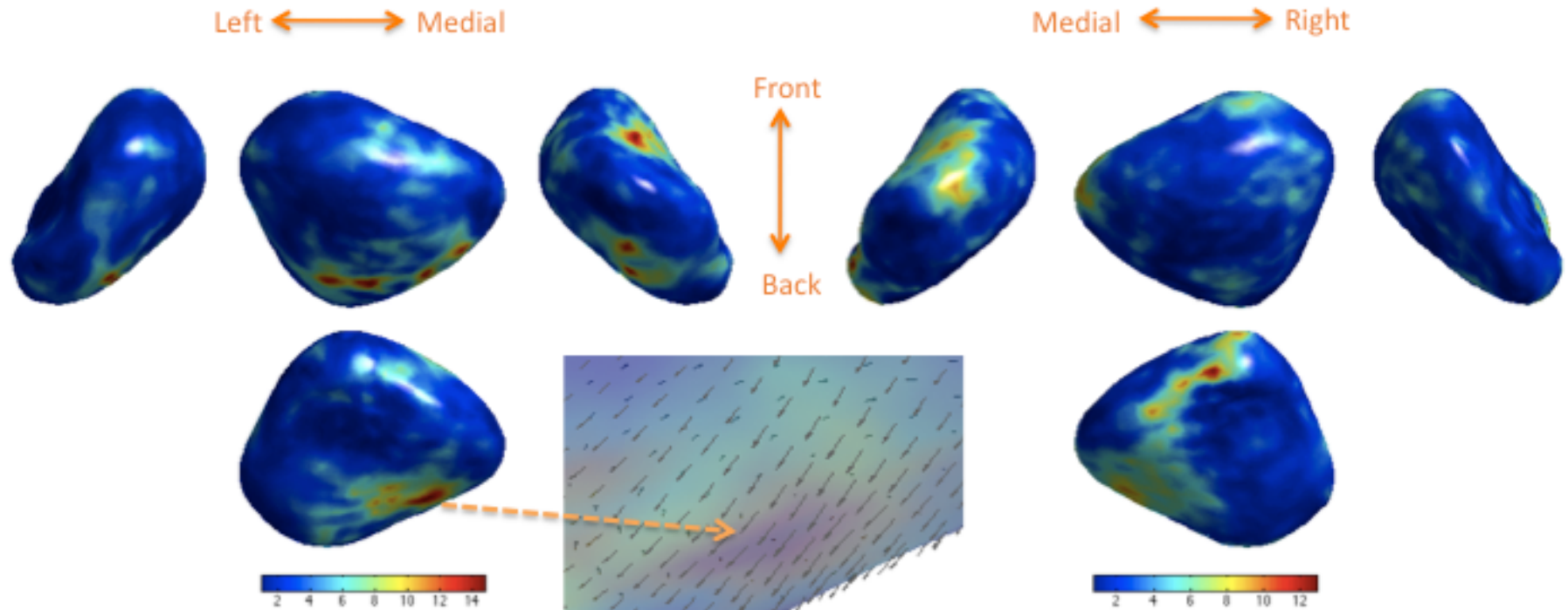


Connectivity Maps





Abnormal amygdala shape difference in autism



Multivariate linear model + Worsley's random field theory

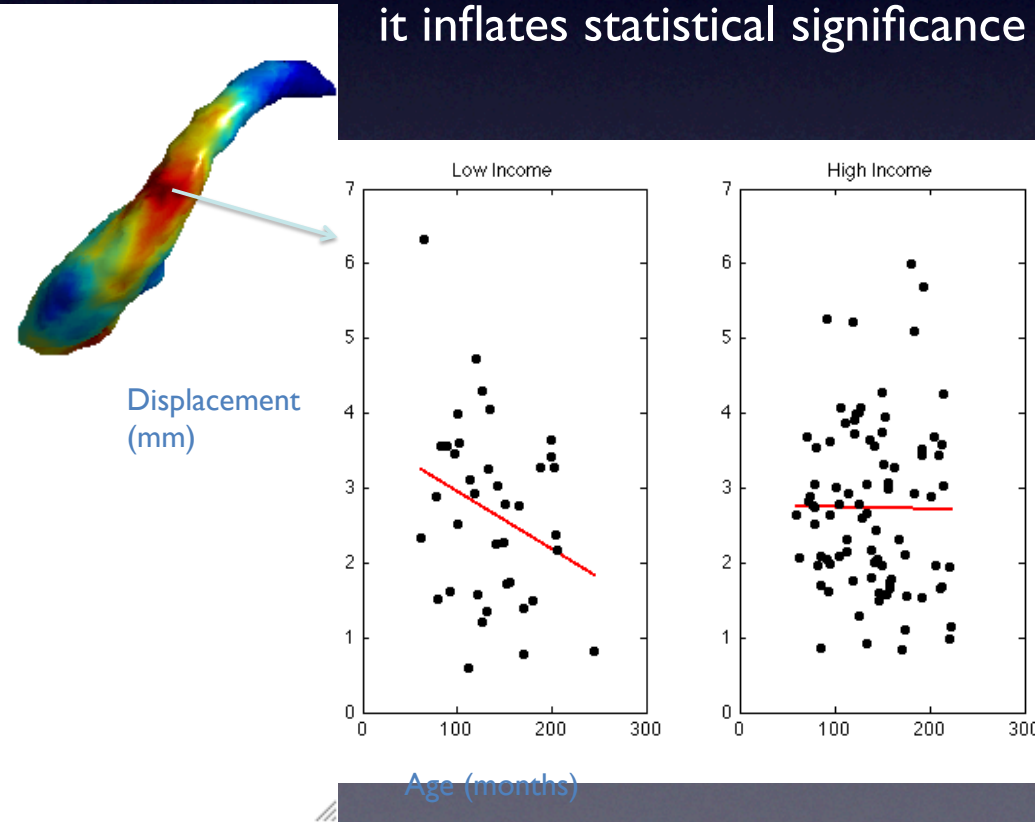
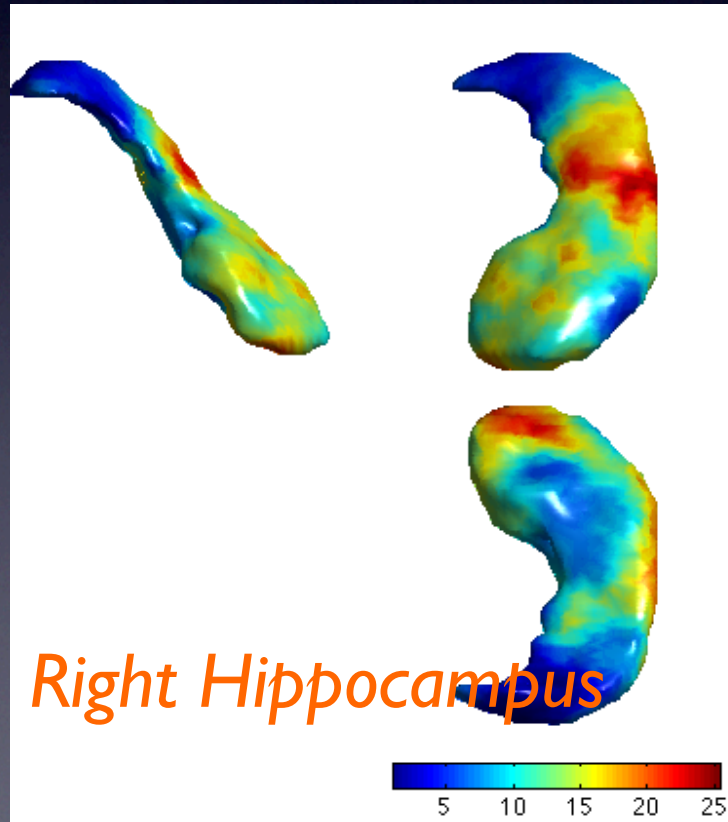
$$P_{n \times 3} = X_{n \times p} B_{p \times 3} + Z_{n \times r} G_{r \times 3} + U_{n \times 3} \Sigma_{3 \times 3}$$

Coordinates = Group + Brain + Age + Noise

Fixed effect model accounting treating multiple scans within a subject as independent

displacement = age + gender + group + age*group

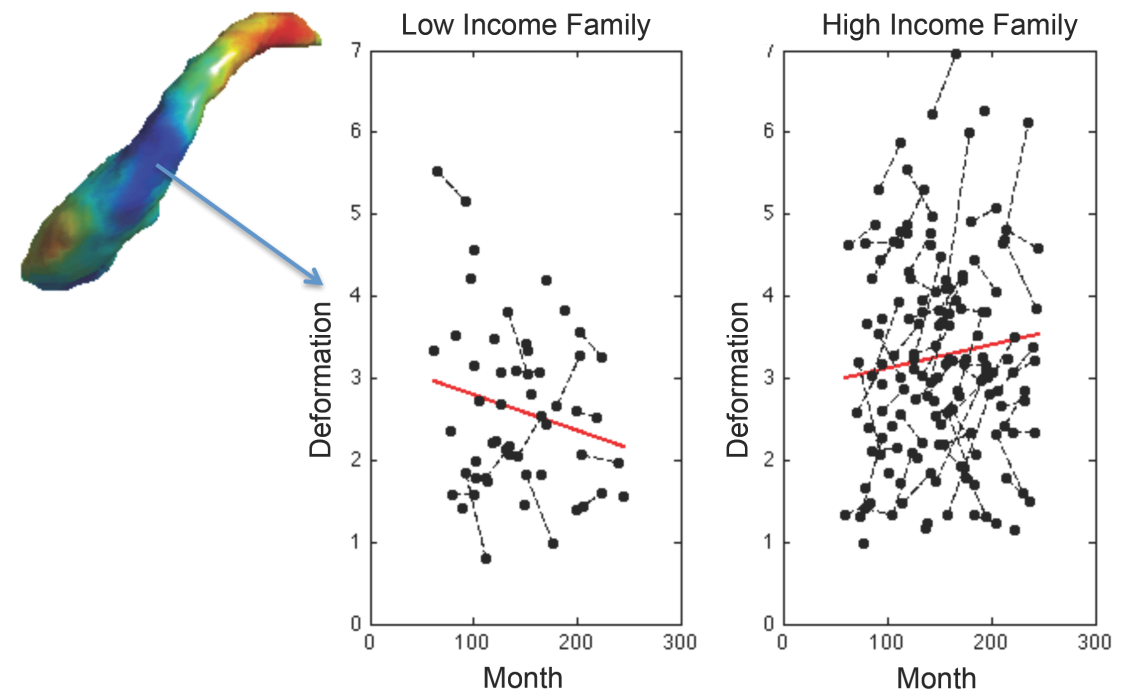
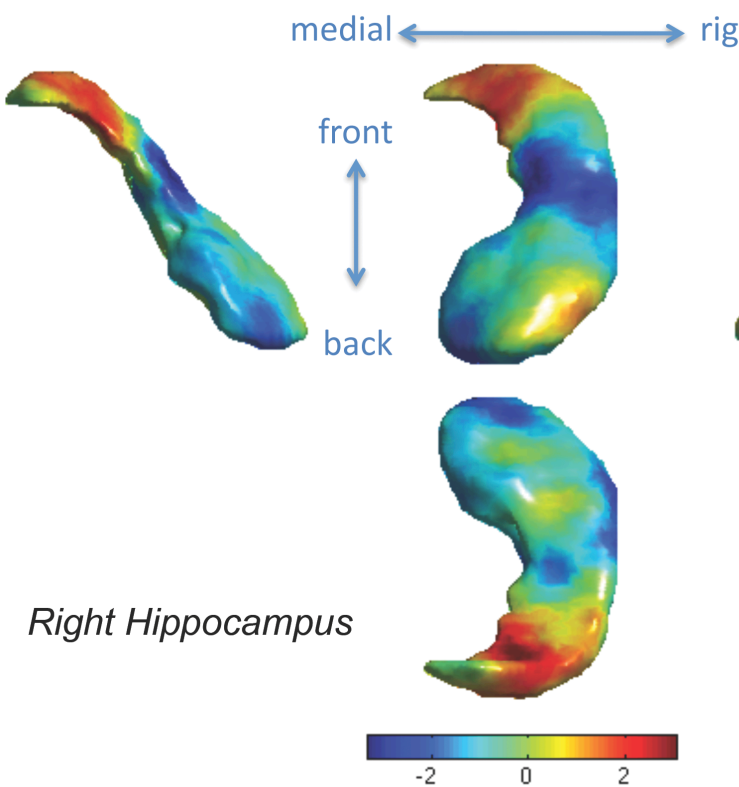
max F = 25.4
corrected pvalue < 0.001
it inflates statistical significance



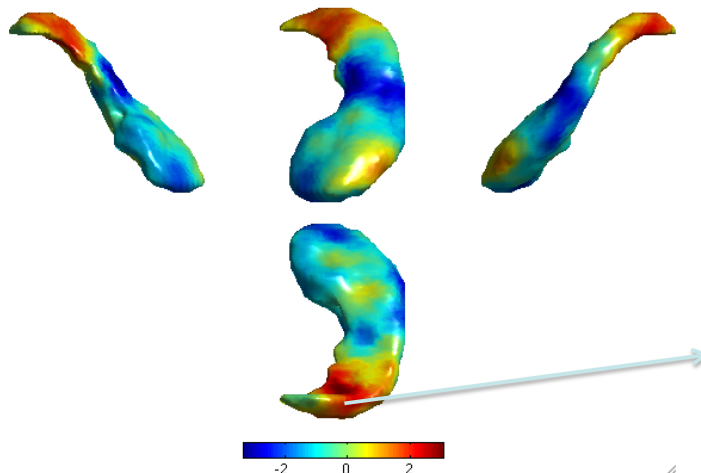
Linear mixed effect model accounting for inter-correlation of multiple scans within a subject

displacement = age + gender + group + age*group

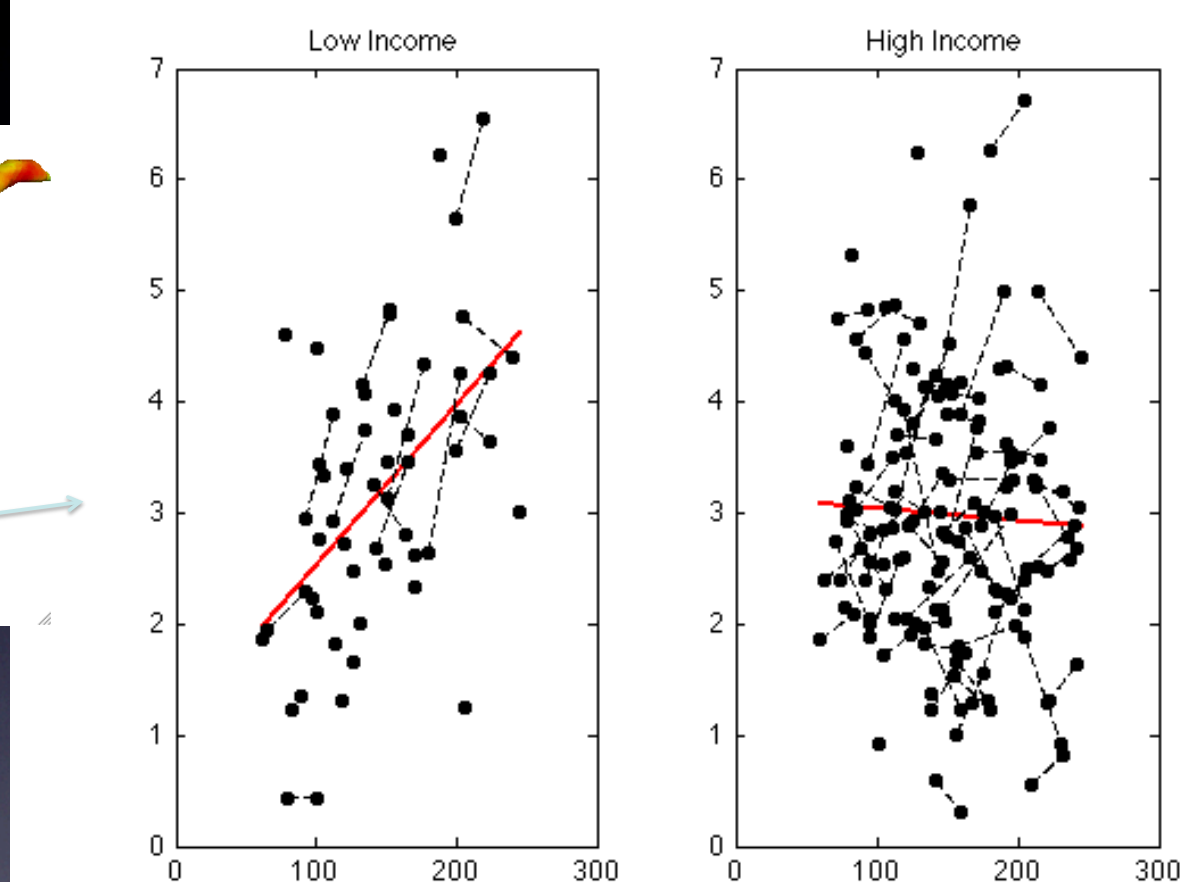
min t = -3.3398,
corrected pvalue = 0.025



Right hippocampus

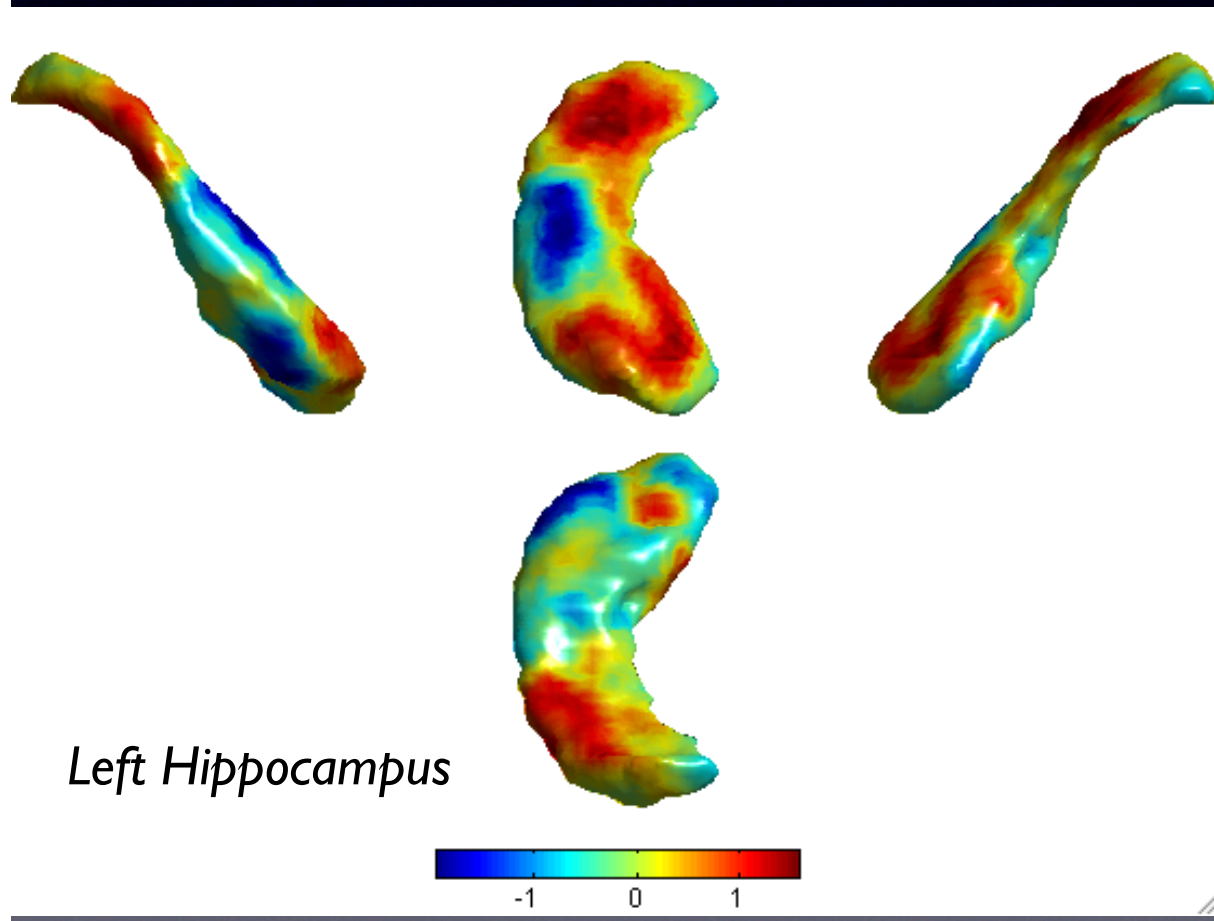


max t = 3.0531
corrected pvalue = 0.05



Linear mixed effect model on left hippocampus

displacement = age + gender + group + age*group



↑
min t = -1.9589,
corrected pvalue > 0.4
Not significant

Thank you. Lunch time!

send email for whatever questions
you have mkchung@wisc.edu

